



**NASA TECHNICAL
HANDBOOK**

National Aeronautics and Space Administration

METRIC/SI

**NASA-HDBK-4007
W/CHANGE 2—REINSTATE
ACTIVE STATUS
2020-10-22**

**Approved: 2016-10-27
Superseding MSFC-STD-531**

**SPACECRAFT HIGH-VOLTAGE PASCHEN AND
CORONA DESIGN HANDBOOK**

NASA-HDBK-4007 W/CHANGE 1

DOCUMENT HISTORY LOG

Status	Document Revision	Change Number	Approval Date	Description
Baseline			2016-10-27	Initial Release
		1	2020-10-16	Administrative Change: Inactive for New Design—This NASA Technical Handbook is no longer authorized for use in new designs, because it is antiquated, and no new updates have been discovered in the last several years
		2	2020-10-22	Administrative Change: Reinstate Active Status—Per NASA Engineering Standards Panel meeting 2020-10-21.

NASA-HDBK-4007 W/CHANGE 2

FOREWORD

This NASA Technical Handbook is published by the National Aeronautics and Space Administration (NASA) as a guidance document to provide engineering information; lessons learned; possible options to address technical issues; clarification of similar terms, materials, or processes; interpretive direction and techniques; and any other type of guidance information that may help the Government or its contractors in the design, construction, selection, management, support, or operation of systems, products, processes, or services.

This NASA Technical Handbook is approved for use by NASA Headquarters and NASA Centers and Facilities. It may also apply to the Jet Propulsion Laboratory and other contractors only to the extent specified or referenced in applicable contracts.

This NASA Technical Handbook establishes an overview of high-voltage electrical/electronic design techniques used to specify and to apply electrical insulation to spacecraft high-voltage parts, components, and systems for spacecraft system designs that are required to meet stringent fault-free operation for a period of days to years in space without maintenance.

Requests for information should be submitted via “Feedback” at <https://standards.nasa.gov>. Requests for changes to this NASA Technical Handbook should be submitted via MSFC Form 4657, Change Request for a NASA Engineering Standard.

Original Signed By
Ralph R. Roe, Jr.
NASA Chief Engineer

10/27/2016
Approval Date

TABLE OF CONTENTS

<u>SECTION</u>	<u>PAGE</u>
DOCUMENT HISTORY LOG.....	2
FOREWORD.....	3
TABLE OF CONTENTS.....	4
LIST OF FIGURES	8
LIST OF TABLES	11
1. SCOPE	12
1.1 Purpose.....	12
1.2 Applicability.....	12
2. APPLICABLE DOCUMENTS.....	13
2.1 General	13
2.2 Government Documents.....	13
2.4 Order of Precedence	13
3. ACRONYMS AND DEFINITIONS	14
3.1 Acronyms and Abbreviations.....	14
3.2 Definitions.....	16
4. OVERVIEW	21
4.1 Background	23
4.2 Partial Discharges, Corona, and Other High Voltage Phenomena.....	24
5. ENVIRONMENTS.....	25
5.1 Introduction	25
5.1.1 Ambient Environment.....	25
5.2 Contamination-Induced Environment.....	26
5.2.1 Implications of Spacecraft Internal Pressure.....	26
5.2.2 Estimating Internal Gas Pressure	27
5.2.3 Outgassing Through Multilayer Insulation	29
5.2.4 Suborbital Flights	33
5.2.5 Gas Purges, Leakage, and Contamination.....	34
5.2.6 Outgassing of High-Voltage Circuits.....	35
5.3 Electromagnetic Environment.....	37
5.3.1 Triboelectric Charging	38
5.3.2 Rocket Motor and Jet Engine Charging	38
5.3.3 Discharges Caused by Improper Grounding	39
5.3.4 Staging Effects	40
5.3.5 Coating Insulators and Windshields.....	40
5.3.6 Antenna Placement With Respect to Dischargers.....	40
5.4 References	40
5.4.1 Government Documents.....	40
5.4.2 Non-Government Documents	41

NASA-HDBK-4007 W/CHANGE 2

TABLE OF CONTENTS (Continued)

<u>SECTION</u>		<u>PAGE</u>
6.	INTERACTIONS.....	43
6.1	Introduction	43
6.2	Electric Field Configurations	43
6.2.1	Field Stress Calculations	43
6.2.2	Configurations	45
6.2.3	Empirical Field Equations	46
6.2.4	Voltage Distribution in Gas Surrounding Solid Dielectrics.....	48
6.2.5	Wire Configurations.....	49
6.3	Breakdown of Gases	49
6.3.1	Paschen's Law	49
6.3.1.1	External Radiation Effects	53
6.3.1.2	Temperature Effects	53
6.3.2	Corona Frequency Spectrum of Air Between Parallel Wires	56
6.3.3	Gas Mixtures	58
6.3.3.1	Helium-Oxygen.....	59
6.3.3.2	Nitrogen-Oxygen.....	59
6.3.3.3	Noble Gases	60
6.3.4	High-Frequency Breakdown	60
6.3.5	Multipactor Phenomena	65
6.3.6	Creepage and Flashover	72
6.3.6.1	Effect of Dielectric Constant on the Flashover Strength	73
6.3.6.2	Effect of Frequency on Flashover Strength	74
6.3.6.3	Effect of Magnetic Field	75
6.3.6.4	Effects of Air Temperature on Flashover Strength	75
6.3.6.5	Effect of Humidity on Flashover.....	76
6.4	Breakdown of Solids	77
6.4.1	Polarization	77
6.4.2	Dielectric Constant and Dissipation Factor.....	78
6.4.3	Dielectric Strength	79
6.4.4	Treeing	82
6.4.5	Breakdown Between Insulated Wires	83
6.4.6	Resistivity.....	86
6.4.7	Temperature Effects	86
6.4.8	Aging.....	87
6.4.8.1	Multifactor Aging.....	90
6.4.8.2	Temperature Effects on Aging	91
6.4.9	Corona Extinction Voltage as a Function of Composite Materials.....	91
6.4.10	Corona Extinction Voltage as a Function of Insulation Thickness.....	92
6.5	References	93

APPROVED FOR PUBLIC RELEASE—DISTRIBUTION IS UNLIMITED

NASA-HDBK-4007 W/CHANGE 2

TABLE OF CONTENTS (Continued)

<u>SECTION</u>		<u>PAGE</u>
6.5.1	Government Documents.....	93
6.5.2	Non-Government Documents	93
7.	DESIGN APPLICATIONS	102
7.1	Introduction	102
7.2	Materials and Processes	102
7.3	Pressure Sensing	103
7.4	System Voltages.....	104
7.4.1	0 to 50 Volts	104
7.4.1.1	0 to 50 Volts Good Workmanship Practices	104
7.4.1.2	0 to 50 Volts Typical Problem Areas.....	104
7.4.2	50 to 250 Volts	105
7.4.2.1	50 to 250 Volts Good Workmanship Practices	105
7.4.2.2	50 to 250 Volts Typical Problem Areas.....	107
7.4.3	Voltages Over 250 Volts	107
7.4.3.1	Voltages Over 250 Volts Good Workmanship Practices and Precautions	107
7.5	Solid Insulation	110
7.5.1	Solid Materials Selection Data.....	110
7.5.2	Conformal Coatings	111
7.5.3	Encapsulated Circuits.....	112
7.5.4	Modularized Electronic Circuits	113
7.5.5	Radiation and Chemical Factors	113
7.6	Packaging	113
7.6.1	Wiring and Connectors	114
7.6.2	Gas Pressure	114
7.6.3	Temperature	115
7.6.4	Gases	115
7.6.5	Mechanical Requirements.....	115
7.6.6	Frequency	115
7.7	Interconnection Systems	115
7.7.1	Connector Test Data.....	116
7.7.2	High-Voltage Connectors.....	117
7.7.3	Feedthroughs	118
7.7.4	Wiring Selection.....	119
7.7.5	Wire Terminations	121
7.7.6	High-Voltage Leads	123
7.7.7	Lead Terminals.....	124
7.7.8	Taps and Plates.....	125
7.7.9	Insulated High-Voltage Wiring.....	125

APPROVED FOR PUBLIC RELEASE—DISTRIBUTION IS UNLIMITED

NASA-HDBK-4007 W/CHANGE 2

TABLE OF CONTENTS (Continued)

<u>SECTION</u>		<u>PAGE</u>
7.7.10	Control Wiring and Circuits.....	126
7.8	Parts and Components.....	126
7.8.1	Resistors	126
7.8.2	High Voltage Capacitors	127
7.8.2.1	Dielectrics for Capacitors	127
7.8.2.2	Acceptable Impregnates	128
7.8.2.3	Ceramic Capacitors	129
7.8.2.4	Mica-Paper Capacitors	131
7.8.2.5	Film Capacitors	131
7.8.3	Solid State and Vacuum Parts	131
7.8.3.1	Diodes	131
7.8.4	Transformers	132
7.9	Printed Circuit Boards.....	132
7.1	Grounding and Bonding.....	133
7.10.1	Composite Structures	133
7.10.2	Composite Joints	134
7.10.3	Static Drain.....	137
7.11	Design Examples of Successful High-Voltage Power Supplies	138
7.12	References	138
7.12.1	Government Documents.....	138
8.	TESTING.....	139
8.1	Introduction	139
8.2	Corona Detection Methods for Electronic Systems	140
8.3	Sensor Constraints.....	140
8.4	Pressure Sensors.....	141
8.5	Ultrahigh Frequency (UHF) Sensor Restraints	142
8.6	Optical Detectors.....	142
8.7	Non-Explicit Detection	143
8.8	Electromagnetic Detectors	144
8.9	Spectrum Analysis ²⁵	144
8.1	Acoustic Detection	145
8.11	References	146
8.11.1	Government Documents.....	146
8.11.2	Non-Government Documents	146

NASA-HDBK-4007 W/CHANGE 2

LIST OF FIGURES

<u>FIGURE</u>		<u>PAGE</u>
1	Spacecraft Internal Pressure	27
2	Effects of Thermal Insulation on Outgassing Rate	30
3	Gas Pressure Inside the Apollo Telescope Mount	31
4	Pressure in Airlock Module Truss Compartment.....	32
5	Payload Pressure for a Vented Payload During Launch	33
6	Partial Discharge Counts Measured in a Sensitive Photomultiplier Circuit	35
7	Delaminated High-Voltage Capacitors	36
8	Insulation Deterioration on the Coil Winding.....	37
9	Utilization Factor for Various Electrode Configurations	44
10	Typical Field Plot of Conductors Showing Curvilinear Squares From Intersecting Equipotential and Field Lines	48
11	Cross Sectional View of (a) Twisted-Pair Wire and (b) Wire-to-Ground Configurations Showing Possible Corona Sites at High Pressure (Shorter Path) and Low Pressure (Longer Path)	49
12	Breakdown Voltage of Several Gases as a Function of pd at Room Temperature	50
13	Paschen Curve of Helium as a Function of pd at Room Temperature.....	51
14	Breakdown Voltage of Hydrogen-Air Mixture as a Function of Hydrogen Percentage in Air.....	51
15	Corona Onset Voltage Between Parallel Plates at Several Spacings	52
16	Corona Between Nichrome Wires in Heated Chamber	54
17	Corona Initiation Voltage as a Function of Temperature and Pressure for Parallel Wires in a Heated Chamber	55
18	Corona Onset Voltage of Nickel-Clad Wires in a Molybdenum- Contaminated Oven.....	56
19	Frequency Spectrum at Corona Pressure	57
20	Frequency Spectrum at 0.75 Torr, 647 Volts for #16 AWG Solid Copper Wires Spaced 4.8 cm	57
21	Frequency Spectrum at Glow Discharge Pressure	58
22	Onset Voltage of Gases and Gas Mixtures Between 0.25-in. Round Rods	59
23	Parallel Plates in Helium-Oxygen	60
24	Round Rods in Nitrogen-Oxygen Gas Mixture	60
25	Breakdown at High Frequency in Air in Inhomogeneous Field	62
26	Breakdown at High Frequency in Air (Smaller Values of d (mm)) in Inhomogeneous Field	62
27	Variation of RF Breakdown Voltage With Pressure Illustrating the Pressure Transition Region From Gas Discharge to Multipactor	63

APPROVED FOR PUBLIC RELEASE—DISTRIBUTION IS UNLIMITED

NASA-HDBK-4007 W/CHANGE 2

LIST OF FIGURES (Continued)

<u>FIGURE</u>		<u>PAGE</u>
28	Breakdown Voltage for a 0.4-mm Gap in Air at Atmospheric Pressure as a Function of Frequency	64
29	Frequency De-rating of Paschen's Law at High Frequencies for Different Electrode Configuration and Spacing.....	65
30	Multipactor Discharge: Electron Resonance in an RF Field with Discharge Sustained by Secondary Emission	67
31	Power Decrease Caused by Multipactor	68
32	Possible Regions of Multipacting Between Parallel Plates	69
33	Multipactor Discharge Characteristics of Various Surface Materials as a Function of f_d for Two Different Operating Frequencies (430 and 100 MHz) for Parallel Plate Electrode Configuration.....	70
33	(Continued) Multipactor Discharge Characteristics of Various Surface Materials as a Function of f_d for Two Different Operating Frequencies (430 and 100 MHz) for Parallel Plate Electrode Configuration	71
33	(Concluded) Multipactor Discharge Characteristics of Various Surface Materials as a Function of f_d for Two Different Operating Frequencies (430 and 100 MHz) for Parallel Plate Electrode Configuration	72
34	Multipacting Region for Coaxial Electrodes With Varying Values of b/a	73
35	Flashover Test Fixture.....	74
36	Effect of Spacing on the Initial Values of Strength for Fixture Shown in 35.....	75
37	Variation of Flashover Voltage With Changing Insulation Dielectric Constant	76
38	Effect of Frequency on Flashover Strength for Configuration Shown in 35.....	77
39	Effect of Frequency on the Electric Strength of PE.....	77
40	Effect of Temperature on 60-Hz Flashover Stress	78
41	Dielectric Polarization.....	80
42	Temperature Effects on ac Dielectric Strength of Kapton® Type-H Film	82
43	High Humidity Effects on the Dielectric Strength of Kapton® Type-H Film	83
44	Insulation Thickness Effects on Dielectric Strength of Kapton® Type-H Film	83
45	Film Area Versus Dielectric Strength of Kapton® Type-H Film.....	84
46	Electrical Treeing in Plexiglass (author: Bert Hickman)	86
47	Corona Initiation and Extinction Voltages of Sample T1, Twisted Pair and Wire-to-Ground Configuration Shown in 11, as a Function of Pressure	87

APPROVED FOR PUBLIC RELEASE—DISTRIBUTION IS UNLIMITED

NASA-HDBK-4007 W/CHANGE 2

LIST OF FIGURES (Continued)

<u>FIGURE</u>		<u>PAGE</u>
48	CIV and CEV Data for Sample P1 Type Wire	87
49	CIV and CEV Data for Sample R3 Type Wire	88
50	CIV as a Function of Altitude (Pressure) of Sample R2 Aged Several Hours at 304 °C	88
51	Volume Resistivity of Kapton® Type-H Film at 1 kHz	89
52	Impedance of Two-Conductor Shielded Cable in Molybdenum Trioxide Vapor	90
53	Life as a Function of Voltage for Kapton® Type-H Film	91
54	Heat Reduces the Time for Kapton® Type-H Film to Fall to Half of Original Dielectric Strength	92
55	Insulation Life as a Function of Field Stress	93
56	Minimum CIV of Several Wire Types and Wire Sizes	95
57	Minimum CIV as a Function of Insulation Thickness	96
58	(a) Outer Jacket Rupture and (b) Center Conductor Delamination	118
59	Round Wire Connector	119
60	Connector—55 Pins in Air at 24 °C Terminals Not Potted	120
61	High-Voltage Connector	121
62	Connector Pin With Air Gap	121
63	Acceptable Stand-Off Connections	122
64	Wire Termination	125
65	Acceptable Solder Terminations	125
66	Unacceptable Solder Terminations	126
67	High-Voltage Lead and Bushing	126
68	High-Voltage Terminals	127
69	High-Voltage Ties	127
70	Round Corners on Encapsulated Coils	128
71	Curved Edge on High-Voltage Plate	128
72	High-Reliability Resistor	129
73	Relative Spacing (Stress) of X7R Dielectric Ceramic Capacitors	132
74	Capacitance Versus Applied Voltage Data for 0.022 mF, 1000 V, X7R Ceramic Capacitors	133
75	Curved and Square-Corner PWB Test Structures	136
76	Multiple Screen Interleaved Lap Joint	138
77	Multiple Exposed Screen, Mechanically Fastened Stepped Lap Joint	138
78	Butt, Scarf, and Stepped Lap Joints	138
79	Mechanically Fastened Joints	139
80	Metal Connector	139
81	Center Screen Stepped Lap Composite-to-Metal Joint	139

LIST OF TABLES

<u>TABLE</u>		<u>PAGE</u>
1	Paschen's Law Breakdown Voltages at the Critical Pressure- Spacing Dimension for Select Gases at dc and 400 Hz	34
2	Maximum Field Strength (Em) With a Potential Difference (V) Between the Electrode Configurations.....	46
3	High-Frequency Voltage Breakdown Criteria	66
4	Comparison of Steady and Impulse Flashover Stress V/cm (Peak) for Glass Epoxy-Bond Laminates.....	75
5	Polyethylene Dielectric Strength (in V/mil) for 30-mil Sheets as a Function of Temperature and Frequency	78
6	Teflon® Dielectric Strength (in V/mil) for 30-mil Sheets as a Function of Temperature and Frequency	78
7	Environmental Effects on Surface Flashover at 60 Hz	79
8	Life Field Stress (1 h)	92
9	Power System Voltages	112
10	Properties of Interest for Insulating Materials	114
11	Summary of Failure Analysis Form	116
12	Conductor Materials.....	124
13	Capacitor Requirements	130
14	Acceptable Impregnates	131
15	Recommendation in Designs Where Graphite/Epoxy is Coupled With Other Materials.....	137
16	Bonding/Grounding Concept Assessment	140

SPACECRAFT HIGH-VOLTAGE PASCHEN AND CORONA DESIGN HANDBOOK

1. SCOPE

This NASA Technical Handbook presents an overview of the current understanding of the electrical design techniques that can mitigate deleterious effects (such as Paschen and corona discharges) resulting from operation of a high-voltage system in space, references common design practices that have been successful in mitigating these effects in the past, and recommends standard practices to eliminate or mitigate such effects in the future.

1.1 Purpose

The purpose of this NASA Technical Handbook is to present an overview of high-voltage electrical/electronic design techniques required to specify and apply electrical insulation to spacecraft high-voltage parts, components, and systems. Of particular interest are spacecraft system designs that are needed to meet stringent fault-free operation for a period of days to years in space without maintenance. The first objective is to develop an understanding of electrical insulation characteristics and the influence of aging. A second objective is to capture decades of lessons learned and present recommended design, analysis, and test methodologies that have been applied to the many successful space vehicle electronic programs during their development, manufacture, final assembly, test, and flight.

1.2 Applicability

This NASA Technical Handbook is applicable to all high-voltage power systems that operate in space. It is not intended to replace the following low Earth orbit or geosynchronous Earth orbit spacecraft charging standards or handbooks: NASA-STD-4005, Low Earth Orbit Spacecraft Charging Design Standard; NASA-HDBK-4006, Low Earth Orbit Spacecraft Charging Design Handbook; ISO-11221, Space Systems—Space Solar Panels—Spacecraft Charging Induced Electrostatic Discharge Test Methods; and NASA HDBK 4002A, Mitigating In-Space Charging Effects—A Guideline. Rather, this NASA Technical Handbook is to complement them to provide for better interior spacecraft high-voltage designs that would prevent Paschen and/or corona discharges, not to deal with plasma interactions that are the purview of other documents.

This NASA Technical Handbook is approved for use by NASA Headquarters and NASA Centers, including Component Facilities and Technical and Service Support Centers. It may also apply to the Jet Propulsion Laboratory or to other contractors, grant recipients, or parties to agreements only to the extent specified or referenced in their contracts, grants, or agreements.

This NASA Technical Handbook, or portions thereof, may be referenced in contract, program, and other Agency documents for guidance. When it contains procedural or process requirements, they may be cited in contract, program, and other Agency documents.

2. APPLICABLE DOCUMENTS

2.1 General

The documents listed in this section are applicable to the guidance in this NASA Technical Handbook.

2.1.1 The latest issuances of cited documents shall apply unless specific versions are designated.

2.1.2 Non-use of specific versions as designated shall be approved by the responsible Technical Authority.

The applicable documents are accessible at <https://standards.nasa.gov> or may be obtained directly from the Standards Developing Body or other document distributors.

2.2 Government Documents

Department of Defense

AFWAL-TR-88-4143	Design Guide: Designing and Building High Voltage Power Supplies, Materials Laboratory, Volumes I and II
------------------	--

NASA

NASA-HDBK-4006	Low Earth Orbit Spacecraft Charging Design Handbook
NASA-STD-4005	Low Earth Orbit Spacecraft Charging Design Standard
NASA-HDBK-4002A	Mitigating In-Space Charging Effects—A Guideline

2.3 Non-Government Documents

ASTM International

ASTM D257	Standard Test Methods for DC Resistance or Conductance of Insulating Materials
-----------	--

2.4 Order of Precedence

This NASA Technical Handbook provides guidance for high-voltage electrical/electronic design techniques but does not supersede nor waive established Agency requirements/guidance found in other documentation.

3. ACRONYMS AND DEFINITIONS

3.1 Acronyms and Abbreviations

ac	alternating current
AFWAL	Air Force Wright Aeronautical Laboratories
AM	airlock module
Ar	argon
ASTM	ASTM International (formerly American Society for Testing and Materials)
AWG	American wire gauge
BEAR	Beam Experiments Aboard a Rocket
°C	degrees Celsius
C	coulomb
CEV	corona extinction voltage
CIV	corona inception (or initiation) voltage
cm	centimeter
C-SAM	C-mode Scanning Acoustic Microscope
dB	decibel
dc	direct current
DWV	dielectric withstanding voltage
EMI	electromagnetic interference
ESL	equivalent series inductance
ESR	equivalent series resistance
°F	degrees Fahrenheit
<i>fd</i>	operating frequency (<i>f</i>) times electrode separation (<i>d</i>)
ft	feet
GHz	gigahertz
GSFC	Goddard Space Flight Center
h	hour
H	hydrogen
HRS	High Resolution Spectrograph
Hz	hertz
HV	high voltage
IEC	International Electrotechnical Commission
IEEE	Institute of Electrical and Electronics Engineers
ITO	indium tin oxide
K	kelvin
kHz	kilohertz
km	kilometer
kV	kilovolt
kW	kilowatt
lbm	pound mass
m	meter
m ³	cubic meter

NASA-HDBK-4007 W/CHANGE 2

MDA	multiple-docking adapter
MHz	megahertz
mil	a thousandth of an inch
min	minute
Mm	millimeter
MoO ₃	molybdenum trioxide
MSFC	Marshall Space Flight Center
MSIS	Mass Spectrometer Incoherent Scatter
MW	megawatt
N ₂	nitrogen
NASA	National Aeronautics and Space Administration
NEMA	National Electrical Manufacturers Association
NO ₂	nitrogen dioxide
NOAA	National Oceanic and Atmospheric Administration
O ₂	oxygen
Pa	Pascal
pC	picocoulomb
<i>Pd</i>	partial discharge
PE	polyethylene
PS/FAS/IU	payload shroud/fixed airlock shroud/instrument unit
psi	pounds per square inch
PWB	printed wiring board
RF	radio frequency
RH	relative humidity
rms	root mean square
S	second
SAE	Society of Automotive Engineers
SLAM	scanning laser acoustic microscope
SPEAR	Space Power Experiments Aboard Rockets
<i>t(rr)</i>	reverse recovery time
Torr	A traditional unit of pressure, now defined as exactly 1/760 of a standard atmosphere. Thus one <i>torr</i> is exactly 101325/760 Pascals (~133.3 Pa).
UHF	ultrahigh frequency
UV	ultraviolet
V	volt
Vdc	volts direct current
VSWR	voltage standing wave ratio

3.2 Definitions

The following definitions are based on AFWAL-TR-88-4143, Volume II, Design Guide: Designing and Building High Voltage Power Supplies.

Adsorption: The adhesion of gas or liquid molecules to the surfaces of solids or liquids with which they are in contact.

Aging: The change in properties of a material with time under specific conditions.

Arc Resistance: The ability of a material to resist the action of a high voltage electrical arc, usually stated in terms of the time required to render the material electrically conductive.

Breakdown Voltage: The voltage at which the insulation between two conductors fails.

Conductance: The reciprocal of resistance. The ratio of current passing through a material to the potential difference at its ends.

Conductivity: The ratio of the current per unit area (current density) to the electric field in a material. Conductivity is expressed in units of siemens/meter.

Conductor: A substance or body that allows a current of electricity to pass continuously along or through it.

Contaminant: An impurity or foreign substance present in a material that affects one or more properties of the material.

Corona: A non-self-sustaining discharge (sometimes visible) caused by ionization of the gas surrounding a conductor around which exists a voltage gradient exceeding a certain critical value for a gaseous medium.

Corona Resistance: The time that insulation will withstand a specified level of field-intensified ionization that does not result in the immediate and complete breakdown of the insulation.

Corrosion: Chemical action that causes destruction of the surface of a metal by oxidation or other chemical combination.

Creep: The dimensional change with time of a material under load.

Creepage (electrical): Electrical leakage on a solid dielectric surface.

Critical Voltage (of gas): The voltage at which a gas ionizes and a corona occurs, preliminary to dielectric breakdown of the gas.

NASA-HDBK-4007 W/CHANGE 2

Delamination: The separation of layers in a laminate through failure of the adhesive.

Dielectric: A material that has very low or no conductivity. A dielectric material is able to sustain an electric field with little or no current flow.

Dielectric Absorption: The effect by which a capacitor that has been charged for a long time discharges only incompletely when briefly discharged.

Dielectric Constant (Relative Permittivity): The property of a dielectric that determines the electrostatic energy stored per unit volume for unit potential gradient.

Dielectric Loss: The time rate at which electric energy is transformed into heat in a dielectric when it is subjected to a changing electric field.

Dielectric Loss Angle (Dielectric Phase Difference): The difference between 90 deg and the dielectric phase angle.

Dielectric Loss Factor (Dielectric Loss Index): The product of dielectric constant and the tangent of dielectric loss angle.

Dielectric Phase Angle: The angular difference in phase between the sinusoidal alternating potential difference applied to a dielectric and the component of the resulting ac having the same period as the potential difference.

Dielectric Strength: The maximum electrical potential gradient that an insulating material can withstand without rupture; expressed in volts per meter of thickness in the SI system.

Dissipation Factor (Loss Tangent; $\tan \delta$ ~ Power Factor): Synonymous terms defined equivalently as the ratio of the magnitude of the conduction current density to that of the displacement current density in a lossy medium., the ratio of the imaginary part of the complex dielectric constant to that of the real part, or the tangent of the loss angle of the insulating material.

Electromagnetic Field: A field of force that consists of coupled electric and magnetic fields moving together through space in time phase and space quadrature, generated by time-varying currents and accelerated charges, orthogonal to each other and their direction of motion, and containing a definite amount of electromagnetic energy.

Flashover: A disruptive electrical discharge around or over the surface of a solid or liquid insulator.

Glow Discharge: A luminous neutral plasma of high charge density. A cathode will have a surface glow at low pressure and higher fields, owing to the excitation of the incoming positive ions and neutralization at the surface.

NASA-HDBK-4007 W/CHANGE 2

Gradient: Rate of increase or decrease of a variable parameter.

Impulse: A unidirectional surge generated by the release of electric energy into an impedance network.

Insulation: Material having a high resistance to the flow of electric current used to prevent leakage of current from a conductor.

Insulation Resistance: The ratio of the applied voltage to the total current between two electrodes in contact with a specific insulator. Also defined as the resistance between two conductors, or between a conductor and earth, when they are separated only by insulating material.

Insulation System: All of the insulation materials used to insulate a particular electrical or electronic product.

Insulator: A material of such low electrical conductivity that the flow of current through it can usually be neglected.

Partial Discharge: In electrical engineering, a localized dielectric breakdown of a small portion of a solid or fluid electrical insulation system under high voltage stress, which does not bridge the space between two conductors. Note: While a corona discharge is usually revealed by a relatively steady glow or brush discharge in air, partial discharges within solid insulation system are not visible.

Partial Discharge Pulse: A voltage or current pulse that occurs at some designated location in the test circuit as a result of a partial discharge.

Partial Discharge Pulse Charge: The quantity of charge supplied to the test specimen's terminals from the applied voltage source after a partial discharge pulse has occurred. Note: The pulse charge is often referred to as the apparent charge or terminal charge. The pulse charge is related to but not necessarily equal to the quantity of charge flowing in the localized discharge.

Partial Discharge Pulse Energy: The energy dissipated during one individual partial discharge.

Partial Discharge Pulse Repetition Rate: The number of partial discharge pulses of specified magnitude per unit time.

Partial Discharge Pulse Voltage: The peak value of the voltage pulse, which, if inserted in the test circuit at a terminal of the test specimen, would produce a response in the circuit equivalent to that resulting from a partial discharge pulse within the specimen. Also referred to as "the terminal corona pulse voltage."

NASA-HDBK-4007 W/CHANGE 2

Permittivity: The ratio of the flux density produced by an electric field in a given dielectric to the flux density produced by that field in a vacuum.

Petticoat Insulator: An insulator made in the form of superposed inverted cups and used for high voltage insulation

Plasma: A gaseous body of ions and electrons of sufficiently low density that considerable charge separation is possible. Note: Because of the mobility of charge, a plasma is normally neutral and free of electric field in its interior, just like a metallic conductor.

Polyamide: A polymer in which the structural units are linked by amide or thioamide groupings.

Polystyrene: A thermoplastic material produced by the polymerization of styrene (vinyl benzene).

Potting: A process similar to encapsulating, except that steps are taken to ensure complete penetration of all voids in the object before the resin polymerizes.

Power Factor: The ratio of the average (or active) power to the apparent power (rms voltage times rms current) of an ac circuit. Also known as phase factor.

Pulse: A wave that departs from a first nominal state, attains a second nominal state, and ultimately returns to the first nominal state.

Resin: An organic substance of natural or synthetic origin characterized by being polymeric in structure and predominantly amorphous. Note: Most resins, though not all, are of high molecular weight and consist of a long chain or network molecular structure. Usually, resins are more soluble in their lower molecular weight forms.

Resistance: The property of a conductor that determines the current produced by a given difference of potential. Note: The ohm is the SI derived unit of resistance.

Resistivity: The ability of a material to resist passage of electrical current either through its bulk or on a surface. Note: The unit of volume resistivity is the ohm-centimeter.

Semiconductor: A solid substance whose electrical conductivity is intermediate between that of insulators and conductors. The conductivity of a semiconductor is often tailored through the addition of impurities and is usually dependent on applied electric or magnetic fields or by temperature effects.

Seta, plural: setae – very small, stiff hair like structures that can form on the surfaces of materials. If the surface is electrically charged, a seta results in very high electric field concentration, sometimes leading to electrical breakdown.

NASA-HDBK-4007 W/CHANGE 2

Silicone: Polymeric materials in which the recurring chemical group contains silicon and oxygen atoms as links in the main molecular chain.

Sparkover (Spark): A short-duration electric discharge caused by a sudden breakdown of air or some other dielectric material separating two terminals, accompanied by a momentary flash of light. Note: Also known as electric spark and spark discharge.

Streamer Discharge – a transient, filamentary electrical discharge that forms when an insulating medium is exposed to large potential differences. It begins as an electron avalanche which in turn causes additional electric field enhancement, which subsequently leads to additional ionization. The ionized region grows quickly to produce a finger-like discharge called a streamer.

Superinsulation: Originally developed originally for thermal insulation of liquid hydrogen or liquid helium handling equipment, this refers to thin, reflective, metallized plastic films designed to virtually eliminate radiant heat transfer.

Surface Leakage: The passage of current over the boundary surface of an insulator, as distinguished from passage through its volume.

Surface Resistivity: The resistance to leakage current along the surface of a dielectric material. Surface resistivity may be measured as the electrical resistance between two parallel electrodes in contact with the specimen surface and separated by a distance equal to the contact length of the electrodes. The resistivity is therefore the quotient of the potential gradient, in V/m, and the current per unit of electrode length, A/m. Since the four ends of the electrodes define a square, the lengths in the quotient cancel and surface resistivities are most accurately reported in ohms, although it is common to see the more descriptive unit of ohms per square. Note: Surface resistivity may vary widely with the conditions of measurement.

Surge: A transient variation in the current and/or potential at a point in the circuit.

Thermoplastic: A plastic that can be readily softened and resoftened by heating without changing its inherent properties.

Tracking: Scintillation of the surface of an insulator. May produce enough heat to leave a degraded track of carbon.

Tracking Resistance: See Arc Resistance.

Transient: That part of the change in a variable, such as voltage or current, which may be initiated by a change in steady-state conditions or an outside influence, and that decays and/or disappears following its appearance.

Treeing: An electrical pre-breakdown phenomenon in solid insulation.

NASA-HDBK-4007 W/CHANGE 2

Triple Point: The junction of a dielectric and a conducting material in the presence of a gaseous or liquid dielectric.

Urethane: A synthetic resin formed by the reaction of an isocyanate resin (nitrogen, carbon, and oxygen radical) with an alcohol.

Volume Resistivity (Specific Insulation Resistance): The electrical resistance between opposite faces of a 1-cm cube of an insulating material, commonly expressed in ohm-centimeters. Note: The recommended test is ASTM D257, Standard Test Methods for DC Resistance or Conductance of Insulating Materials.

Yield Strength: The lowest stress at which a material undergoes plastic deformation. Below this stress, the material is elastic; above it, the material is elastic-plastic.

4. OVERVIEW

In general, a detailed knowledge of electrical insulation and high-voltage design techniques is essential if reliable high-voltage systems are to be designed and manufactured for space applications and other uses. The trend is toward more advanced systems operating at higher voltages in compact, economical packages that have been submitted to a battery of controls to ensure a high-quality assembly. If materials are to be operated under much more demanding specifications, better information is required on the limits of these materials and on their design and manufacturing techniques.

Although section 3.2 gives definitions of many terms used in this NASA Technical Handbook, for better clarification, it is important to provide additional explanation for the following major terms:

a. The term “high voltage” in this NASA Technical Handbook is defined as the voltage above which electrical breakdown phenomena are likely to occur. The absolute voltage for a breakdown event, however, is dependent upon the electrical parameters (frequency and magnitude) and structural, geometric, and environmental constraints. Breakdown voltages can range from tens of volts in microwave systems to thousands of volts in utility systems.

b. “Electrical insulation” is a generic term given to vacuum, or to gaseous, liquid, and solid materials exhibiting high electric resistivity that may be used to electrically isolate two or more conducting surfaces.

c. “Dielectric” refers to an electrical insulator that can be polarized by an applied electric field.

d. “Insulator” is the generic expression for a solid material used to mechanically support and electrically isolate one or more conducting elements.

APPROVED FOR PUBLIC RELEASE—DISTRIBUTION IS UNLIMITED

NASA-HDBK-4007 W/CHANGE 2

e. “Insulation systems” may consist of one or more materials or classes of materials used to electrically isolate two or more conducting surfaces.

f. “Partial discharge” is an electrical discharge that does not bridge the electrodes, such as internal discharges in the cavities within the solid dielectric, surface discharges along the surface of insulator, and corona discharges around a sharp edge (usually around the electrode surface). Usually, the magnitude of such discharges is small; however, they may cause progressive deterioration of the insulation and lead to ultimate failure.

g. “Pure air”: The composition of air is variable with respect to several of its components (e.g. CH₄, CO₂, H₂O) so 'pure' air has no precise meaning. The composition of the major components in dry air is relatively constant (percent by volume given): nitrogen, 78.084; oxygen, 20.946; argon, 0.934; carbon dioxide, 0.033; neon, 0.0018; helium, 0.000524; methane, 0.00016; krypton, 0.000114; hydrogen 0.00005; nitrous oxide, 0.00003; xenon, 0.0000087. The concentrations of carbon dioxide, methane, nitrous oxide, the chlorofluorocarbons and some other species of anthropogenic origin are increasing measurably with time. For purposes of this document, “pure air” is assumed to consist of such a mixture that is free of any contaminant that could possibly alter its electrical or dielectric behavior.

For early spacecraft missions, techniques were developed for the detection of partial discharges in spacecraft electronic equipment. Use of these techniques clearly showed that the reduction of partial discharges enhanced equipment life, and thereafter testing incorporating such techniques made mandatory to eliminate faulty insulation and flawed workmanship. Some examples of representative instrumentation and test techniques, both of which have matured and improved over time, are described later in this NASA Technical Handbook.

In the modern spacecraft electronics industry, dense packaging is required to make the equipment fit within a restricted volume. Likewise, weight is restricted to economize on fuel and maximize space for the payload. Consequently, high electrical field stresses, which enhance partial discharge activity, are often present. Such partial discharge activities can be a contributing factor in insulation degradation.

Continuous partial discharge or corona activities are a serious problem usually associated with insulation degradation, electromagnetic interference (EMI), and the upset of poorly protected sensitive circuits without proper shielding or noise suppression. Insulated conductors may be highly susceptible to continuous corona or partial discharges when operated at very low pressure gaseous environments, because the corona, or breakdown initiation voltage, is a function of both the density and content of the gaseous environment. For example, helium has a much lower breakdown voltage at low pressures than air or nitrogen. The insulated and non-insulated conductors, terminations, and other electrical/electronic parts may be susceptible to this phenomenon in the high field stresses caused by the dense population of parts within the system design. Some insulation systems, however, can endure partial discharge or corona activities for microseconds to milliseconds, for thousands of repetitive occurrences, as experienced with pulse power applications.

Electrical and electronic equipment used in space applications should be designed to operate over a range of pressures and temperatures from sea level conditions to the space environment. Most terrestrial low-voltage equipment can be designed to meet the sea-level requirement by using conformal coatings on all parts and boards and by using properly spaced parts and circuits. However, at low-pressure or vacuum conditions, these techniques may not be applicable. Hence, spacecraft equipment designs should consider rarefied gas or air as an essential packaging design criterion. Lightweight, small volume packaging dictates that circuitry operating in rarefied air may require special consideration, such as pressurization or encapsulation. Gas-filled packages require conformal coatings to prevent corrosion, voltage breakdown, and flashover between closely spaced electrodes when operated at higher voltages. Furthermore, many equipment failures are caused by corroding circuitry related to exposure to wide temperature ranges, humid environments (manned spacecraft), contamination (collection and deposition of debris, oils, and dirt), or a very dry, hot environment (unmanned spacecraft) while operating. Additionally, delamination of insulating materials has also caused problems. When designing high-voltage systems for space applications, these issues also should be addressed.

4.1 Background

Electrical insulation research and development for electrical and electronic equipment is a continuing process for applications in manned and unmanned spacecraft. The initial studies and test evaluations began following World War II and continue for modern aerospace equipment. All of the testing techniques and procedures for the data presented herein were initiated in the early 1950s and should continue well into the 21st century.

Some of the better insulation compositions containing asbestos were deleted from use in space programs in the 1960s but may be reinstated for very special applications in the future. Although mica is a material with excellent electrical, temperature, and chemical characteristics, it is difficult to apply to long, thin conductors at present; therefore, most electrical insulating materials consist of organic, inorganic, and glass fiber composite insulation systems. Among these, most organic composite materials have an upper long-life temperature limit of less than 260 °C. While this temperature range is adequate for some space applications (e.g. avionics), for many others their use may be limited. The electrical and electronics industries have been making concerted efforts to reduce the weight and size of parts in their various systems, as time and technology progress. Along with this, the insulation on flat and round conductors has been reduced to a minimum that can provide the necessary mechanical, chemical, thermal, and electrical characteristics.

One other major concern with space power systems is the life of the insulation, because servicing a high-voltage system in space would be a challenging task and systems insulation should have life similar to the spacecraft itself. The true rating for an insulation system is the voltage at which the insulation life becomes infinite on a voltage-time curve as determined experimentally. If an excessively high voltage is applied to the insulation system repeatedly, the life will be shortened. There is a much lower voltage at which the life becomes infinite. This is the voltage at which the curve becomes asymptotic to the lifetime axis. In some insulation systems, it is often noted that

the rated voltage, as determined by the lifetime curve, is also the corona inception (or initiation) voltage (CIV). System operation above the CIV seriously degrades the insulation life. This implies that to ensure maximum life, there must be no corona or partial discharges in the system.

For given applications, a shorter-than-maximum life may be acceptable. However, other important secondary factors related to corona and transients include radiated and conducted EMI, production of ozone and other noxious gases, and power loss associated with the partial discharge energy. This implies that a calculation of the corona inception voltage for a given insulation system is a logical approach in determining a maximum voltage rating for a given system.

4.2 Partial Discharges, Corona, and Other High Voltage Phenomena

By nature, any discharge or breakdown taking place in the bulk of the insulation without bridging the electrodes is termed partial discharge. Potential sites of such discharges are voids or gaseous inclusions in the bulk of solid insulation or in bubbles in liquid dielectric material (e.g. transformer oil), which could be distributed randomly either because of natural defects or by way of manufacturing. A partial discharge is the breakdown of such a void between two surfaces with a voltage difference between them.

When an electric field is applied in a gas-filled region, no current flows, apart from capacitive current, unless there are free electric charges present. When the applied electric field strength is low, the current flow is usually related to external sources and is not sufficient to cause any partial discharges. However, at higher applied electric field strengths, the free charged particles can gain energies from the field, resulting in ionization of the gaseous species by elastic or inelastic collisions. In gaseous environments and uniform fields, buildup of charge leads to an unstable situation, in which the current increases very rapidly while the applied voltage collapses. This usually results in a discharge bridging the electrode gap. However, in a highly non-uniform field, the charges can form a kind of electrostatic shield around the electrode where the electric field strength is greater and, therefore, causes quenching of the self-sustained discharge. The resulting discharge does not bridge the gap and usually is called the corona discharge. Further, this discharge may be either pulsating or continuous, and the average current may be relatively low (in the milliamperage range).

In practice, the term “corona” is often used interchangeably with the term “partial discharge.” However, corona is local ionization of a gaseous medium caused by a high electric field stress around a point or wire, whereas partial discharge occurs in a void or bubble in the dielectric material or insulation.

The voltage threshold for corona initiation is dependent upon multiple factors:

- a. Gas density.
- b. Size of the bubble or gap.

- c. Shape of electrodes or void.
- d. Impedance of solid insulation.
- e. Nature of gas or gas mixture in the bubble or gap.
- f. Thickness of insulation.

The voltage at which a partial discharge starts, however, does not depend on the type of the bulk of the dielectric material but on the stress in the cavity (shape dependent) and the breakdown strength of the cavity (type of the gas species; density dependent). Since cavity shape and characteristics of the gas inside it cannot be predicted precisely, the partial discharge initiation voltage predictions are relatively more difficult than corona initiation predictions.

5. ENVIRONMENTS

5.1 Introduction

Some spacecraft systems, including high-voltage components, are contained in sealed pressure vessels, effectively isolating the system from the external environment. In this case, the environment is part of the system design and accounts for high voltages present. Pressurization is often considered impractical because it requires heavy, tight enclosures with special high-quality seals. Nevertheless, when this approach is taken, one can assume that significant high-voltage interactions will not occur; therefore, this case is not considered further in this NASA Technical Handbook.

In general, a spacecraft's interaction with its environment is of paramount concern for spacecraft design and operation. High-voltage systems require special precautions because of the ever-present possibility of gas discharge phenomena. The following are outlined in this section:

- a. The ambient or natural environments that a spacecraft will encounter.
- b. The induced environment resulting from modifications that the vehicle makes to its own environment.
- c. The electromagnetic effects resulting from sources internal or external to the spacecraft.

5.1.1 Ambient Environment

The dominant environment between 100 and 1000 km altitude is the neutral atmosphere. In this essentially collisionless regime, the gases are in hydrostatic equilibrium. Below about 100 km, where the atmosphere is homogeneous, the composition is approximately 80 percent nitrogen (N₂) and 18 percent oxygen (O₂) with traces of nitrogen dioxide (NO₂), argon (Ar), and other gases. Above 100 km, atomic oxygen, which is made from the photo dissociation of molecular

oxygen (O_2), comes to dominate. Above about 800 km, the atmosphere is largely atomic hydrogen (H). At a 500-km altitude, the number density of neutral species varies from 2×10^6 to $3 \times 10^8 \text{ cm}^{-3}$, depending on the level of solar activity and position in the orbit. The kinetic temperature of the gas is usually between 500 and 2000 K, and the ambient pressure is in the range of 10^{-10} to 5×10^{-8} Torr.

The neutral gas environment has been well explored and quantified. Empirical models based on in situ neutral composition and satellite drag measurements have evolved over the years into reliable predictors of the average composition and thermal structure of the thermosphere. The most notable of these models are the Mass Spectrometer Incoherent Scatter (MSIS) model (Goddard Space Flight Center (GSFC)) based on in situ satellite observations of neutral concentrations, the Marshall Space Flight Center (MSFC) version of the Jacchia model derived from satellite drag measurements, and the United States (U.S.) Standard Atmosphere (National Oceanic and Atmospheric Administration (NOAA)). These models provide good estimates of the thermosphere environment as functions of altitude, longitude, latitude, local time, magnetic activity, and solar activity and are continually updated as new information becomes available. Of particular interest is AIAA standard Guide to Reference and Standard Atmosphere Models, which provides guidelines for selected reference and standard atmospheric models including consideration of their content, uncertainties, and limitations.

5.2 Contamination-Induced Environment

A spacecraft never operates in a clean environment. The environment in which a spacecraft operates is a combination of the ambient and various gaseous components originating from outgassing and other contamination sources from the vehicle itself. Outgassing from the spacecraft structure and its subsystems begins to rapidly increase from the moment of launch, while the ambient pressure quickly decreases from sea-level atmospheric pressure (760 Torr) to that of orbit ambient pressure (less than 10^{-6} Torr). This external pressure change takes only a few minutes, whereas the pressure next to the spacecraft surface and the spacecraft interior pressure will remain at a higher pressure throughout the life of the spacecraft, because of the outgassing of electrical, structural, and purging systems aboard the spacecraft.

5.2.1 Implications of Spacecraft Internal Pressure

Vacuum is normally considered an excellent insulator. In fact, the theoretical dielectric strength of dry air at a pressure of 10^{-6} Torr is greater than $5 \times 10^5 \text{ V/cm}$, a value 16 times the dielectric strength of air at sea level. This is because there are few charge carriers, and the mean free path of electrons exceeds the gap length between closely spaced electrodes. For internal volumes of a spacecraft and even for external adjacent spaces, such vacuum conditions are seldom achieved. The designer should assume, therefore, that the environment is characterized by a low-pressure gaseous environment.

In a typical case, a system can be described as a vented enclosure within which sources of gas production will reach equilibrium with venting. Sources include the following:

- a. Leakage from pressure vessels and onboard propellant tanks.
- b. Periodic operation of purge systems.
- c. Continuous outgassing of materials, cabling, insulation, and electronic equipment.

It has been observed in the past that these sources are capable of maintaining a spacecraft pressure of about 0.01 Torr for several minutes to hours even though the external pressure is less than 10^{-6} Torr. Figure 1, Spacecraft Internal Pressure, shows data for a particular spacecraft (Sutton and Stern, 1975).

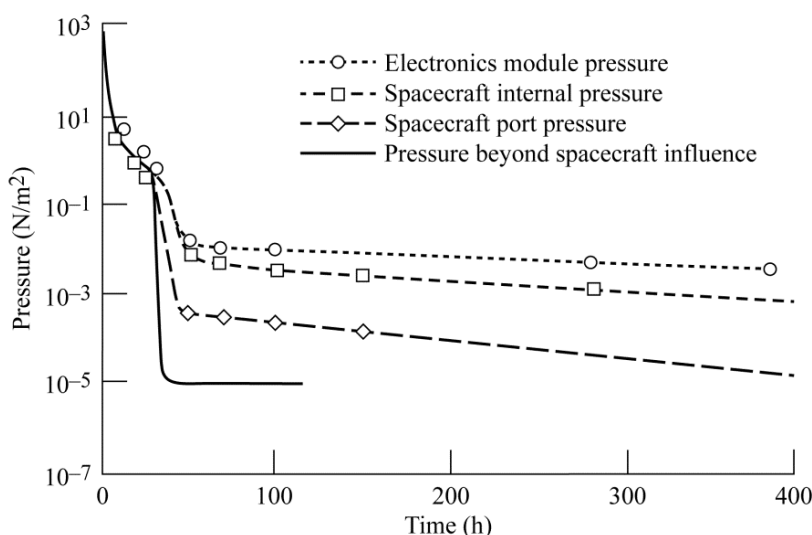


Figure 1—Spacecraft Internal Pressure

One aspect of electronic design that is easily overlooked is the provision for partial discharges and voltage breakdown at low gas pressures. Enclosed electronic equipment with restricted venting, which delays outgassing, may be a cause of faults within high-voltage equipment.

5.2.2 Estimating Internal Gas Pressure

During the boost phase, most of the gas escapes rapidly from the spacecraft interior for the first 30 km into space, while continuum flow exists. During this interval, the interior pressure of the spacecraft is nearly the same as the external pressure. As the spacecraft continues on its projected course, its internal pressure will be greater than the external pressure. This is because of slow outgassing and venting through small orifices, tubes, and cracks for gases entrapped in electrical and thermal insulation and structural materials.

There are several ways to calculate the internal gas pressure and flow rates through the openings, cracks, or orifices for a spacecraft. Depending on the gas density, these calculations can be in the

NASA-HDBK-4007 W/CHANGE 2

molecular flow region, viscous flow region, or transition region (Dushman and Lafferty, 1965). For a spacecraft with small amounts of outgassing products and operating in a low-pressure environment, the flow can be characterized as molecular flow because the mean free path of the molecules is much larger than the dimensions of the orifice or the openings. Then, the gas flow can be calculated by the Clausing equation (Dushman and Lafferty, 1965).

$$C = 3638K A \left(\frac{T}{M}\right)^{1/2} \quad (Eq. 1)$$

where

C is the flow conductance of the orifices in cm^3/s

A is the total area of the orifices in cm^2

T is the internal temperature in K

M is the molecular weight of the gas in g/mole

K is a dimensionless function of orifice (tube) length over diameter and is tabulated in (Dushman and Lafferty, 1965).

In this simplified form of the Clausing equation, the parameter 3638 has the units

$$\text{cm}\cdot\text{s}^{-1}(\text{gm}/(\text{T}\cdot\text{mole}))^{1/2}$$

and accounts for the Boltzmann constant, the conversion from mass to molecular weight, and absorbs several dimensionless integers. This equation can be used for estimating the flow of gas from chamber to chamber in a multiple chamber vacuum system.

Scialdone (1974) calculated and measured spacecraft compartment and equipment outgassing rates. He showed that the depressurization time constant τ is V/C , where τ is the time for the pressure to decrease to 36 percent of its initial pressure, V is the volume in cubic centimeters, and C is the flow conductance for the orifices in cubic centimeters per second, given by

$$C = \frac{1}{4} \bar{v} A k \quad (Eq. 2)$$

where

$$\bar{v} = \left(8 \frac{kT}{\pi m}\right)^{1/2} \text{ cm/s (molecular flow speed)}$$

A_k is the area of the k orifices in square centimeters

m = mass of the gas molecule in grams

k is the Boltzmann constant

Air and nitrogen have a time constant of approximately 0.4 s when bled through a 1- cm^2 opening in a steel sphere (Scialdone, 1969). NASA experience (Sutton and Stern, 1975) has shown that a 0.1 time constant ensures adequate outgassing around high-voltage circuits.

These equations work well with known vent port sizes, spacecraft sizes, and non-outgassing parts. Most spacecraft, however, have thermally insulating coatings, fibrous insulation,

electrically insulated parts, semi-shielded boxes, and boxes within modules. In addition, compressed gases for orbit adjustment are carried and released. With these complexities, it is more appropriate to qualify the design by testing the completely assembled spacecraft. This can be done in a thermal vacuum chamber to measure the real internal and external spacecraft pressures and the outgassing rate, instead of relying on calculated outgassing values for the system integrity.

5.2.3 Outgassing Through Multilayer Insulation

Multilayer thermal insulation may be necessary within a spacecraft design. In this case, caution should be taken, because the outgassing rates for multilayer insulation are different from the outgassing (or venting) through orifices. This can be seen in an experiment performed using 100 layers of super insulation across the center of a vacuum chamber. The chamber was pumped only from the side labeled Volume A in figure 2, Effects of Thermal Insulation on Outgassing Rate (Dunbar, 1988), while Volume B was isolated by the layered insulation. During the initial pumpdown, gas exhibited bulk flow through interstitial spaces in the insulation. As a result, during the first 15 min of pumpdown, the pressure in the chamber dropped from sea-level pressure to 0.1 Torr, with the gauge on the thermally insulated side of the chamber following pump pressure within 5 percent. As the pump pressure dropped further, entering the high vacuum regime, the pressure on the insulated side of the chamber decreased very slowly as gas was released into the chamber by purging and outgassing from the many layers of insulation. This experiment shows clearly that designers who specify such insulation to control radiative transfer need to be aware of the lengthy time required to eliminate both trapped and adsorbed gas. Should high voltage be present in the affected part of the system, such gas might pose a breakdown threat during the purging process.

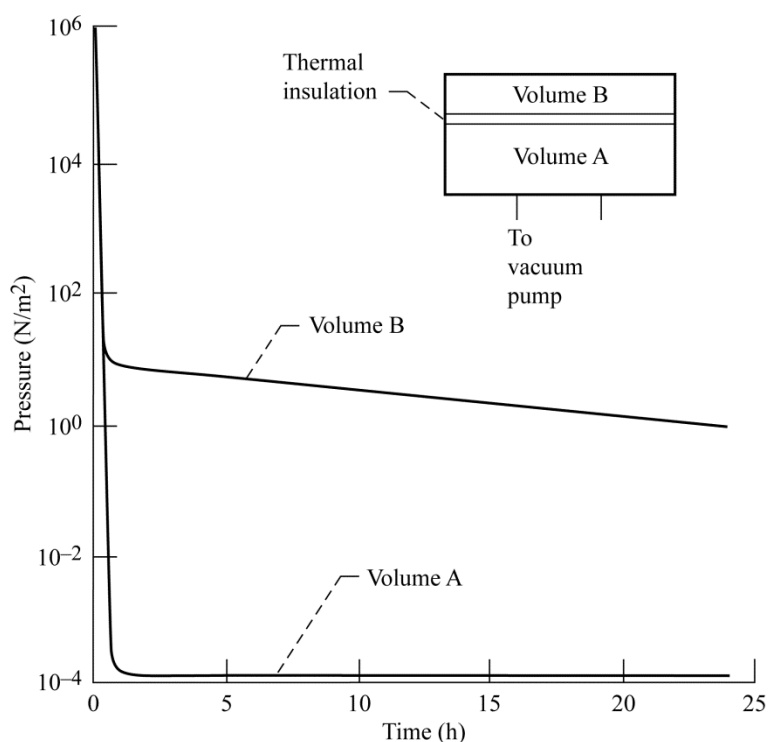


Figure 2—Effects of Thermal Insulation on Outgassing Rate

In the Apollo telescope mount of the Skylab spacecraft, the area of the outgassing ports was approximately 1 sq. cm per liter volume, the value recommended for adequate spacecraft outgassing for high-voltage experiments and equipment onboard Skylab. The resulting pressures are summarized in figure 3, Gas Pressure Inside the Apollo Telescope Mount (Dunbar, 1973). The Apollo telescope mount volume included several hundred feet of Teflon[®]-insulated instrumentation and low power wiring, plus the telescopes and ancillary electronic equipment. Wiring requires significant time for purging since the entrapped gas has to travel up to half the length of the wire to escape from each end. Clamping can further restrict the gas flow within the electrical strands.

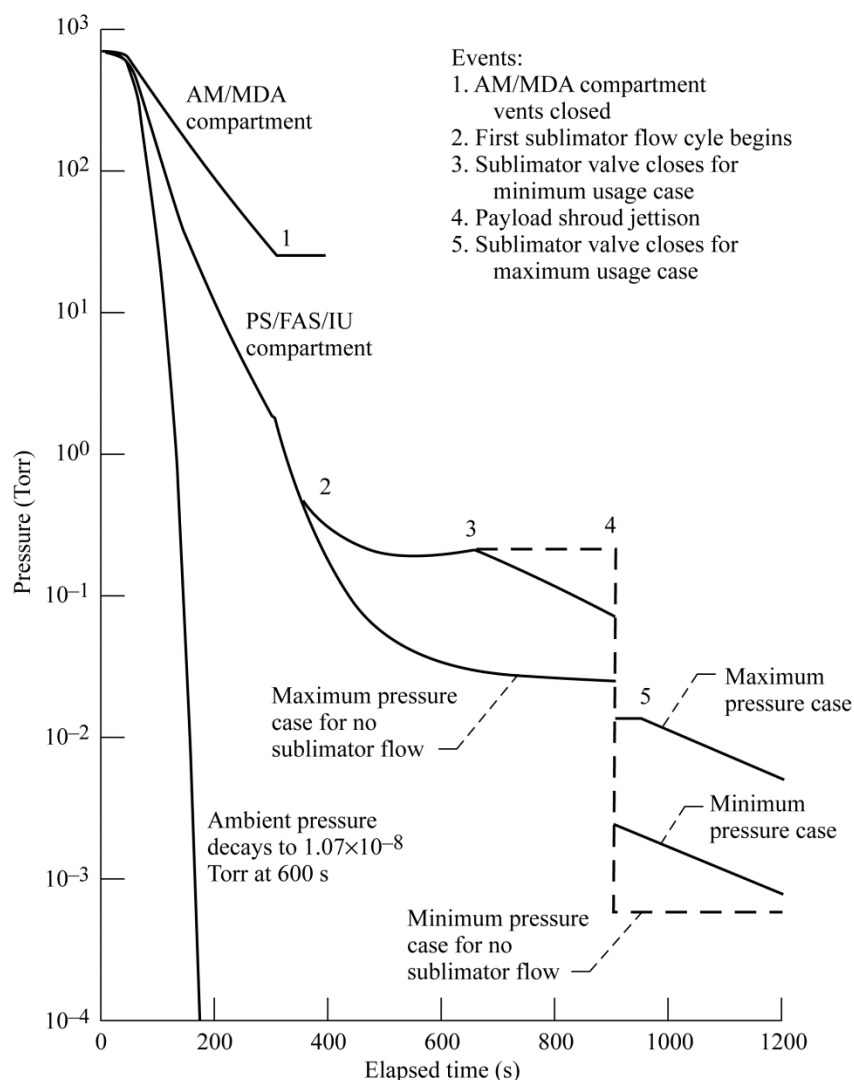


Figure 3—Gas Pressure Inside the Apollo Telescope Mount

The Skylab space vehicle had several separate modules, including the airlock module (AM), multiple-docking adapter (MDA), and the payload shroud/fixed airlock shroud/instrument unit (PS/FAS/IU). During launch, the vent valves were purposely left open to allow modules to outgas freely. The module internal pressure was allowed to outgas to a minimum pressure of 25 Torr. At that time, the multiple docking adapter vent was closed; the remaining vent valves remained open as shown in figure 3. As the Skylab proceeded toward space, at time 600 s after lift-off, the external (space) pressure was 1.07×10^{-8} Torr, but the internal pressures remained above 10^{-3} Torr for 20 min. The module internal pressure as a function of time is shown in figure 4, Pressure in Airlock Module Truss Compartment. The sublimator pressure pulses shown in figure 4 had a flow rate of 0.01156 lbm/s for 300 s per pulse.

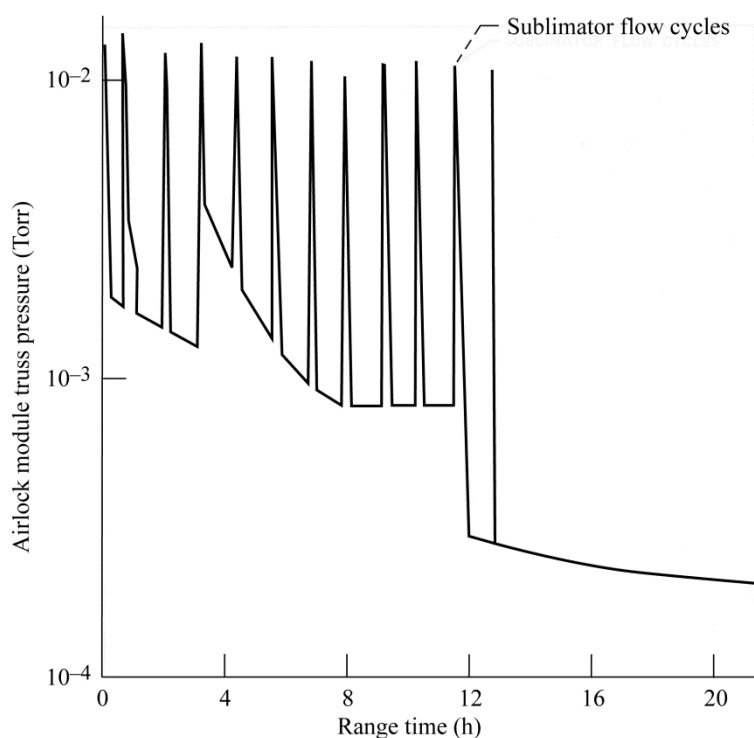


Figure 4—Pressure in Airlock Module Truss Compartment

Foams can be used in electrical and electronic equipment as dielectric material or supporting (cushioning) material. These foams are very porous, however, and contain large volumes of captured gas. Since outgassing is very slow and becomes a constant contamination source in vacuum, use of these foam materials should be avoided in high-voltage systems. The equation to calculate the diffusion coefficient (D) for a foam can be found in work by Cuddihy and Moacanin (1965) when needed. They also found that the calculated values for outgassing rates in polyurethane foam used for electrical/electronic insulation were within a factor of 2 of experimentally measured values (Cuddihy and Moacanin, 1965). Furthermore, Scannapieco (1970) gives the outgassing rates of spacecraft materials as a function of temperature and effects of outgassing on voltage breakdown.

The super insulation, Apollo telescope mount, and polyurethane foam tests discussed above show that the spacecraft internal pressure may be significantly greater than the external pressure for several days after orbital insertion. Furthermore, outgassing products within a high-voltage module may keep the pressure near the minimum breakdown potential region for safe, reliable operation of high-voltage circuits, making it advisable to delay their turn on. Likewise, the outgassing products of the spacecraft and reaction control propellants increase the pressure in the vicinity of the spacecraft as shown in figure 1.

5.2.4 Suborbital Flights

Suborbital spacecraft have all the short-time outgassing problems of orbital spacecraft, except that the electronics have to operate from Earth's surface, to apogee, and back to Earth's surface. For example, the X-33 experimental spacecraft was designed for a flight profile commencing at Earth's surface, progressing to a maximum apogee of 150,000 ft altitude, and returning to Earth. Maximum external pressure of the vehicle would be as great as 760 Torr at launch (Earth's sea-level average pressure). Minimum external airframe pressure would be that of maximum apogee or less than 0.01 Torr.

A very good example of the outgassing rates for several modules aboard the Beam Experiments Aboard a Rocket (BEAR) spacecraft is reported by Nunz (1990). An example of outgassing is shown for the BEAR space orbiter electronics compartment in figure 5, Payload Pressure for a Vented Payload During Launch. The curve designated as region 2 in figure 5 was for an electronic component facing space with the side of the spacecraft open to space. In 10 min time, the pressure remained at 0.05 Torr, that is, BEAR had a large outgassing area compared to the total surface area. The curve designating the diagnostic region, containing wiring and many components inside a semi-enclosed compartment, is shown to have had pressure greater than 0.5 Torr for the full 10 min flight time. In addition, there were no purge gases supporting the pressurization of BEAR. Some suborbital vehicles will have purge gases. Based on the BEAR pressure profile and continuous outgassing, it is estimated that the pressure around all components and wiring within the confines of the air frame will have pressure greater than 0.1 Torr for a suborbital flight duration. Figure 5 can be found in Nanevics and Hilbers (1973).

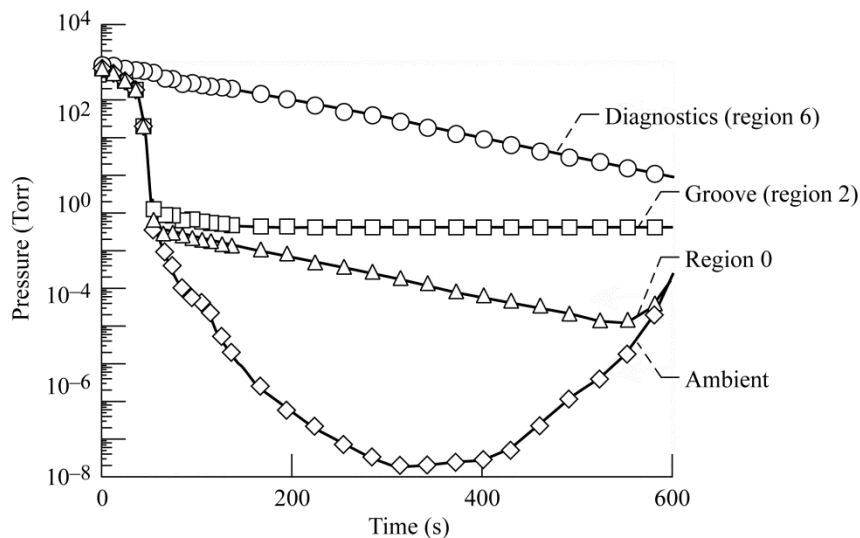


Figure 5—Payload Pressure for a Vented Payload During Launch

Similar data exists for the Space Power Experiments Aboard Rockets (SPEAR) series of experiments. The SPEAR Program (completed in 1994) included 3 tests finishing with a high

voltage rocket launch (SPEAR 3). The series tested a variety of very high voltage methods for using the vacuum as an insulator. See Rustin et al (1993) and Cohen et al. (1995).

5.2.5 Gas Purges, Leakage, and Contamination

Outgassing products come from many sources, such as entrapped air, pressurizing gases in the compartments that escape by laminar gas flow, continuous leakage of hydrogen or helium through tank walls, nitrogen purges of the electronics bay, and the outgassing of parts and components.

Before launch, purges with dry nitrogen are often conducted to remove residual air, moisture, and external debris. Helium has also been used as a purge gas; however, compared to other gases, it has a very low breakdown voltage when depressurized and exacerbates the corona problem. When helium gas is chosen as the purge gas, a significant amount of residual helium will be trapped in the porous insulation, such as fiberglass, and inside some electronic components and parts, such as transformers and power conversion equipment, during the first flight. Subsequent flights will commence with a higher helium content in the air-helium gas mixture. This can result in continual corona inside or between components following initiation for the duration of the flight.

A nitrogen purge is preferred to a helium purge. Nitrogen is plentiful and cost effective and has a breakdown voltage similar to that of air, which is higher than the helium breakdown voltage. A small amount of air mixed with nitrogen (less than 5 percent air) gives the mixture approximately the same breakdown and corona inception characteristic as that of pure air. It is impossible, therefore, to completely void the airframe with a single nitrogen purge. From a voltage breakdown or CIV initiation characteristic, a purge with nitrogen is recommended. The voltage breakdown characteristics of air, helium, hydrogen, and nitrogen are shown in table 1, Paschen Law Breakdown Voltages at the Critical Pressure-Spacing Dimension for Select Gases at dc and 400 Hz.

Table 1—Paschen’s Law Breakdown Voltages at the Critical Pressure-Spacing Dimension for Select Gases at dc and 400 Hz

GAS	BREAKDOWN VOLTAGE	
	dc (V)	ac (V)
Air	327	230
Helium	189	132
Hydrogen	292	205
Nitrogen	265	187

5.2.6 Outgassing of High-Voltage Circuits

High-voltage circuits used in testing usually heat up during operation. When heated, local pressure will increase by outgassing of conformal coatings frequently used in such circuits, potentially resulting in partial discharges. As an example, it was observed in a sensitive photomultiplier circuit that a mere increase in temperature from 0 to 15 °C raised the ambient gas pressure to the extent that the partial discharge counts increased from 10 to 1000 times normal (Dunbar, 1973). This is shown in figure 6, Partial Discharge Counts Measured in a Sensitive Photomultiplier Circuit (Dunbar, 1973), where corona-pulse count increases with temperature.

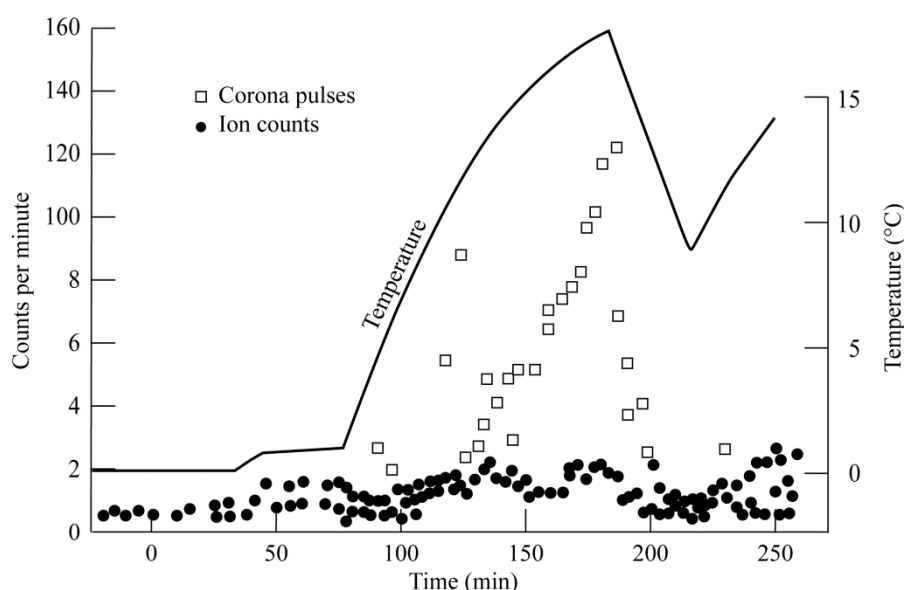


Figure 6—Partial Discharge Counts Measured in a Sensitive Photomultiplier Circuit

Neglecting these partial discharges is a risk to design. All circuits should be tested at operating temperatures and pressures with sensitive instruments. When signals from high-voltage circuits show unexplained or unpredicted noise, especially if the noise is temperature dependent, the engineer should carefully investigate possible partial discharge activities within the circuitry. Such partial discharge will initially produce only noise, but in time, the conformal coating may crack or debond, exposing a bare electrode that would then provide a supply of free electrons, resulting in system failure.

Cracks, voids, and improperly bonded surfaces account for most failures within totally encapsulated circuits. An example of an improperly bonded surface on a capacitor is shown in figure 7, Delaminated High-Voltage Capacitors (Dunbar, 1983). Applying high voltage to the capacitor will ionize the gas in the crack, heating the gas and the insulation surfaces, and further increasing the outgassing rate. Gas escaping from the cracks alters the pressure-spacing dimension, generating circuit noise. Continuous partial discharges eventually overheat the insulation, enlarge cracks, and ultimately can produce voltage breakdown.

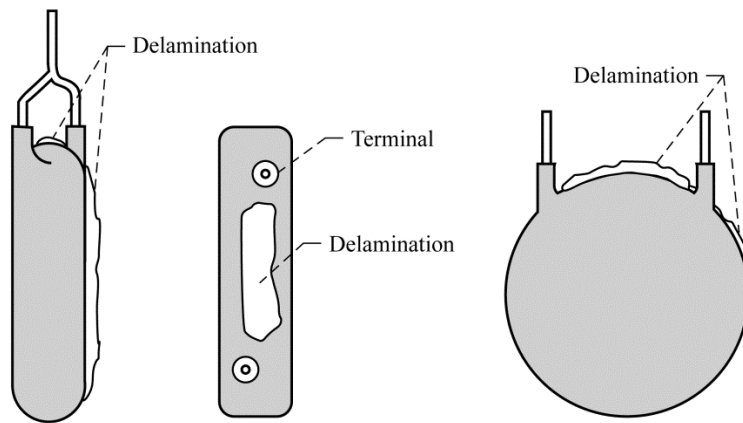


Figure 7—Delaminated High-Voltage Capacitors

Fillers are sometimes added to an encapsulant to enhance structural strength. For example, if the filled encapsulant is poured over a coil winding or over the end of a stranded wire, voids will be created, usually either between windings or between the windings and metal core where partial discharges can occur. Figure 8, *Insulation Deterioration on the Coil Winding*, shows the resulting deteriorated insulation on the coil winding. The figure shows a cut away view of an encapsulated coil at three different magnifications. The clear region around the coils indicates that the potting compound merely covered the wires without penetrating the regions between them, creating a void chamber in which the charged conductors can interact through Paschen discharge. The outer surface of the insulation is only slightly pervious to the products of internal outgassing and will allow the internal pressure to rise toward the Paschen minimum for the spacing involved. Initially, most voids are between 1×10^{-3} cm (0.4 mil) and 5×10^{-2} cm (20 mil). The pressure at the Paschen minimum for these voids is between 20 and 750 Torr. This pressure can be sustained with continuous outgassing through infinitesimal outgassing ports.

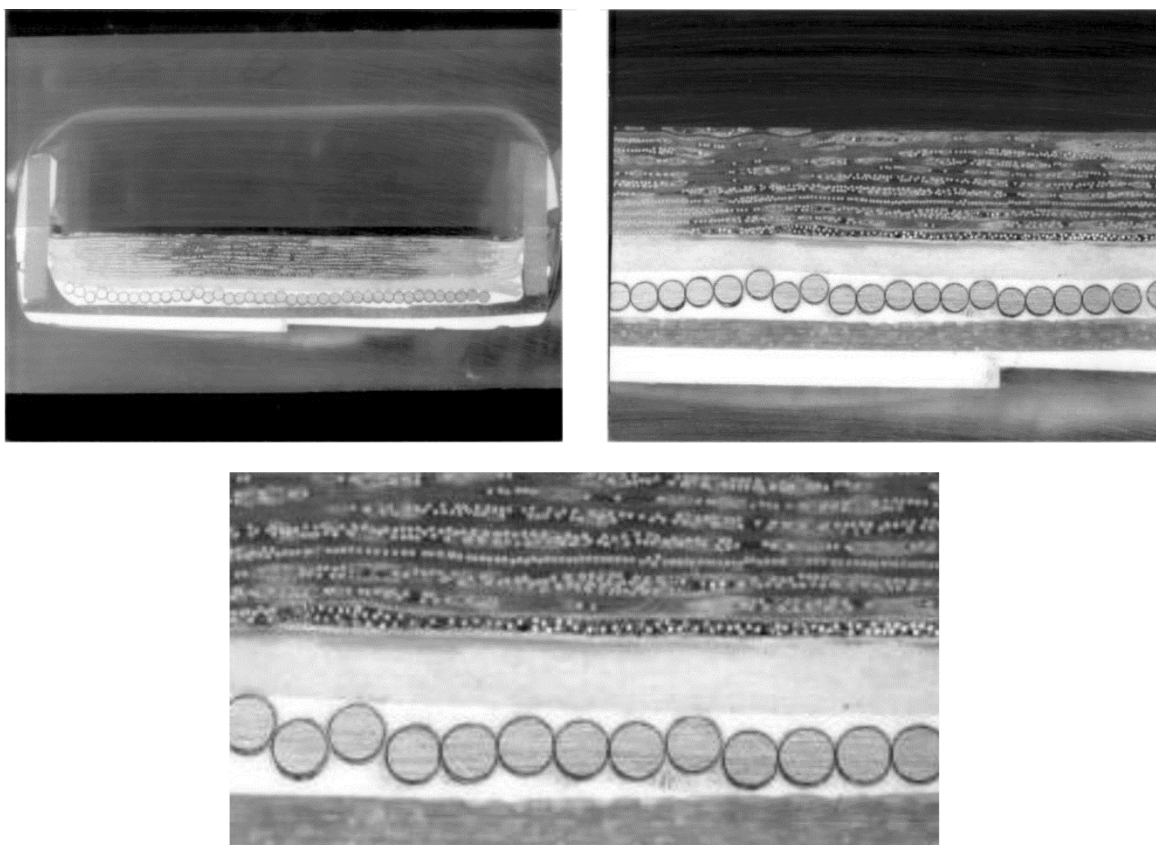


Figure 8—Insulation Deterioration on the Coil Winding

A development test should be made to prove that the encapsulation process has successfully precluded voids, cracks, and improperly bonded regions. For transparent encapsulants, it is recommended that sample discs of the potting material be poured. Cracks, voids, and delaminations are easily detected through a polarizing lens. Translucent and opaque materials require either a destructive examination or a very sensitive measurement of partial discharges.

5.3 Electromagnetic Environment

While the chief concern for the designer is usually the contamination that results in a system-induced environment, there is another concern that, in many cases, will be more important. It is generally assumed that circuit and surface potentials present throughout the system at all times are known in advance because of design. Electromagnetic effects on systems and spacecraft surfaces can dramatically alter these potentials, leading to achievement of CIV and subsequent breakdown. In this section, we review electromagnetic effects on systems and spacecraft surfaces.

5.3.1 Triboelectric Charging

Triboelectric charging occurs whenever two dissimilar materials come in contact with each other and then separate. One material pulls charges (mainly electrons) from the other, leaving the first one (the one with the excess electrons) with a positive charge and the second with a negative charge. An example of this occurs when a space vehicle flies through moisture containing ice crystals. The ice crystals lose electrons to the spacecraft. As a result, the spacecraft ends up with a large negative potential because of the accumulation of this negative charge (Tanner and Nanevich, 1961). As more ice particles impinge upon the surface of the spacecraft, charge will accumulate until the corona threshold is exceeded. Then, corona may initiate, with the corona discharge current equaling the charging current. It is a good approximation to regard triboelectric charging as a constant current source.

Vehicle charging resulting from triboelectrification can be detrimental when the vehicle skin is composed of dielectric or dielectric-coated sections, in contrast to a metal skin. Charge accumulated on a dielectric material cannot easily flow away from the point of deposition. Charge thus accumulates on the surface until the electric field along the surface is large enough to support a streamer discharge over the dielectric surface to a nearby metal structure. If the dielectric strength of the insulator is exceeded before the streamer occurs, however, then the charge may be relieved by a spark discharge that punctures the dielectric and travels to an underlying conductor. Streamer discharges, like spark discharges, seek the lowest impedance path to the vehicle structure. During the course of its operational life, a spacecraft may encounter a number of sources of triboelectric charging. Natural sources include cosmic dust and micrometeoroids while manmade sources arise from materials spalled by cosmic dust impacts with spacecraft surfaces, outgassing products, and small particles arising from various orbital debris interactions.

Since windshields and windward-facing windows are made of insulating materials, similar effects occur with them as with other dielectric materials. Streamer discharges from windshields and windows are a source of radio frequency (RF) noise (Rupke, 2002).

5.3.2 Rocket Motor and Jet Engine Charging

Exhaust from the rocket motors and jet engines may not be considered a detrimental effect. Before any conclusive measurements on rockets were made, it was assumed that the rocket engine could have one of three effects on the electrostatic potential of the spacecraft:

Case a.—If the engines were capable of charging the vehicle to the potentials above the vehicle threshold potential, then corona discharges and EMI would accompany each launch. (This is the worst-case scenario.)

Case b.—When the conductivity of the exhaust is sufficient to limit the vehicle to some value below the corona threshold potential, then there will be no corona discharges or associated EMI related to engine charging. Other charging sources, however, still could cause corona discharge.

Case c.—If the rocket engine exhaust was so effective a discharger that the vehicle would be held below the corona threshold even when other charging sources were present, then the rocket engine would tend to alleviate, rather than aggravate, the vehicle charging problem. (This is a positive effect.)

From measurements made on Titan III C rockets, however, it was found that rocket engine exhaust is an excellent discharger (Case c) (Nanevich and Hilbers, 1973). Similarly on Voyager (and many other spacecraft) it was reported that the rocket exhaust could be “heard” in the VHF antenna experiment due to a global discharge of the spacecraft when the engines were fired. Jet engine exhaust, being at a lower temperature, corresponds to the second possibility (Case b).

Nonetheless, discharges in the exhaust occurring as a series of discrete impulses of short duration and rapid rise time related to turbulence are able to produce RF noise over a broad spectrum. This interference may disable radio receiving systems and, in some cases, may induce spurious pulses in the electronic systems controlling stage sequencing and vehicle guidance.

5.3.3 Discharges Caused by Improper Grounding

One other place where the effect of vehicle charging can be damaging is where the conducting sections of the vehicle are not properly connected together. For example, when a rocket vehicle is charged triboelectrically on the forward surfaces and discharged from the skirt at the aft end and the forward section is not electrically connected to the aft section, then charge acquired on the forward section cannot flow to the aft section freely. Thus, the vehicle is differentially charged, unless the potential difference between the sections becomes large enough for a spark discharge to occur. This electrical isolation occurs as a result of improper electrical connection at the interface of two sections. When a spark or arc discharge event takes place between differentially charged sections, it may be destructive, depending on the magnitude of the discharge.

These spark discharges can be quite energetic, since the capacitance between the sections may be several thousand picofarads and the sparkover voltage may be several kilovolts. Furthermore, the spark discharges will seek the easiest electrical path between the sections. If there is some electrical wiring routed across this gap, it is possible that the spark will travel through a shorter gap from the front section to the wiring and then through another short gap to the aft section. This, of course, would put a tremendous noise pulse on any data line. Also, there is the possibility that these spark discharges could fire electro-explosive devices when they are onboard and in the vicinity of the sparkover site. In the past, electro-explosive devices on rockets have occasionally been initiated by corona or streamer discharge (Bennett, 1968). The development of the current NASA Standard Initiator (NSI-2) included prevention of such initiation as a priority design goal (Roberts Research Laboratory, June 1988). This effort was successful as more than 20 years of experience with this NSI has shown no problems with electrostatic discharge initiation. For other electro-explosive devices, discharges between unbonded sections especially present a real danger; therefore, proper connection between sections of the spacecraft is essential.

5.3.4 Staging Effects

It had been conjectured that electrostatic discharges could occur between stages as they are separated. In fact, it was shown that the separation of two dissimilar objects could cause substantial voltage difference between the bodies (Haffner, 1966). Experiments by Nanevicz and Vance (1966) have shown, however, that the two parts of the staging vehicle will be electrically connected through the conductive exhaust plume as long as the motor plume is in contact with the expended stage. It does not seem conceivable that significant differences in potential, that is, more than a few tens of volts, can be developed between separating sections during a staging event in which the upstage motor is ignited at or before the time of stage separation. For launch vehicle designs where tens of seconds can pass between stage separation and upper stage ignition (e.g., Saturn 5), engineers must be aware of the electrostatic risk.

5.3.5 Coating Insulators and Windshields

It has been found that a high-resistance conductive coating over the dielectric surface is quite effective in eliminating streamers and the noise they cause. The conductive coating drains away the charge as rapidly as it arrives and prevents the electrostatic potential buildup, which can produce streamer discharges. The coatings (Schmitt, 1972) used for nontransparent dielectrics are usually opaque and have a surface conductivity (the inverse of surface resistivity) on the order of a $1 \text{ M}\Omega^{-1}$. Most windshields are made of either glass or acrylic plastics. Glass has a lower surface resistivity ($1 \times 10^{12} \Omega$) than the acrylics ($1 \times 10^{16} \Omega$). This is attributed to the open silica network in glass that allows hydration. It has been shown that a surface resistivity of $1 \times 10^8 \Omega$ is sufficient to bleed off accumulating charge (Schmitt, 1972).

The principal coating currently used for glass outer panels is indium tin oxide (ITO). ITO can be fused into the glass exterior surface to sufficient depth that erosion should not seriously reduce the conductivity of the external surface coating during the life of the windshield.

5.3.6 Antenna Placement With Respect to Dischargers

The proper choice of antennae and their placement can provide significant suppression of corona-generated noise. In one case involving a loop antenna on an aircraft, it was shown that correct placement reduced the noise factor by 25 dB (Tanner and Nanevicz, 1961). It was further shown that at least 25 dB of noise suppression can be obtained with dipole antennas if two of them are correctly placed and balanced.

5.4 References

5.4.1 Government Documents

None.

NASA-HDBK-4007 W/CHANGE 2

5.4.2 Non-Government Documents

AIAA. *Guide to Reference and Standard Atmosphere Models*, (2004). NSI/AIAA G-003B-2004.

Bennett, J (June 1988). *Pyrotechnic System Failures: Causes and Prevention*. NASA TM 100633. Washington, DC: National Aeronautics and Space Administration.

Cohen, Herbert A.; Lehr, F. Mark; Engel, Thomas G. (1995). *SPEAR II: High Power Space Insulation*. Lubbock, TX: Texas Tech University.

Cuddihy, E.F.; Moacanin, J. (1965). *Outgassing Rates in Polymeric Foams*. Report Nos. JPL-TR-32-840 and NASA CR-69727. Pasadena, CA: Jet Propulsion Laboratory.

Dunbar, W.G. (1973). *Skylab High Voltage Systems Corona Assessment*. Paper presented at the 11th Electrical/Electronics Insulation Conference. Chicago, IL.

Dunbar, W.G. (1983). High Voltage Design Guide. Report No. AFWAL-TR-82-2057-VOL-4. Wright-Patterson Air Force Base, OH: Air Force Wright Aeronautical Laboratory.

Dunbar, William G. (August 1988). Design Guide: *Designing and Building High Voltage Power Supplies, Volume 2; Topical Interim Report*. Report No. AFWAL-TR-88-4143-Volumes I and II. Wright-Patterson Air Force Base, OH: Air Force Wright Aeronautical Laboratories.

Dushman, Saul; Lafferty, James M. (1965). *Scientific Foundations of Vacuum Technique: Second Edition*. New York, NY: John Wiley & Sons, Inc., p. 93.

Haffner, J.W. (December 1966). *The Generation of Potential Differences at Stage Separation*. Report No. JPL-TM-33-280. Pasadena, CA: Jet Propulsion Laboratory.

Nanevicz, J.E.; Vance, E.F. (June 1966). *Rocket Motor Charging Experiments Scientific Report No. 2*. Report No. AFCRL-66-497. Menlo Park, CA: Stanford Research Institute.

Nanevicz, J.E.; Hilbers, G.R. (July 1973). *Titan Vehicle Electrostatic Environment; Final Report*. Report Nos. SRI Project 8428 and AFAL-TR-73-170. Menlo Park, CA: Stanford Research Institute.

Nunz, G.J. (1990). *Beam Experiments Aboard a Rocket (BEAR) Project, Volume 1*. Report Nos. LA-11737-MS-VOL-1 and BEAR-DT-7-1. Los Alamos, NM: Los Alamos National Laboratory.

Roberts Research Laboratory (June 1988). *Final Report on Contract NAS 9 – 17249 Development and Verification of NASA Standard Initiator – 2 (NSI -2)*. NASA CR-172069. Washington, DC: National Aeronautics and Space Administration.

APPROVED FOR PUBLIC RELEASE—DISTRIBUTION IS UNLIMITED

NASA-HDBK-4007 W/CHANGE 2

Rupke, E. (March 2002). *Lightning Direct Effects Handbook*. Report AGATE-WP3.1-031027-043. Lightning Technologies Inc., Pittsfield, MA

Rustan, P., et al. (1993) "High Voltages in Space. Innovation in Space Insulation", IEEE Trans. on Elec. Insulation, 28, No. 5, 855-865.

Scannapieco, J.F. (June 1970). *The Effects of Outgassing Materials on Voltage Breakdown*. Published in Proceedings of the Second Workshop on Voltage Breakdown in Electronic Equipment at Low Air Pressure, March 1969; Report No. JPL TM 33-447. Pasadena, CA: Jet Propulsion Laboratory, pp. 203.

Schmitt, George F., Jr. (December 1972). "Conductive Polymeric Coatings for Combined Anti-Static Properties and Erosion Resistance." In 1972 *Lightning and Static Electricity Conference*. Report No. AFAL-TR-72-325. Wright-Patterson Air Force Base, OH: Air Force Avionics Laboratory, pp. 88.

Scialdone, J.J. (August 1969). *Internal Pressures of a Spacecraft or Other System of Compartments, Connected in Various Ways and Including Outgassing Materials, in a Time-Varying Pressure Environment*. Report No. NASA TM-X-63869. Washington, DC: National Aeronautics and Space Administration.

Scialdone, J.J. (April 1974). *The Outgassing and Pressure in a Spacecraft*. Paper presented at the Cost Effectiveness in the Environmental Sciences; Proceedings of the Twentieth Annual Meeting. Institute of Environmental Sciences, Washington, DC, pp. 164-169.

Sutton, J.F.; Stern, J.E. (April 1975). *Spacecraft High Voltage Power Supply Construction*. Report No. NASA TN D-7948. Washington, DC: National Aeronautics and Space Administration, p. 39.

Tanner, R.L.; Nanevich, J.E. (April 1961). *Precipitation Charging and Corona-Generated Interference in Aircraft*. Report No. AFCRL 336, Contract AF 19(604)-3458, Technical Report 73. Cambridge, MA: Air Force Cambridge Research Laboratory.

6. INTERACTIONS

6.1 Introduction

In the previous section, we reviewed the basic environments that are important to the designer. In this section, we will characterize the interactions that result when high-voltage systems are exposed to these environments. In the following sections, we will review electromagnetic fields within materials, break-down phenomenon in gaseous and solid media, and cover interactions of high-voltage systems with a plasma environment typical of Earth orbits.

6.2 Electric Field Configurations

Selection of electrical components and their mounting configurations are critical to a high-density, high-power packaging design. For high-voltage equipment, additional emphasis should be placed on electromagnetic field stress and material selection and application. The following section gives an overview of electromagnetic field calculations for common geometry in electric power system construction.

6.2.1 Field Stress Calculations

To select and design insulation for electrical equipment properly, it is often essential to make plots of the field distribution. As technology advances, the structures become more and more complicated and analytical methods to calculate the electric field lines and potential gradients become less effective. Therefore, numerical methods are being developed to calculate field lines and potential gradients. Currently, there are many computer package programs to simulate electromagnetic fields for a given structure. These programs operate based on either finite-element or finite-difference techniques. Also researchers have developed in-house computer programs to meet specific applications.

These field-plotting techniques are used to determine the maximum stress value in the configuration for both operating and test voltages. From the breakdown field (E_s) for an insulating medium, the breakdown voltage (V_s) can be approximately calculated from the relationship (Ryan, 1967 and Ryan and Walley, 1967):

$$V_s = \eta g E_s \quad (Eq. 3)$$

where

g is the electrode separation

η is the utilization factor, defined as the ratio of average to maximum gradient in the gap.

In practice, for the breakdown voltage calculation, η is numerically equal to the required voltage de-rating, because it is equal to the ratio of the field stress between parallel plates and the maximum field at the smaller electrode of a non-uniform configuration with identical spacing. For the breakdown voltage calculation, E_s is usually taken as the breakdown field in the uniform field case.

For simple applications for most frequently used configurations, plots of the utilization factors as a function of electrode spacing are shown in figure 9, Utilization Factor for Various Electrode Configurations (Dunbar, 1988), for several electrode geometries.

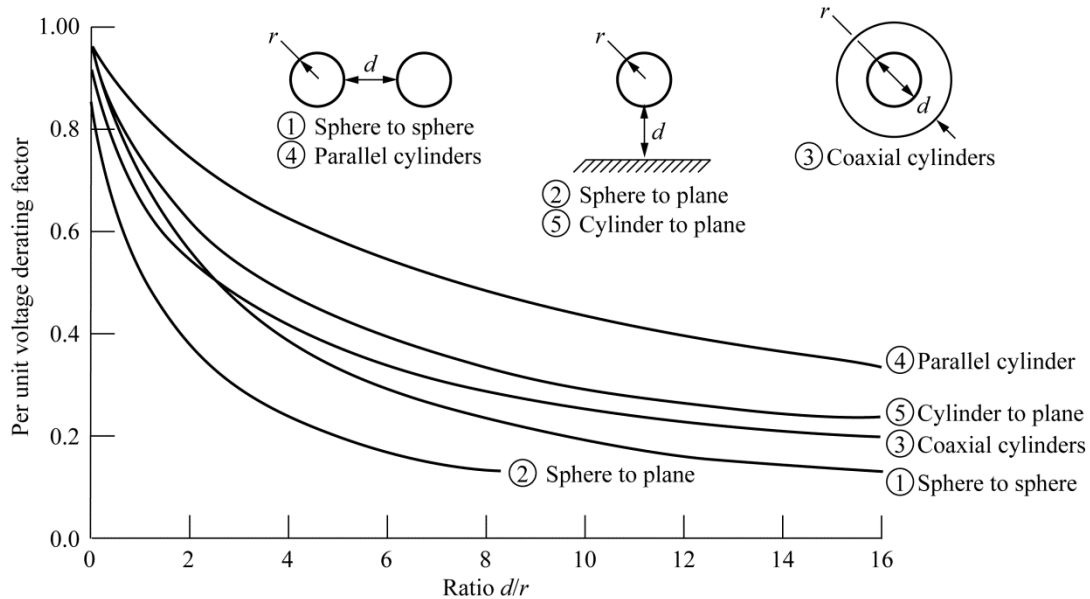


Figure 9—Utilization Factor for Various Electrode Configurations

The utilization factor, which provides a way to estimate quickly the maximum field stress of a configuration, can also be used to estimate the minimum electrode radius for a given spacing when the electrical stress capability of the dielectric is known. The utilization factor is numerically equal to the required voltage de-rating of a configuration. In equation form, it is

$$\eta = \frac{E}{E_m} < 1 \quad (Eq. 4)$$

where

E is the local electric field strength between two electrodes spaced at some distance apart (for example, in kV/mm)

E_m is the maximum electric field strength within the space between two conductors spaced at some distance apart (for example, in kV/mm).

A treatise on electric field theory can be found in most texts on electricity and magnetism or fields and waves. Von Hippel (1954), Greenfield (1972), and Schwaiger and Sorensen (1932) have written texts on dielectrics that explain the basic principles from field theory. A small sample of the many relevant texts describing field plotting and analysis are those by Moore (1927a and 1927b) Bewley (1948), Smythe (1968), Stratton (1941), and Weber (1950).

6.2.2 Configurations

For electrodes of any given shape, the variation in potential as a function of the distance from one electrode to the other electrode can be calculated by solving the differential equations for the electrostatic field. For simple geometries, such as parallel plates, concentric spheres, and coaxial cylinders, the equations for the field strength (Schwaiger and Sorensen, 1932) are given below:

- a. Parallel plates

$$E_x = \frac{V}{s} \quad (Eq. 5)$$

where

E_x is the voltage gradient at a distance x between the electrodes in V/cm

V is potential at the electrodes in volts

s is the spacing between the electrodes in cm

- b. Concentric spheres

$$E_m = \frac{V}{r_1} \frac{r_2}{r_1 + r_2} \quad (Eq. 6)$$

where

r_1 is the inner sphere radius

r_2 is the outer sphere radius both in cm

The maximum field gradient E_m is at the surface of the inner (smaller) sphere.

- c. Coaxial cylinders

$$E_m = \frac{V}{r_1 \ln \frac{r_2}{r_1}} \quad (Eq. 7)$$

where

r_1 is the inner cylinder radius

r_2 is the outer cylinder radius both in cm

E_m is the maximum field gradient at the inner conductor surface in V/cm

d. Sphere-gap

$$E_m = \frac{V}{x} \left(\frac{r+x/2}{r} \right) \quad (Eq. 8)$$

where

r is the radius of the spheres (cm)

x is the distance between them (cm)

This is the case where two spheres are located side by side with a gap between them.

e. Parallel cylinders

$$E_m = \frac{V}{2r} \left(\frac{1}{\cosh^{-1} \left(\frac{(s/2)-r}{r} \right)} \right) \quad (Eq. 9)$$

where

r is the radius of the cylinders

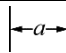


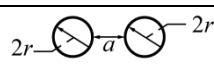
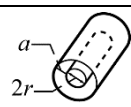
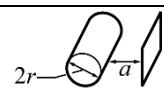
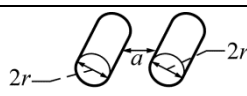
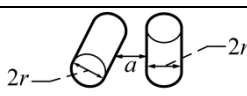
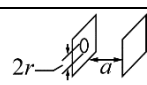
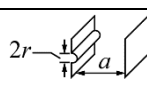
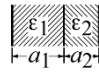
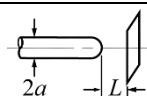
s is the distance between them

6.2.3 Empirical Field Equations

An empirical field equation or formula is the shortened, simplified form of a complex equation. Complex equations, manageable with computers, have traditionally been viewed as difficult and time consuming to use in everyday design work, especially if the design has to be assembled piecewise. This is changing with the availability of considerable computing power even in mobile devices suitable for field work. It is still sometimes advantageous to use empirical equations for first-order estimations. Furthermore, maximum stress is often the only value needed in a design, and the plotting of the complete field using a complicated equation is not necessary. Empirical equations for the maximum field stresses at the smaller electrode spacing for several electrode configurations are given in table 2, Maximum Field Strength (E_m) with a Potential Difference (V) Between the Electrode Configurations (Bowers and Cath, 1941).

NASA-HDBK-4007 W/CHANGE 2

Table 2—Maximum Field Strength (E_m) With a Potential Difference (V) Between the Electrode Configurations

CONFIGURATION		FORMULA FOR E_m
Two parallel plane plates		$\frac{V}{a}$
Two concentric spheres		$\frac{V}{a} \cdot \frac{r+a}{r}$
Sphere and plane plate		$0.9 \cdot \frac{V}{a} \cdot \frac{r+a}{r}$
Two spheres at a distance from each other		$0.9 \cdot \frac{V}{a} \cdot \frac{r+a/2}{r}$
Two coaxial cylinders		$\frac{V}{2.3 r \ln \frac{r+a}{r}}$
Cylinder parallel to plane plate		$0.9 \cdot \frac{V}{2.3 r \ln \frac{r+a}{r}}$
Two parallel cylinders		$0.9 \cdot \frac{V/2}{2.3 r \ln \frac{r+a/2}{r}}$
Two perpendicular cylinders		$0.9 \cdot \frac{V/2}{r \ln \frac{r+a/2}{r}}$
Hemisphere on one of two parallel plane plates		$\frac{3V}{a}$; where $a \gg r$
Semi-cylinder on one of two parallel plane plates		$\frac{2V}{a}$; where $a \gg r$
Two dielectrics between plane plates		$\frac{V \epsilon_1}{a_1 \epsilon_2 + a_2 \epsilon_1}$
Point and plane, where $(L/a) = 160$		$\frac{0.605V}{a}$

Electrical stresses calculated with these equations are within 10 percent of values obtained from analytical solutions. Empirical equations for sparkover gradients in air and sulfur hexafluoride are published by Mattingley and Ryan (1973) for the configurations shown in figure 9. As an example, the sparkover electric field for parallel cylinders, at atmospheric pressure in air, was found to be equal to:

$$2.98 \left(1 + \frac{0.96}{\sqrt{r}} \right) \quad (Eq. 10)$$

where

r is the radius of the cylinders (same for both cylinders) and is $0.098 \leq r \leq 4.64$ mm.

6.2.4 Voltage Distribution in Gas Surrounding Solid Dielectrics

In solids, as in gases, the start of repetitive ionization is the beginning of dielectric breakdown. Since solid insulation generally has much greater dielectric strength than gaseous insulation, corona is expected to occur first in the gas surrounding a homogeneous solid dielectric supporting the electrodes. The CIV in gases can be determined by using established breakdown curves for various gap distances and electrode configurations because the measurements in the literature show that the breakdown voltage of a gas in a uniform field is the same as the CIV for that gas. However, an electrical system is composed of gaps or voids, dielectric material supporting the electrodes, and electrode material, forming various shapes and electric field distribution within. Then, the problem is establishing the applied voltage distribution between the gas and solid portions of the dielectric to predict breakdown threshold voltages. This complex structure can be modeled in terms of capacitors in series with different dielectric constants to evaluate the overall system's dielectric strength. Table 2 shows the potential of two dielectrics between parallel plates. The potential of capacitors in series can be determined using this information.

The voltage applied to two insulated wires is divided into three components as the voltage across each wire's insulation and the voltage across the space between the insulation. This voltage distribution is unlike that encountered in series capacitors where the voltage across the air capacitor is proportional to the voltage across the solid-insulation capacitor for all applied voltages. With parallel wires, the thickness of the insulation is constant around the wire, but the thickness of the gap between wires varies from a minimum in the space between the wires to a maximum from the far side of one conductor to the far side of the other conductor. This results in a nonlinear electric field as shown in figure 10, Typical Field Plot of Conductors Showing Curvilinear Squares from Intersecting Equipotential and Field Lines (MSFC-STD-531).

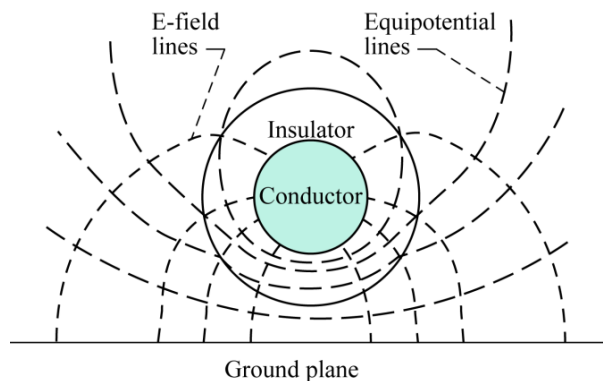


Figure 10—Typical Field Plot of Conductors Showing Curvilinear Squares From Intersecting Equipotential and Field Lines

6.2.5 Wire Configurations

Round, solid-insulated conductors have a unique field stress, which depends upon the insulated conductor's construction and its position with respect to a ground plane. In the case where there is an air spacing between two solid-insulated round conductors, the electric field configuration is more complicated, especially as the gas density decreases to a value where the Paschen minimum is reached. For example, for an insulated wire next to a ground plane, the minimum spacing will be the thickness of the insulation to the ground plane; for a twisted pair configuration, the minimum spacing will be twice the thickness of the insulation. Depending on the operating pressure, the possible breakdown paths, which correspond to the Paschen minimum, are shown in figure 11, Cross-Sectional View of Twisted-Pair Wire and Wire-to-Ground Configurations Showing Possible Corona Sites at High Pressure (shorter path) and Low Pressure (longer path) (MSFC-STD-531, High Voltage Criteria).

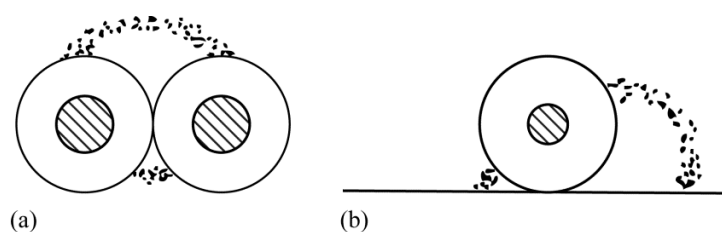


Figure 11—Cross Sectional View of (a) Twisted-Pair Wire and (b) Wire-to-Ground Configurations Showing Possible Corona Sites at High Pressure (Shorter Path) and Low Pressure (Longer Path)

6.3 Breakdown of Gases

Electrical breakdown of gases occurs as a result of collisions between electrons and gas molecules in the presence of an electric field. After the primary collisions produce new electrons and ions, these charged particles will gain energy from the field. If the field exceeds some threshold potential, a fully developed discharge will be established within the electrodes as electrons multiply through collisions with the molecular gas. Additional electrons are produced from charged particles colliding with the electrode surfaces. The result will be a fully developed gaseous discharge. The initiation of this discharge is usually referred to as “the electrical breakdown” or “gaseous breakdown.”

6.3.1 Paschen's Law

Paschen's Law states that the breakdown voltage of a gas in a uniform field is constant if the product (pd) (where p is the gas pressure, and d is the distance between spaced parallel plate electrodes), is held constant (Paschen, 1889; Meek and Craggs, 1978). Paschen's Law dictates that for all gases, the function $V = f(pd)$ has a typical form with a distinct minimum. Gas breakdown voltage has been shown to also be affected by electrode material and configuration, and by operating temperature. Paschen's Law is valid over a wide pressure region, except pressures beyond 2 to 3 atm and pressures below 10^{-7} Torr (Von Hippel, 1954). Note for highest

accuracy, at an absolute temperature T (in K) differing from room temperature ($T_0 = 293$ K), the breakdown voltage should be read at the abscissa value of $(pd) \times (T_0/T)$ (Kind and Karner, 1985). As gas pressure is increased from standard temperature and pressure, the breakdown voltage is increased because at higher gas densities the molecules are closer together, and a higher electric field is required to accelerate the electrons to ionizing energies within the mean free path. The breakdown voltage decreases as gas density is decreased from standard temperature and pressure because the longer mean free path permits the electrons to gain more energy before a collision. As density is further decreased, the voltage decreases until it reaches a minimum value. When the density is further decreased, the breakdown voltage starts to increase because the density of the gas is not sufficient to sustain a chain reaction of any ionization at that potential. Finally, the pressure (therefore, the density) becomes so low that most electrons travel from one electrode to the other without colliding with a molecule. Examples of Paschen curves for several gases are shown in figure 12, Breakdown Voltage of Several Gases as a Function of pd at Room Temperature (Dunbar, 1988).

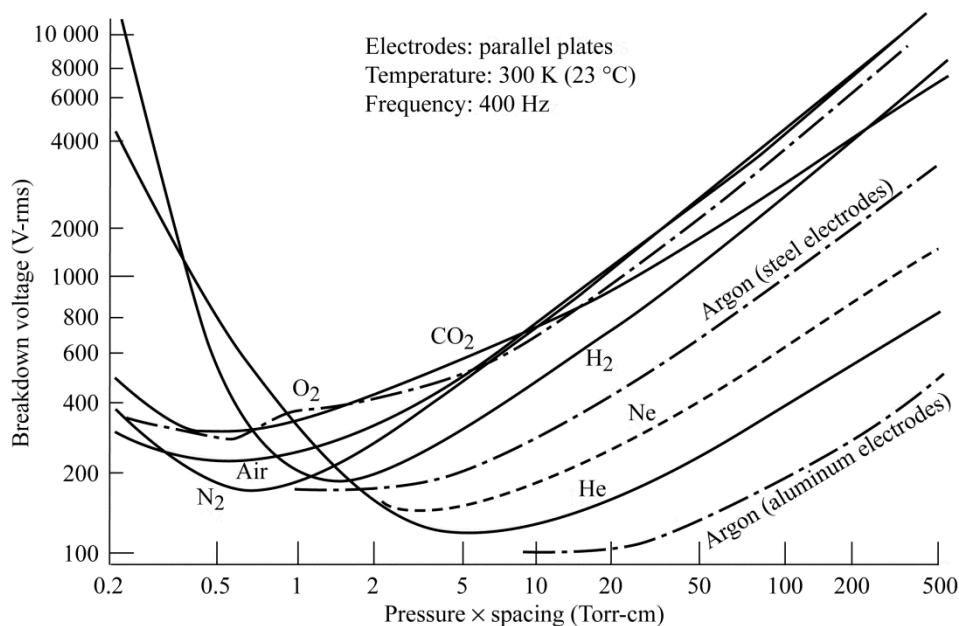


Figure 12—Breakdown Voltage of Several Gases as a Function of pd at Room Temperature

In some cases, there will be a gas other than pure air surrounding the wire, cables, parts, and components. Pure air has a relatively high CIV characteristic for either coated or insulated conductors that allows transients of 320 to 350 V-peak to exist in a corona-free region, depending on insulation thickness and dielectric properties. Other pure gases such as helium, hydrogen, and nitrogen or mixtures of one or more of these gases with air during a purge may result in a lower breakdown voltage characteristic, since the breakdown characteristic is also a function of the gas composition as well as the pd values. The breakdown voltage of helium as a function of the product pd is shown in figure 13, Paschen Curve of Helium as a Function of pd at Room Temperature. A mixture of 10 percent hydrogen in air will have a breakdown voltage of

0.91 times that of pure air, as shown in figure 14, Breakdown Voltage of Hydrogen-Air Mixture as a Function of Hydrogen Percentage in Air.

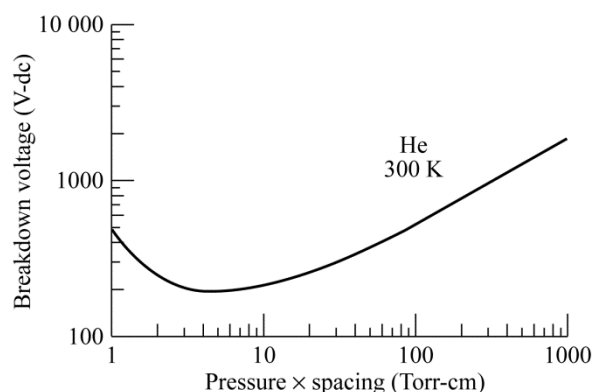


Figure 13—Paschen Curve of Helium as a Function of pd at Room Temperature

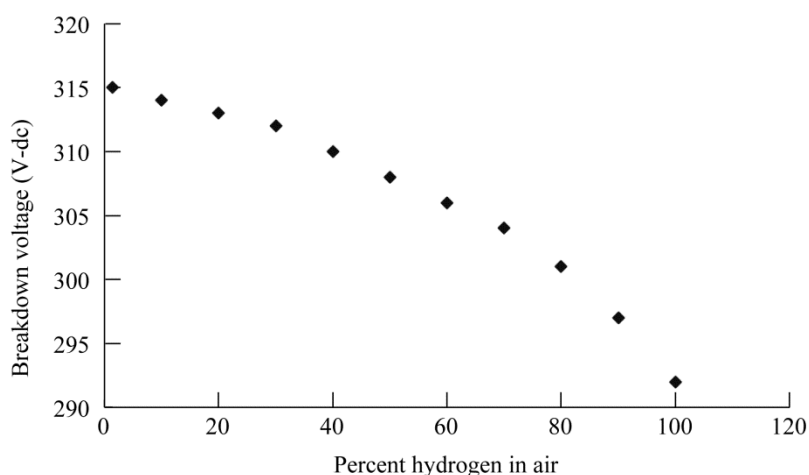


Figure 14—Breakdown Voltage of Hydrogen-Air Mixture as a Function of Hydrogen Percentage in Air

The Paschen minimum voltage for air, which is 327 Vdc, occurs at a pd dimension of 0.7 Torr-cm at room temperature (23 °C). Wires and parts may have spacing from less than 0.1 mm to a few centimeters, depending upon the construction, application, location, and shielding requirements. This implies that some parts within the electrical system may be subjected to either voltage breakdown, corona, partial discharges, or glow discharges when the space vehicle is at altitudes greater than approximately 12.19 km (40,000 ft) during launch and approximately 9.15 km (30,000 ft) during reentry. The reason for the lower altitude during reentry is the higher temperature and inhibited airflow into the compartments during reentry.

Where possible, it is advisable to design high voltage systems so that the separation between high voltage surfaces is smaller than the electron mean free path for a collision. The pressure

corresponding to minimum CIV depends on the spacing of the electrodes. For a 1-cm spacing in air at room temperature, this pressure occurs between 0.5 and 1.0 Torr. A representative minimum CIV for air is 327 Vdc. In comparison, the CIV for the same contact configuration at 760 Torr (1 atm) is 31.2 kV.

In general, for each electrode spacing there is a unique pressure at which minimum CIV occurs as shown in figure 15, Corona Onset Voltage Between Parallel Plates at Several Spacings (Dunbar, 1966). Thus, the minimum CIV will occur over a wide range of altitudes in the electrical system on a space vehicle having many components with a variety of spacing between conductors, contacts, and terminations. The minimum pd dimension is constant for a wide pressure variation and for many spacings inside a space vehicle. Since the CIV and breakdown voltage of a gas are functions of gas density and spacing (pd), the corona or breakdown can start when the pressure between closely spaced (2 mils or 5.1×10^{-3} cm) electrodes is as high as 125 Torr and continues through to the longest distance between an energized electrode and a ground plane, until a pressure of less than 0.02 Torr (spacing = 20 cm) is obtained (Dunbar, 1966). Initially this appears extreme until the designer can visually observe the length of the breakdown path between an electrode on a card and the furthest metal ground plane.

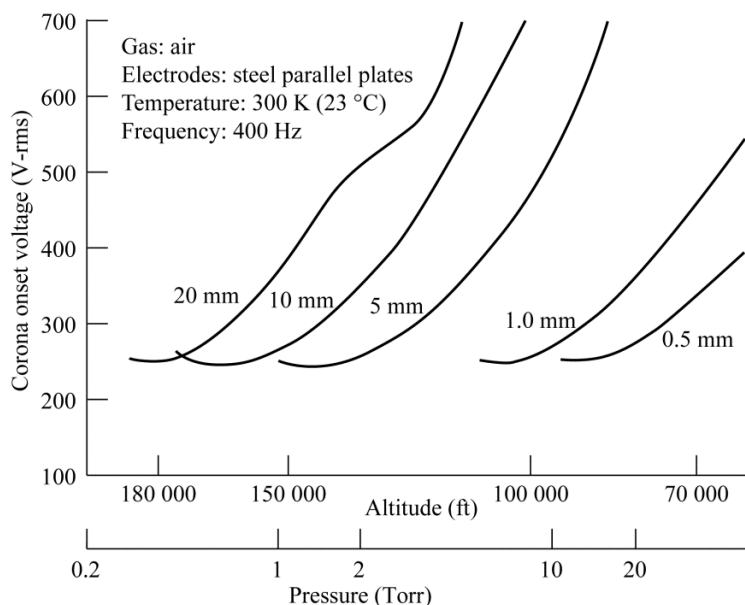


Figure 15—Corona Onset Voltage Between Parallel Plates at Several Spacings

It should be noted that the pressure between electrodes is different from the external pressure and would be greatly reduced through ventilation as the vehicle is traveling between Earth and space. In some instances, the time lag can exist until well after the vehicle reaches orbit altitude because of outgassing of insulation and containers within the vehicle.

6.3.1.1 External Radiation Effects

Corona, under normal conditions, has no well-defined starting voltage because its initiation may depend on an external source of ionization as well. There is generally a time delay between the application of voltage and corona. This time delay varies statistically and is a function of the difference between the applied voltage and the critical voltage. Ultraviolet (UV) and high-energy radiations reduce the time delay considerably.

Below the critical voltage, there is a potential (V_g) where pulses of corona start but are not self-sustaining, hence are extinguished. The region from V_g to the critical voltage is called the Geiger-counter regime (Loeb, 1965). The frequency of the pulses in this region generally depends on the intensity of the external ionizing agents present.

When radioactive cobalt-60 or a gamma emitter is used as an ionizer, it affects corona in three ways. First, it lowers the CIV of the gaseous environment slightly; second, it raises the intensity of the intermittent corona; and third, it may alter the mechanical and electrical properties of the insulation to make the material either more or less corona resistant. Irradiated polyethylene is an example of a material that is changed by radiation to be more corona resistant. Its increased corona resistance after irradiation results from an increase in ability to shrink and bond to itself to form a structure with fewer voids (Von Hippel, 1954). Radiation effects on dielectric materials are investigated by Stojadinovic et al. (2001); Mackersie et al. (2001); Amjadi (2000); Krieg et al. (2000); Given et al. (2000); and Lee et al. (2000).

6.3.1.2 Temperature Effects

In the space environment, the ambient temperature variation can be large because of solar heating effects. The onboard instrumentation and power systems are designed to operate in this wide ambient temperature range, typically from negative 55 °C to positive 155 °C for vehicles in low Earth orbit. In addition to this ambient temperature variation, the instruments can see local temperature changes related to dielectric losses, partial discharges, corona discharges, electrical breakdown, or fully developed arc or glow discharges. This section discusses testing needed to ensure that high voltage systems can operate under conditions of significant temperature excursion. Failure to do so is potentially catastrophic since the physical effects discussed with respect to test will also occur in operations.

The test conditions for simulating a given operating altitude and temperature can be calculated by using the relationship derived from the ideal gas law as

$$P_t = P_0 \frac{T_t}{T_0} \quad (Eq. 11)$$

where

T_0 is room temperature in K (293K)

T_t is operating temperature of the equipment in K (maximum temperature of the equipment)

P_0 is nominal operating pressure in Torr

P_t is test chamber pressure in Torr

Also, the breakdown voltage may be related to temperature and altitude by using the U.S. Standard Atmosphere—Pressure chart, which gives the air-density factor as a function of altitude. Thus, for corona test purposes, it is possible to simulate any altitude and temperature in a room-temperature chamber containing gas at an appropriate pressure. However, this simulated test environment ignores higher order effects from chemical and thermal dielectric deterioration, which would occur at a temperature other than room temperature.

The CIV and corona extinction voltage (CEV) are key parameters used to determine the likelihood of corona, glow discharge, or electrical breakdown. Any sustained discharge will heat the gas locally (around conductors) as well as in enclosed spaces (voids). The resulting temperature rise will change the extinction voltage, thus giving inconsistent results. This effect has less impact in the vicinity of the Paschen minimum. Readings at higher pd values will be influenced by temperature rise during the test. When testing for partial discharges in voids of solid dielectrics, internal temperature rises because of sustained discharges affecting CIV and CEV. When the walls of the void are heated by dielectric losses, the insulation outgases, changing the gas pressure and possibly the gas mixture inside the void. This affects the voltage difference between the CIV and CEV across a simple void in a solid dielectric, resulting in test results that are not representative of operational conditions. When testing for pd or corona, test engineers must keep in mind that testing itself can temporarily alter the sample. Caution should be taken to obtain valid data.

For example, the CIV data as a function of gas pressure and temperature for round nichrome wires having two different fixed spacings are shown in figure 16, Corona Between Nichrome Wires in Heated Chamber (Dunbar, 1988), and figure 17, Corona Initiation Voltage as a Function of Temperature and Pressure for Parallel Wires in a Heated Chamber (Dunbar, 1988). The test data indicate a small variation in the minimum CIV at temperatures between 500 and 1100 °C but little or no change from 23 to 500 °C.

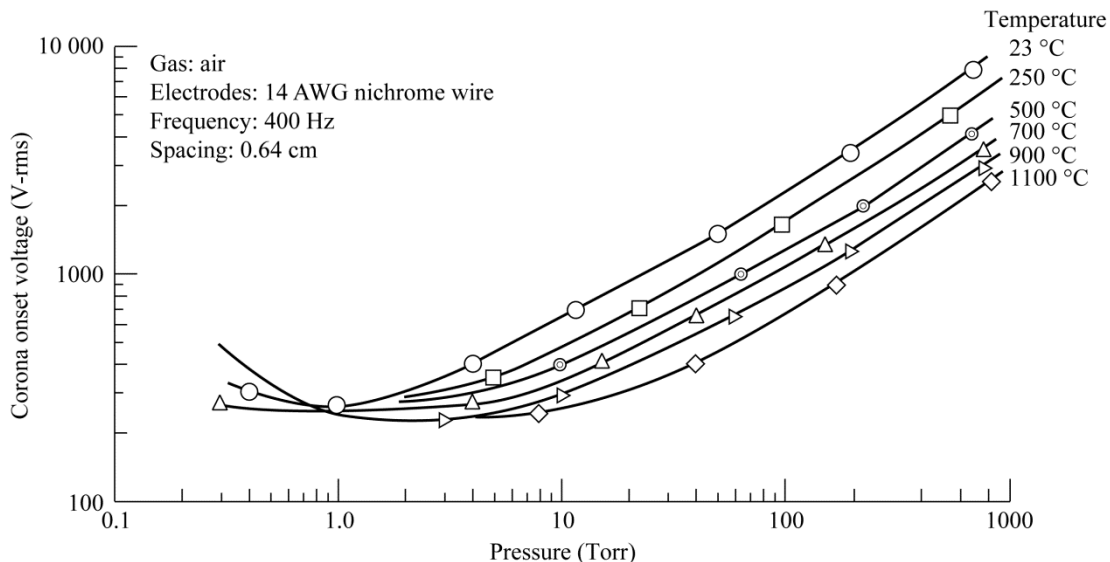


Figure 16—Corona Between Nichrome Wires in Heated Chamber

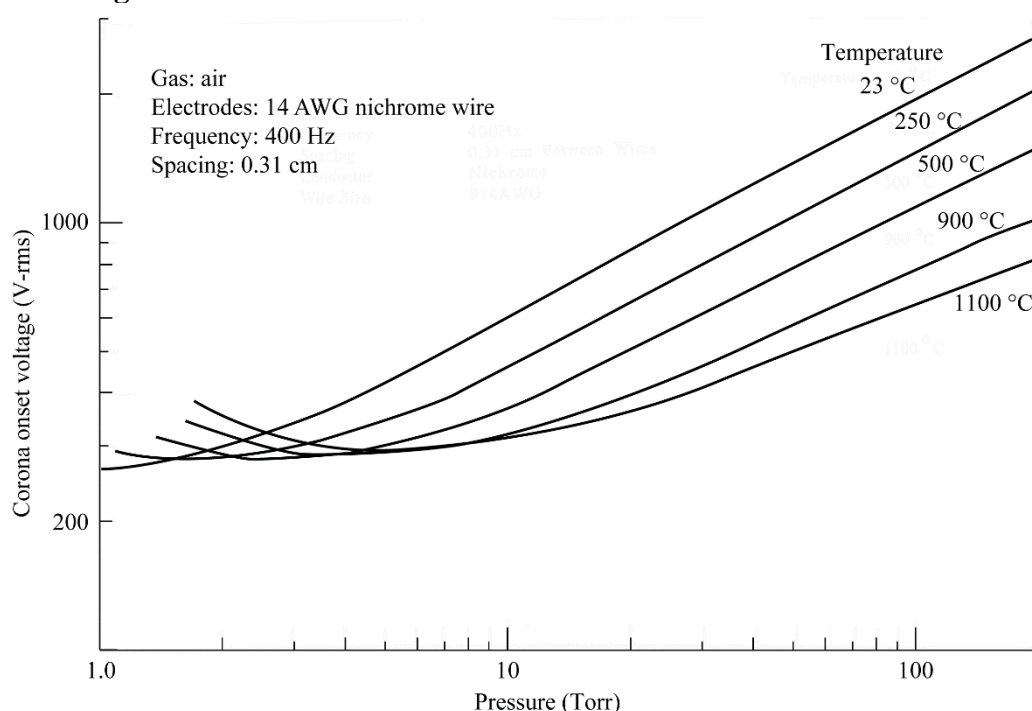


Figure 17—Corona Initiation Voltage as a Function of Temperature and Pressure for Parallel Wires in a Heated Chamber

When subject to high temperature, molybdenum and tungsten sensors, conductors, and parts are to be protected from oxidation by either an inert gas or vacuum environment. In addition, when molybdenum materials are located in an oxidizing atmosphere they should be isolated to prevent molybdenum trioxide (MoO_3) formation from evaporating and depositing on cooler parts. The CIV data, as a function of temperature and pressure, obtained between two MoO_3 -contaminated titanium wires spaced in a depressurized air-filled chamber is shown in figure 18, Corona Onset Voltage of Nickel-Clad Wires in a Molybdenum-Contaminated Oven. The wires did not corrode or show signs of evaporation at temperature less than 500 °C. As the temperature was increased, MoO_3 evaporated and deposited on the cooled vacuum chamber walls. The multitude of MoO_3 molecules between the conductors carried the conduction current when a voltage exceeding the CIV was applied to the wires (Harwood, 1958).

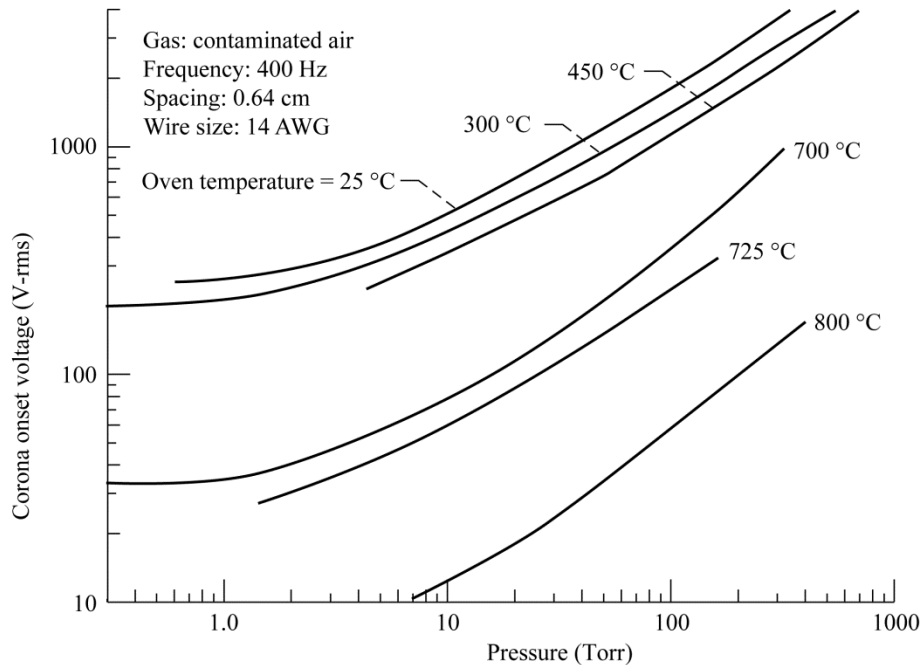


Figure 18—Corona Onset Voltage of Nickel-Clad Wires in a Molybdenum-Contaminated Oven

6.3.2 Corona Frequency Spectrum of Air Between Parallel Wires

As discussed in section 5.2.6, partial discharges or corona usually generate high-frequency noise that can interfere with the operation of other equipment. In one study, when the frequency spectrum of the noise generated by discharges between parallel wires was measured at three pressure-spacing (pd) dimensions, the following results were obtained (Dunbar, 1983).

- a. The corona frequency spectrum for one atmosphere air is sufficient to generate EMI from 60 Hz to over 1 GHz.
- b. As pressure is decreased to 30 Torr, the higher frequencies are attenuated significantly as shown in figure 19, Frequency Spectrum at Corona Pressure (Dunbar, 1983).
- c. Two situations exist for the low-pressure region. For glow discharge inception, the frequency range is from 15 to 30 kHz as shown in figure 20, Frequency Spectrum at 0.75 Torr, 647 Volts for #16 AWG Solid Copper Wires Spaced 4.8 cm (Dunbar, 1983). The data were taken between parallel wires using EMI test requirements and equipment. However, if the voltage is raised to include streamers (sparking) within the glow discharge region, which is an over-voltage of at least 30 V-peak above glow discharge initiation, the frequency spectrum increases to the values shown in figure 21, Frequency Spectrum at Glow Discharge Pressure (Dunbar, 1983).

NASA-HDBK-4007 W/CHANGE 2

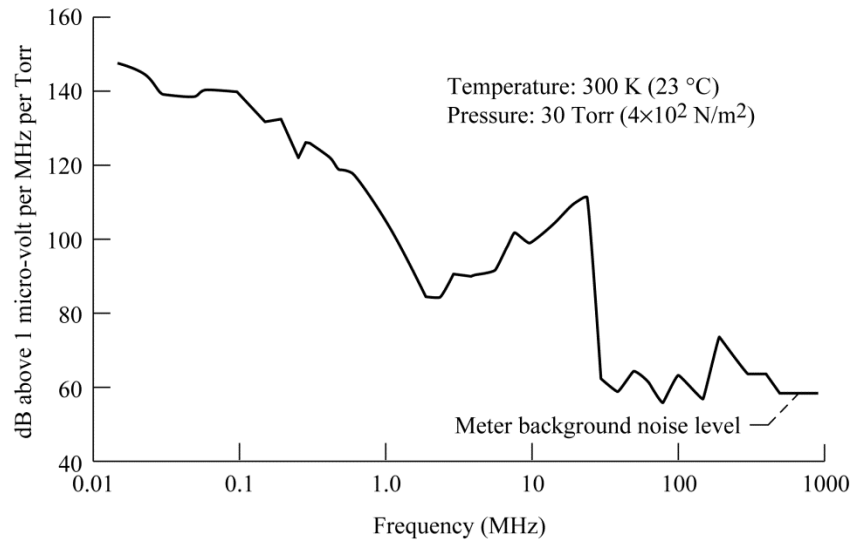


Figure 19—Frequency Spectrum at Corona Pressure

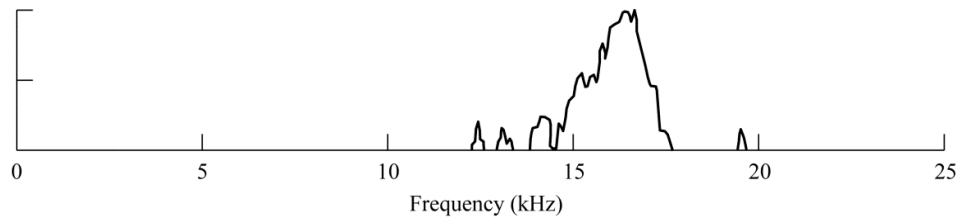


Figure 20—Frequency Spectrum at 0.75 Torr, 647 Volts for #16 AWG Solid Copper Wires Spaced 4.8 cm

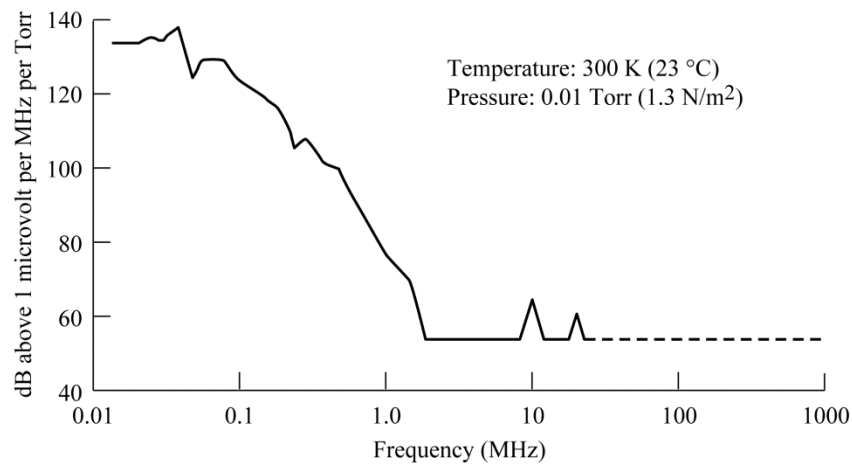


Figure 21—Frequency Spectrum at Glow Discharge Pressure

These data are important when measuring corona discharges at low pressure with corona system test equipment. As an example, test equipment that has a low-frequency cut-off at 40 kHz will not detect the lower frequencies of glow discharge at initiation. The low-intensity radiated emissions spectra produced by a glow discharge may not be considered detrimental to electrical and electronic system hardware, but this should be confirmed by comparison with the certification performance data for the hardware under consideration.

6.3.3 Gas Mixtures

Manned spacecraft systems use a gas or a gas mixture to pressurize the manned module, usually a mixture of oxygen, nitrogen, and hydrogen. Although nitrogen has a much lower breakdown characteristic than oxygen, a highly electro-negative gas, the presence of oxygen in nitrogen will raise the breakdown voltage as shown in figure 22, Onset Voltage of Gases and Gas Mixtures between 0.25-in. Round Rods (Dunbar, 1966). Other outgassing products and gases will also combine with the nitrogen-oxygen mixture, but the small quantity will not have any significant effect on the total breakdown characteristic.

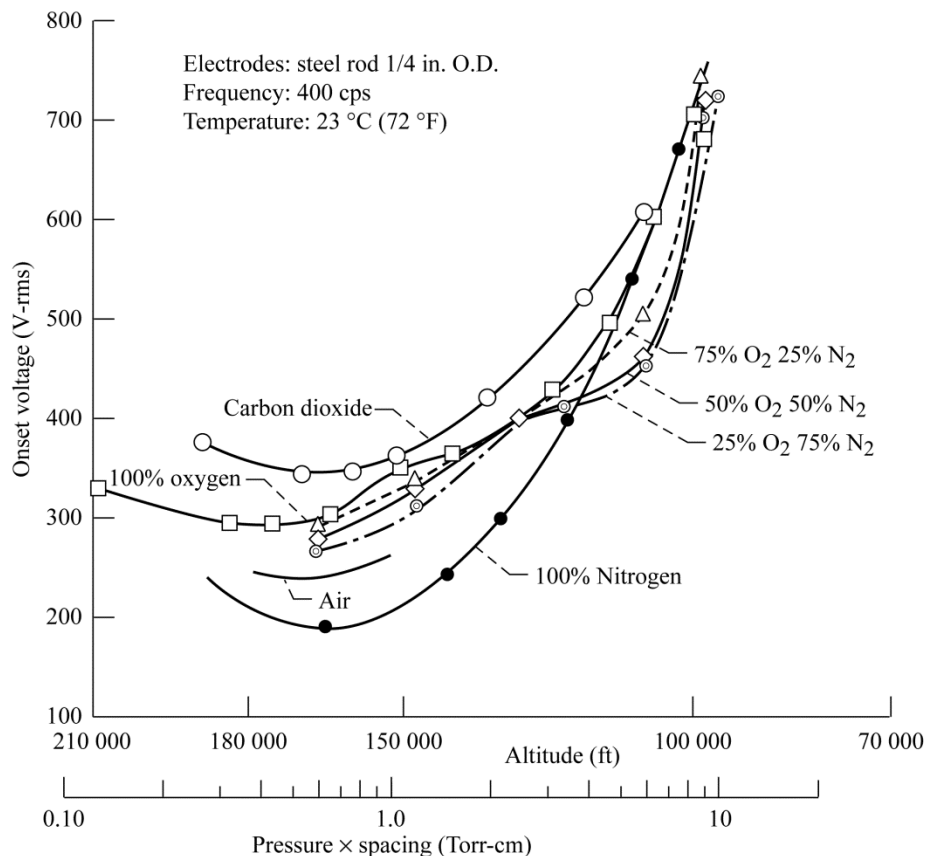


Figure 22—Onset Voltage of Gases and Gas Mixtures Between 0.25-in. Round Rods

6.3.3.1 Helium-Oxygen

The breakdown voltage between a pair of 5.0-cm diameter parallel plate circular electrodes spaced 0.2, 2.0, and 5.0 cm apart was determined for pure helium, pure oxygen, and helium-oxygen mixtures. The data shown in figure 23, Parallel Plates in Helium-Oxygen (Dunbar, 1966), imply that corona and voltage breakdown can appear on the bare or very thinly insulated conductors of a 200 V-rms ac electrical system when the mixture contains more than 80 percent helium by volume. Such a system would require special corona and voltage breakdown precautions.

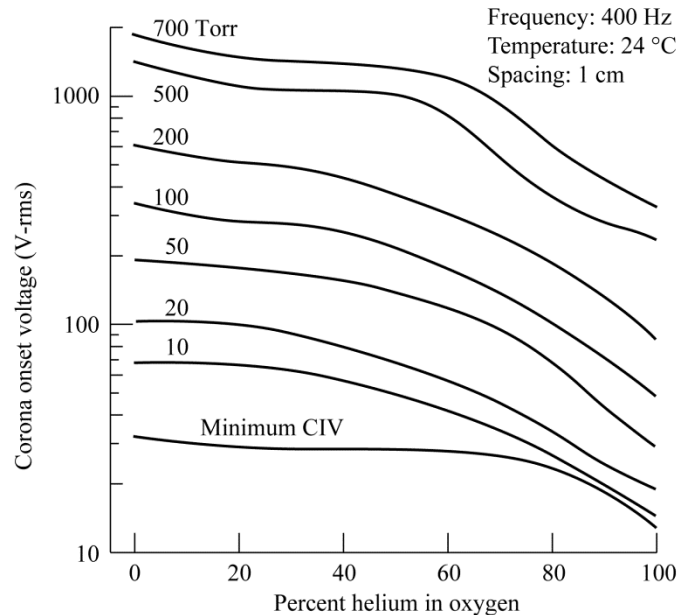


Figure 23—Parallel Plates in Helium-Oxygen

6.3.3.2 Nitrogen-Oxygen

The breakdown voltages of nitrogen-oxygen mixtures were tested with the same equipment as the helium-oxygen gases. The test results are shown in figure 24, Round Rods in Nitrogen-Oxygen Gas Mixture (Dunbar, 1966). These curves show that the CIV cannot be determined by a linear interpolation of the component gases. For some gas mixtures, there are pressures and spacings where the CIV is less than that of either component gas. Either neon or argon when mixed with oxygen shows this characteristic.

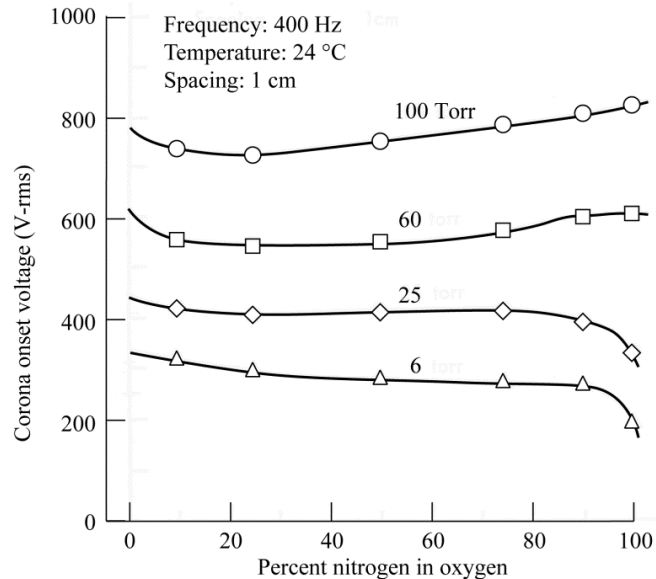


Figure 24—Round Rods in Nitrogen-Oxygen Gas Mixture

6.3.3.3 Noble Gases

Gas mixtures with neon and/or argon may have very low CIV. Such mixtures are used in neon lights to keep the starting or initiation voltage within acceptable limits for display purposes. These gases, if used in spacecraft hardware, should be kept away from high voltage to avoid corona issues.

6.3.4 High-Frequency Breakdown

Most high-voltage breakdown and partial discharge information available in the literature has been developed for 60-Hz utility power system equipment. In spite of the lack of information for systems operating above 60 Hz, spacecraft electrical and electronic designers have used published power system partial discharge and corona testing techniques and data for power conversion designs with reasonable success. However, it was determined early in the space program that the use of very low frequency partial discharge criteria leads to failures when applied to high-frequency, high-density packaging, specifically when non-sinusoidal frequencies greater than 20 kHz were introduced for weight and volume saving (Bunker, 1970). Fortunately, many of the early designs used vacuum tube technology, which included reasonably slow rise times compared to today's high-speed switching devices. Instead of determining the cause of the failures for the early power conversion components, it was agreed among engineers that spacecraft high-voltage packages should have average electric field stresses less than 2000 V/mm and maximum field stresses less than 5000 V/mm. This field stress limitation reduced the failure rates to acceptable limits.

Later, experimental data published in August et al. (1967) and August and Chown (1970) showed that the high-frequency breakdown between conductors spaced greater than 0.04 cm

apart was considerably less than the breakdown voltage at very low frequencies for pd values greater than 50 Torr-cm. For very closely spaced electrodes (less than 0.04 cm), the breakdown voltage was the same for frequencies from 50 Hz to 2 MHz for pd values greater than 50 Torr-cm. At pd values greater than Paschen's minimum, Paschen's Law does not hold for high frequencies (figure 25, Breakdown at High Frequency in Air in Inhomogeneous Field (Prowse, 1950 and Lassen, 1931), and figure 26, Breakdown at High Frequency in Air (Smaller Values of d/mm)) in Inhomogeneous Field (Pim, 1949).

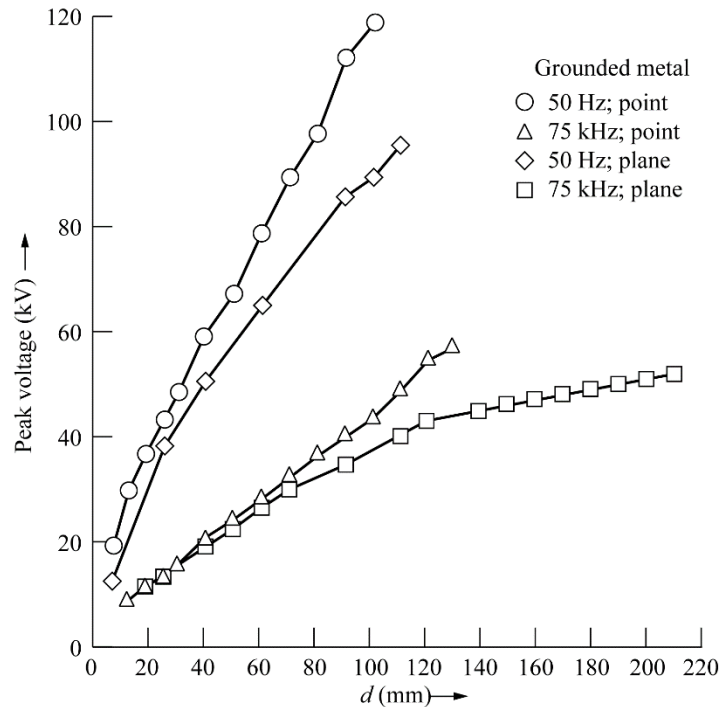


Figure 25—Breakdown at High Frequency in Air in Inhomogeneous Field

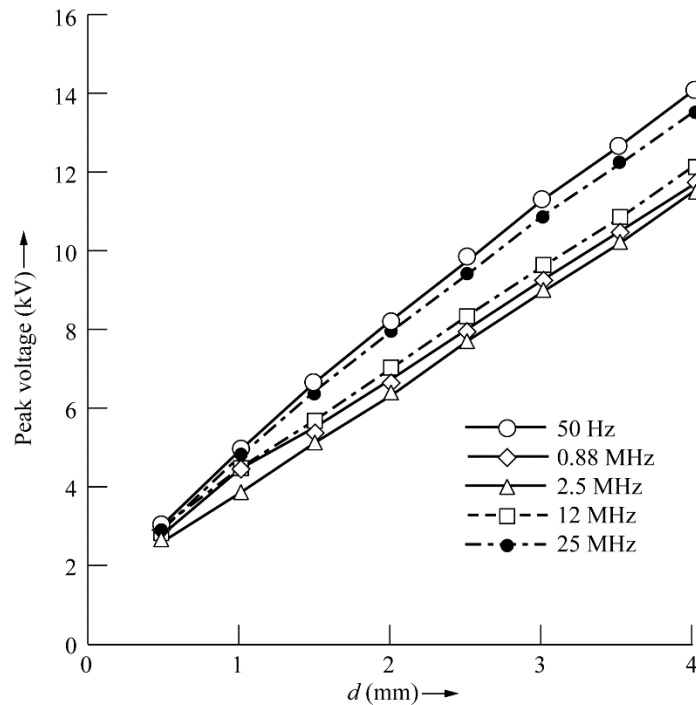


Figure 26—Breakdown at High Frequency in Air (Smaller Values of d (mm)) in Inhomogeneous Field

During the first reported spacecraft high-frequency electronic failure (Bunker, 1965 and Bunker, 1970), it was assumed that the breakdown phenomenon that occurred at pressures between 1 Torr and vacuum were related to high-frequency effects. This led to the development of the voltage breakdown versus high-frequency breakdown curve shown in figure 27, Variation of RF Breakdown Voltage With Pressure Illustrating the Pressure Transition Region From Gas Discharge to Multipactor (August and Chown, 1969, and August and Chown, 1970). This curve was based on the limited information published in the book by Meek and Craggs (1978) plus the high-frequency and multipactor voltage breakdown reports given in Prowse (1950); Lassen (1931); Pim (1949); Labrum (1947); Hughes Aircraft Company (July 1966); Vaughn (1968); Mohr and Putz (1966); Lewis and McCarty (1966); Wachowski (1964); Woo (1968a); Ishamaru and Woo (1967); MacDonald and Brown (1949); and Herlin and Brown (1948). The subject of multipactor is developed more fully in section 6.3.5.

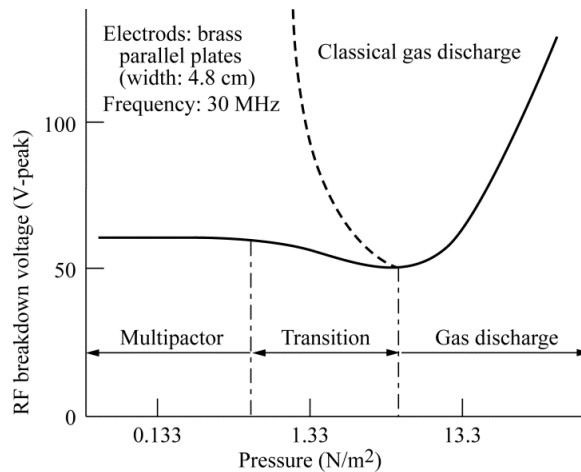


Figure 27—Variation of RF Breakdown Voltage With Pressure Illustrating the Pressure Transition Region From Gas Discharge to Multipactor

The breakdown voltage for very low RF frequencies is the same as the dc value; however, at high frequencies, the breakdown mechanism is complicated by electron resonances resulting in cumulative ionization. Hence, lower breakdown voltages are experienced relative to those predicted on the basis of dc (Bunker, 1966).

Figure 28, Breakdown Voltage for a 0.4-mm Gap in Air at Atmospheric Pressure as a Function of Frequency (Prowse, 1950), is a plot of data in the literature and is limited to pressure-spacing dimensions greater than 30 Torr-cm for frequencies where multipaction is not an issue. This curve is presented based on available data in the literature: region A is by Lassen (1931), B is by Pim (1949), and C is by Labrum (1947). The curve intends to illustrate main features only, since continuous observations over the whole range of frequency do not exist.

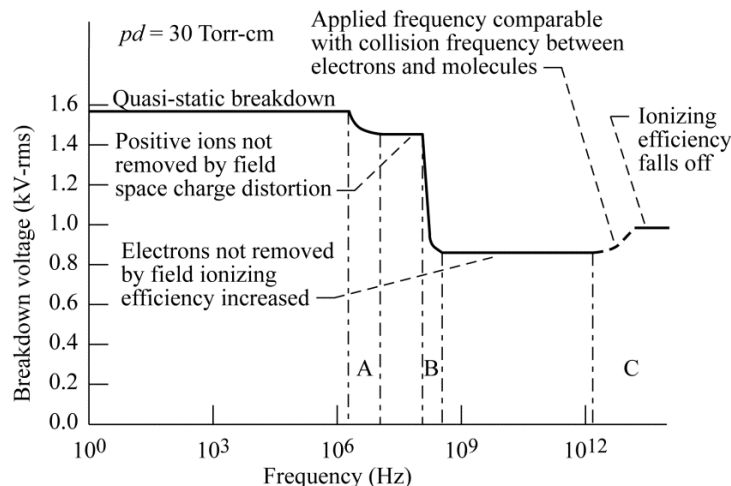


Figure 28—Breakdown Voltage for a 0.4-mm Gap in Air at Atmospheric Pressure as a Function of Frequency

As solid-state devices developed, switching speeds increased. Also, improved magnetic material development led to power conversion repetition rates ranging from 20 kHz to over 100 kHz. Further, high-density packaging development progressed through the selection of higher frequencies. With these developments, physically smaller electrical parts reduced the spacing between small rounded surfaces and part volumes and weights, forcing designers to pay more attention to the electrical field stresses within the insulation system.

Figure 29, Frequency De-rating of Paschen's Law at High Frequencies for Different Electrode Configuration and Spacing, shows the results of an experiment (Dunbar et al., 1998) to determine the corona initiation of a long antenna in a very large diameter vacuum chamber. Measured parameters were the CIV and CEV at frequencies from 60 Hz to over 60 kHz at pressures of 10 to 50 Torr. The results of these experiments concluded that the corona initiation in air was reasonably stable from 60 Hz to 40 kHz. As seen in the curve labeled "antenna," the CIV decreased above 40 kHz to 85 percent of the 60 Hz value. This was a significant finding, implying very small conductors or square-edged conductors, as used on printed circuit boards, surrounded by an air gap will have lower CIV when the frequency exceeds 40 kHz for pd dimensions greater than 50 Torr-cm. The data in figure 29 are taken from published literature. Dotted lines are expected (or extrapolated) curves, and the large dots are the data in the literature.

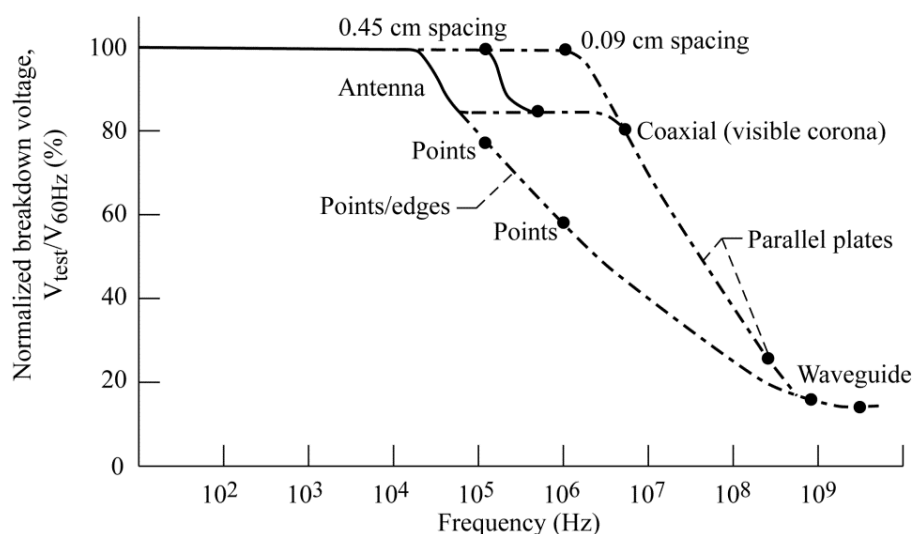


Figure 29—Frequency De-rating of Paschen's Law at High Frequencies for Different Electrode Configuration and Spacing

Every component that has to pass an EMI qualification can be tested for partial discharges using the same EMI detection equipment with little modification to the EMI specification. Normally, the EMI test is determined in a "room ambient" environment. For the partial discharge part of the test, the test article should be placed in a vacuum chamber, if viable, to simulate the operational environment. For spacecraft equipment, the test pressure should be adjusted to assure coverage of the Paschen minimum pd dimensions for the test article while conducting EMI measurements. By comparison of the radiated emissions signature at one atmosphere pressure with those at

lower operational pressures, differences in the frequency spectra can be identified that may be attributed to glow discharges and partial discharges. The discharge frequencies to be assessed are well defined by Pfeiffer (1991a and 1991b) and Pfeiffer et al. (1987). Note that published data indicate the breakdown voltage in air between parallel plates spaced less than 1 mm apart is constant from 20 Hz to 100 kHz (Prowse, 1950; Lassen, 1931; Pim, 1949; Labrum, 1947; Dunbar et al., 1998; Pfeiffer, 1991a; and Buchalla, et al., 1992).

Research has also shown the breakdown voltage of air at 23 °C as a function of frequency shows little change in the Paschen minimum from 50 Hz to 2 MHz for breakdown between parallel plates. Above 2 MHz, there is a drastic drop to the multipactor breakdown region, which continues up to 200 MHz. Above 5 GHz, the minimum breakdown voltage rises again, because the multipactor phenomena are not observed since the resonant electrons cannot keep up with this high frequency of the field. (Walter and Hershberger, 1946; Herlin and Brown, 1948; Prowse, 1950; He and Hall, 1984; Sato and Haydon, 1984a and 1984b; Damas and Robiscoe, 1988; Seebok and Koehler, 1988; Suganomata et al., 1989; Vlieks et al., 1989; Bourat and Joly, 1989; Saito, 1995; and Galstjan and Ravaev, 1995).

As more data become available, it is recommended that a plot of voltage breakdown as a function of frequency be made available to engineers developing high-density packaging for spacecraft. In the meantime, designers are encouraged to use the following partial discharge initiation voltage information shown in table 3, High-Frequency Voltage Breakdown Criteria (Woo, 1968a).

Table 3—High-Frequency Voltage Breakdown Criteria

FREQUENCY RANGE	VOLTAGE (V-PEAK)	ELECTRODE CONFIGURATION
0.06 to 980 kHz	327	Parallel plate (spaced: 0.01 to 0.04 cm)
0.06 to 40 kHz	327	Antenna
60 kHz to 1.0 MHz	260	Antenna and sharp edges
950 MHz to 3 GHz	39	Waveguide (all metal)
60 GHz	327	Waveguide

The subject of RF breakdown continues to be an active area of research. A recent Air Force handbook, Graves (2014), captures much of the work done in the past ten years and will prove an invaluable reference.

6.3.5 Multipactor Phenomena

Multipactor phenomena are only observed in RF systems. Multipaction, or the multipactor effect, is a resonant RF discharge, sustained by the emission of secondary electrons from the walls of the RF devices such as waveguides and RF connectors. Multipactor breakdown may occur when secondary electrons are produced on an electrode surface and are accelerated in a gap toward another electrode surface so that they reach the second electrode in a half-period of the applied RF field. Upon striking the second electrode, the electrons create new secondary electrons, which are accelerated back across the gap toward the primary electrode during the next half-period,

producing more electrons there, as shown in figure 30, Multipactor Discharge: Electron Resonance in an RF Field With Discharge Sustained by Secondary Emission (Dunbar, 1983). These electrons accelerated across the gap gain their energy from the applied RF field (Hughes Aircraft Company, 1966; Wachowski, 1964; Woo, 1968a and 1968b; and Galan et al., 1988). For most materials, the secondary electron emission yield, that is, the ratio of emitted secondary electrons to the number of incident electrons becomes greater than unity if the impact energy is sufficiently high. Thus, the number of electrons participating in a discharge increases when the coefficient of secondary emission is greater than 1.0 and multipactor breakdown occurs. Occurrence of a multipactor discharge depends primarily on the RF voltage and frequency levels, gap spacing, electrode surface condition (roughness and cleanliness), secondary electron emission coefficient of the electrode material, and the operating pressure (vacuum environment). Since the multipactor discharge is an electron resonance phenomenon, it is independent of the nature of the gaseous environment under which the RF system is operating.

In practical systems, operating pressure is usually very low such that the mean-free-path of electrons for collision with molecules is much larger than the gap length, (d), and the voltage level is in a range such that the accelerated free electrons can gain the right amount of kinetic energy from the field to be in resonance.

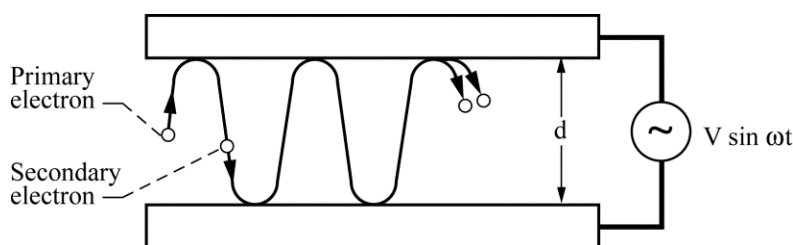


Figure 30—Multipactor Discharge: Electron Resonance in an RF Field with Discharge Sustained by Secondary Emission

Generally speaking, the existence of multipaction does not imply an immediate component failure. However, long-term effects, such as erosion or physical damage of the cables and other component surfaces, may lead to an eventual failure. For instance, it is possible for multipaction to occur in a transmitting antenna in which only a small percentage of the transmitted power is dissipated in the multipactor, resulting in localized heating. The result in decreased or increased radiated power and an increase in the voltage standing wave ratio (VSWR) may be negligible, and the system may continue to operate with no other adverse effects. On the other hand, if the antenna were used in a duplex system where transmitting and receiving occurred simultaneously on different channels, the antenna noise caused by the multipactor may blank out the receiving channel and thus make the system partially inoperable. The total system should be considered to estimate the effects of multipaction with respect to system performance.

When designing RF equipment, sufficient safety margins are to be provided to ensure that multipaction will not occur. Frequency-temperature-pressure testing should be required to ensure product multipactor-free acceptability.

Although a multipacting breakdown is a resonance phenomenon, it is not required that a unique set of operating conditions occur (Nanevich and Vance, 1967; Hughes Aircraft Company, 1966; and Galan et al., 1988). There is a wide range of combinations of gap spacing, operating frequency, and voltage over which multipacting may be observed. However, there is a lower threshold voltage below which the discharge does not occur. In addition, for a given electrode spacing, there exists a cut-off frequency below which the discharge does not occur. Multipactor discharges can occur over a wide range of frequencies above the cut-off frequency. Furthermore, in a configuration where more than one path length is available, less frequency selectivity would be experienced.

Multipaction is usually experienced at frequencies greater than 70 MHz. The effect of multipacting on the Paschen curve over a range of pressures is illustrated in figure 27. Multipaction does not occur until the mean free path is larger than the gap, that is, below the Paschen minimum. Most communications between a spacecraft and a ground station take place at frequencies in the 20 MHz to 30 GHz range. The design and fabrication practices for this frequency range are different than for 60 Hz-ac or dc systems.

The transmitting system is affected in many different ways by multipaction (Hughes Aircraft Company, 1966). There is some RF power lost in exciting the electrons. When sufficient gas molecules are present, ionization can occur, which can cause corona with the resultant breakdown between plates. The impact of the electrons on the surface can cause heating and outgassing. When the load on the RF source is reactive, it causes detuning of the output circuits. Multipaction would usually generate higher order harmonics in the output of the transmitter. Also, RF noise is generated by multipactor effects, which can interfere with nearby receiving equipment. All these effects may not happen at the same time, and the antenna may be perfectly useful as a radiator after a breakdown. However, its efficiency with respect to total radiated power will be drastically reduced as shown in figure 31, Power Decrease Caused by Multipactor (Dunbar, 1983), for an RF coupler with intermittent multipaction. These symptoms of multipactor effects should not be interpreted as indication for other failure modes.

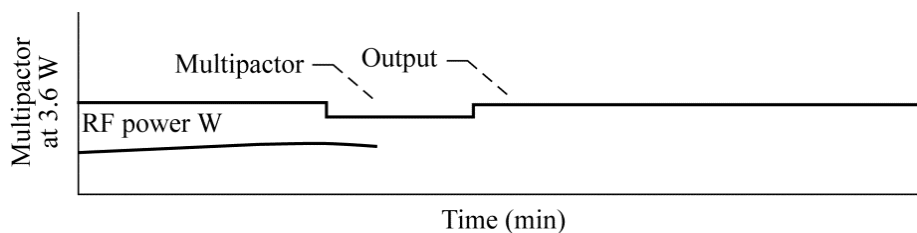


Figure 31—Power Decrease Caused by Multipactor

Electrode spacing, frequency, electrode configuration, and the applied voltage are all to be considered when evaluating design parameters for the elimination of multipaction. Figure 32, Possible Regions of Multipacting Between Parallel Plates (Dunbar, 1983), displays one set of relationships among those parameters. The top scale is electrode separation divided by wavelength, both in the same units. The three regions indicated by $1/2$, $3/2$, and $5/2$ are where multipacting can occur. The electrons that correspond to the region marked $1/2$ have a transit

time of $T/2$, where $T=1/f$. Those in region $3/2$ have a transit time of $3T/2$, and $5/2$ is $5T/2$. Unfortunately, a general plot of this sort cannot be relied upon for design data, because the values depend on factors such as the number of electrodes, electrode material, surface conditions, and geometry, for example, parallel plates, coaxial, or edges. The designer is forced to test each design at various stages of fabrication to be certain that multipacting does not occur.

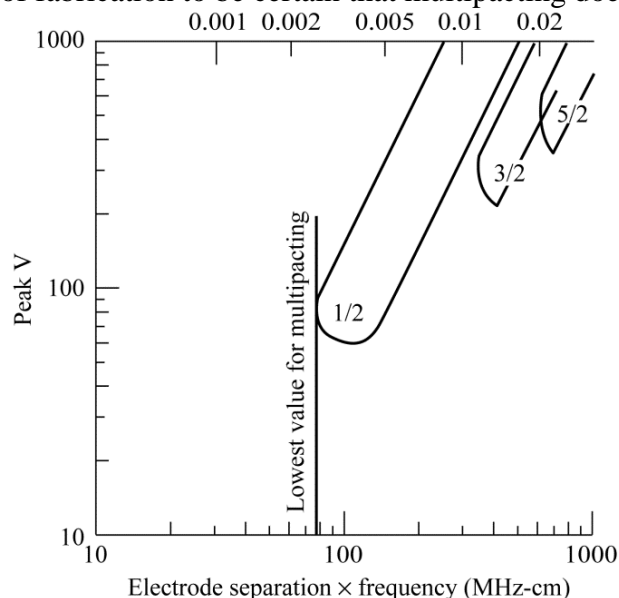


Figure 32—Possible Regions of Multipacting Between Parallel Plates

Some design features that should be considered are included in Hughes Aircraft Company (1966):

- a. Treatment of the electrode surfaces to change their secondary electron emission characteristics, such as a micro-thin coating with polyurethane or other suitable material
- b. Application of a dc bias to the electrodes to suppress secondary electron emission
- c. Pressurization of the space between electrodes
- d. Selection of electrical and mechanical dimensions to reduce the possibility of multipactor events

When considering the use of foam, the designer is to consider the density of the foam, its application, the gas enclosed in the cells, and the cellular breakdown of the foam. For some applications, the foam may be ineffective or detrimental as a function of time in the presence of temperature cycling.

Examples of breakdown discharge data for parallel plate electrode configuration are shown in figure 33, Multipactor Discharge Characteristics of Various Surface Materials as a Function of fd for Two Different Operating Frequencies (430 and 100 MHz) for Parallel Plate Electrode Configuration, Hughes Aircraft Company (1966), for several electrode materials as a function of

NASA-HDBK-4007 W/CHANGE 2

fd , the operating frequency (f) times electrode separation (d) for two frequencies. These data may be used to closely estimate the minimum breakdown voltage for a particular fd dimension and a particular electrode material. Specifically, the data show that dielectric materials have higher multipactor initiation voltage than the metallic electrodes (Hughes Aircraft Company, 1966). Therefore, using an anti-corrosion coating (dielectric material) on waveguide internal metallic surface improves the multipactor initiation voltage. The anti-corrosion material needs to be only a few microns thick, but it must be well bonded to the waveguide metallic surface (100 percent bonding).

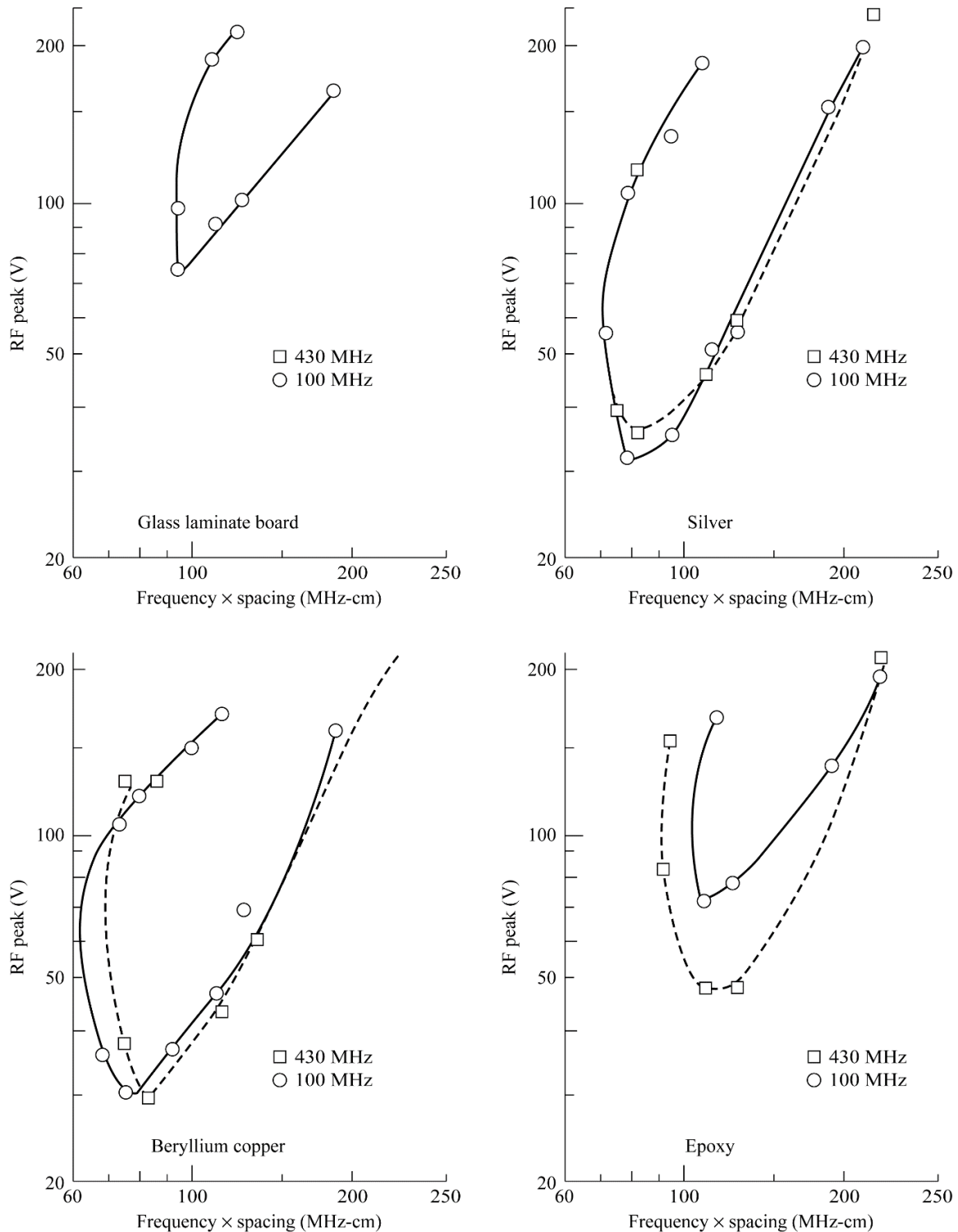


Figure 33—Multipactor Discharge Characteristics of Various Surface Materials as a Function of fd for Two Different Operating Frequencies (430 and 100 MHz) for Parallel Plate Electrode Configuration

Multipactor effect and breakdown can also be seen in coaxial transmission lines or coaxial electrode geometries operating in the space environment (Woo 1968a; and Ishimaru and Woo (1967). Figure 34, Multipacting Region for Coaxial Electrodes With Varying Values of b/a (Woo, 1968a), shows the RF breakdown voltage data as a function of fd obtained for coaxial electrodes in vacuum where b and a are the radius of the outer and inner conductors, respectively.

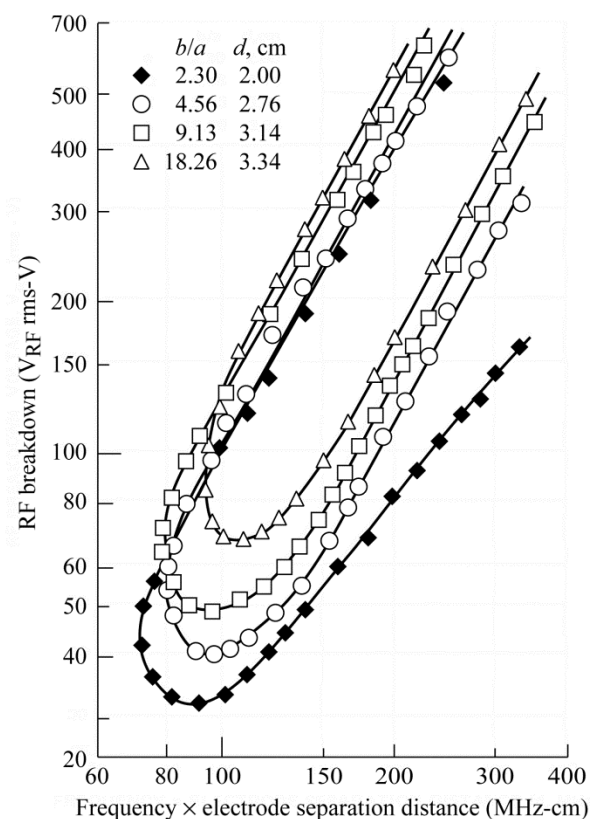


Figure 34—Multipacting Region for Coaxial Electrodes With Varying Values of b/a

In summary, multipactor breakdown is a hazard that may occur in RF equipment subjected to low-pressure space environments. Components such as printed circuit boards, conventional wiring, multi-pin connectors, and variable capacitors have all experienced multipaction in space. Failure experience usually initiates with multipaction, followed by dielectric heating, materials outgassing, and finally gaseous breakdown. Potting, foaming, or dielectric coatings tend to reduce the risk of multipactor breakdown phenomena; however, small open voids between electrodes within a foam or improper coating may result in multipaction. As a rule, foam products are considered a poor choice because there is a high probability of open pores between closely spaced electrodes. Using a solid dielectric is the best way to eliminate multipaction. However, joints and connectors with very small spacings between mated surfaces can result in multipaction. Printed circuit board and component cleanliness is mandatory. Dust particles or small setae will result in lowered multipactor voltage breakdown. Pressurization of RF

equipment is a positive method for multipactor elimination when viable. Finally, the correct choice of materials and configuration is very important as shown in figure 33.

6.3.6 Creepage and Flashover

Current flowing across the surface of an insulator, especially when slightly wetted and containing a conductive contaminant may produce enough heat to generate a track of carbon. This conductive path tends to reduce the capability of the insulator to hold off the voltage and may result in electrical breakdown. The surface erodes without producing a track in some materials. Fillers effectively reduce the tracking tendency of organic materials. Eroding materials, such as acrylics, do not require filler protection. To lengthen the surface creepage path, tracking can also be controlled by reducing the voltage stress on the surface by applying petticoat insulation configurations. A bibliography on surface flashover, surface creepage, and tracking on or within solid insulation is cited in Bashara et al. (1965); Billings and Humphreys (1968); Billings et al. (1967); Billings et al. (1971); Chapman et al. (1955); Dakin and Mullen (1972); Frisco and Chapman (1956); Kurtz (1971); Mason (1960); Orbeck and Niemi (1973); Toriyama et al. (1971); Wallace and Bailey (1967); Wu and Cheng (1978).

New porcelain insulators may be coated with a cycloaliphatic epoxy coating containing inorganic filler. The finished product will then be able to withstand higher voltage stress than the original porcelain. In time, surface erosion and exposure to UV radiation will degrade the epoxy-based laminate to a level inferior to the porcelain.

Figure 35, Flashover Test Fixture (Dunbar, 1988), shows the test fixture used to evaluate the flashover voltage measured between 1.9 cm-diameter washers mounted on an uncoated glass epoxy-bond laminate. The flashover voltage initiation as a function of spacing is shown at three frequencies in figure 36, Effect of Spacing on the Initial Values of Strength for Fixture Shown in figure 35 (Dunbar, 1988). The impulse and steady-state flashover voltage stresses are shown for the same configuration in table 4, Comparison of Steady and Impulse Flashover Stress V/cm (peak) for Glass Epoxy-Bond Laminates (Dunbar 1988).

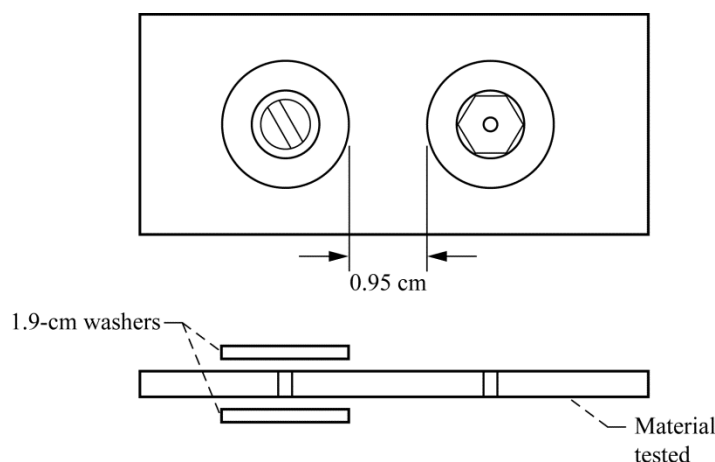


Figure 35—Flashover Test Fixture

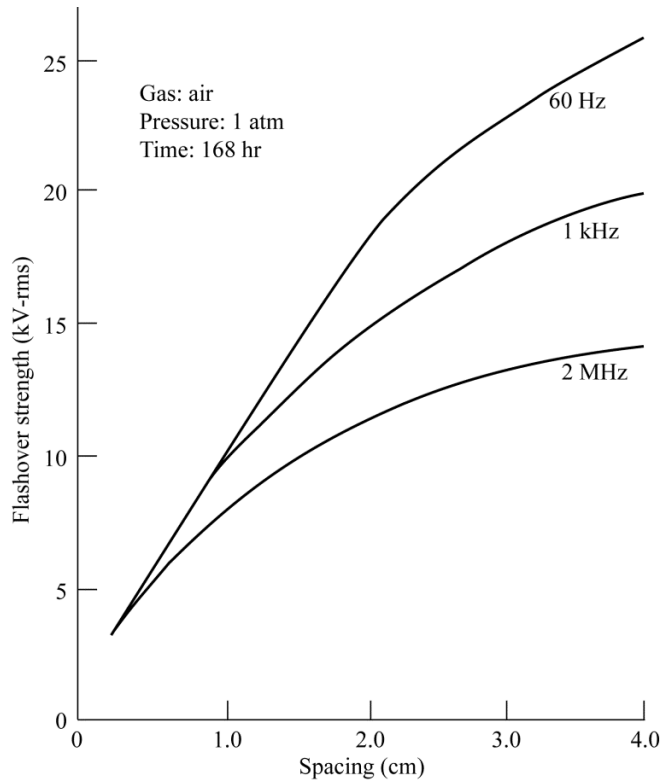


Figure 36—Effect of Spacing on the Initial Values of Strength for Fixture Shown in Figure 35

Table 4—Comparison of Steady and Impulse Flashover Stress V/cm (Peak) for Glass Epoxy-Bond Laminates

TEST (DURATION: 1 MIN)		AVERAGE FLASHOVER STRENGTH FOR 1-CM SPACING (KV)
Steady-state	60 Hz	14.1
	dc Positive	14.9
	dc Negative	16.7
Pulse	Positive	17.1
	Negative	18.6

6.3.6.1 Effect of Dielectric Constant on the Flashover Strength

Flashover strength is affected by dielectric constant. Polyethylene, which is representative of the low-loss, low-dielectric-constant class of material, exhibits the smallest decrease in flashover strength with respect to increasing frequency.

High dielectric constant materials have much lower resistance to surface voltage creepage than the low dielectric constant materials. Figure 37, Variation of Flashover Voltage with Changing

Insulation Dielectric Constant (Luck, 1967), is an illustration showing the advantage in selecting the correct dielectric constant. The flashover breakdown factor in the illustration represents the results of many measurements, showing how a decreasing flashover voltage can be expected across the dielectric when insulations of progressively higher dielectric constants are used.

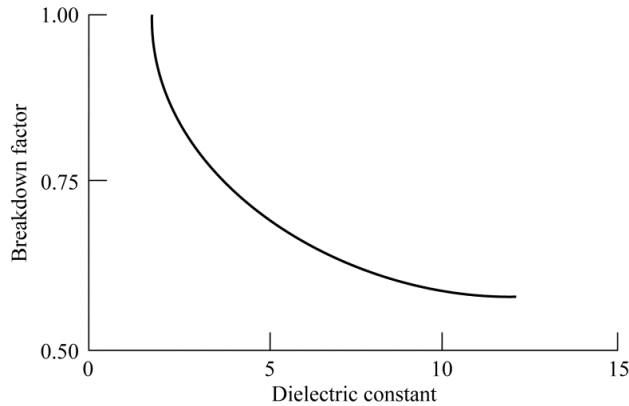


Figure 37—Variation of Flashover Voltage With Changing Insulation Dielectric Constant

6.3.6.2 Effect of Frequency on Flashover Strength

All materials have lower flashover strength at higher frequencies. The example given in figure 38, Effect of Frequency on Flashover Strength for Configuration Shown in figure 35, illustrates that the surface flashover strength changes magnitude with frequency. The flashover strength of glass-cloth epoxy-based laminate (G-10) is shown at three different frequencies as a function of spacing in air at 23 °C in figure 36, and the effect of frequency on surface flashover for polyethylene (PE) is seen in figure 39, Effect of Frequency on the Electric Strength of PE. Further, table 5, Polyethylene Dielectric Strength (in V/mil) for 30-mil Sheets as a Function of Temperature and Frequency (Luck, 1967), and table 6, Teflon® Dielectric Strength (in V/mil) for 30-mil Sheets as a Function of Temperature and Frequency (Luck, 1967), show the dielectric strength of PE and Teflon® (respectively) as a function of frequency and temperature (Luck, 1967).

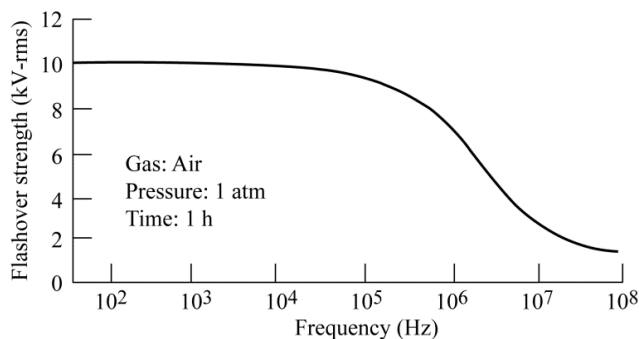


Figure 38—Effect of Frequency on Flashover Strength for Configuration in Figure 35

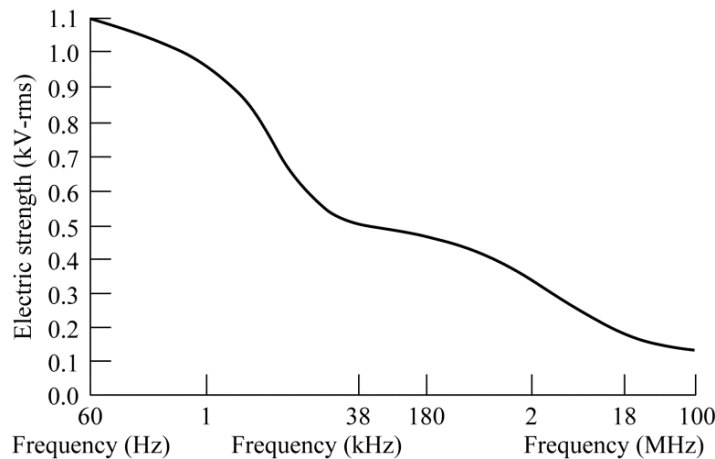


Figure 39—Effect of Frequency on the Electric Strength of PE

6.3.6.3 Effect of Magnetic Field

Limited data indicate improvement or degradation of the flashover properties of materials when the system is subjected to a combination of magnetic field and impulse voltages. Few effects are noted for magnetic fields less than 3 to 4 Tesla. For higher magnetic fields, the flashover strength is either improved or degraded, depending on the polarization of the interacting fields (Korzekwa et al., 1989).

6.3.6.4 Effects of Air Temperature on Flashover Strength

It is useful to determine the relationship between flashover strength at 25 °C and other temperatures. For gaseous breakdown in a uniform field, this relationship involves the ratio of the gas densities at the two temperatures. To test this relationship, it is only necessary to multiply the 25 °C value by the factor $(25 + 273)/(T + 273)$, which is the inverse ratio of the absolute temperatures involved. This ratio is part of the well-known air density correction factor, which is commonly used in spark-gap measurements over a considerable range of density and gap spacing. However, this may not hold true for surface flashover, because there are other factors, such as outgassing, surface charging, and triple point effects, involved in surface flashover events. Figure 40, Effect of Temperature on 60-Hz Flashover Stress (Dunbar, 1988), displays the effect of temperature on a 60-Hz surface flashover stress. The broken lines in this figure show the values obtained when this factor is applied to 25 °C flashover values. Thermionic emission does not become a factor until the temperature approaches 700 °C for most metals or until the material tends to change state via severe outgassing or polymerization. As a rule, the flashover voltage appears to increase as temperature in the system increases as shown in tables 5 and 6.

NASA-HDBK-4007 W/CHANGE 2

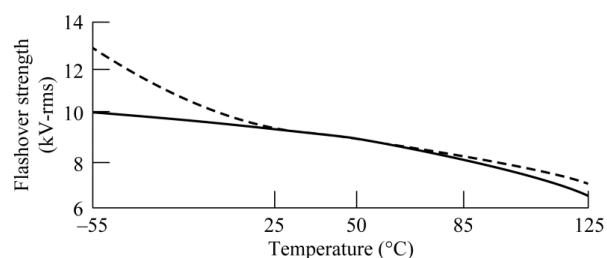


Figure 40—Effect of Temperature on 60-Hz Flashover Stress

**Table 5—Polyethylene Dielectric Strength (in V/mil) for 30-mil Sheets
as a Function of Temperature and Frequency**

TEMPERATURE (°C)	FREQUENCY						
	60 Hz	1 kHz	38 kHz	180 kHz	2 MHz	18 MHz	100 MHz
–55	1,660	1,270	750	700	410	190	160
25	1,300	970	500	460	340	180	130
50	1,140	910	590	580	280	150	150
80	980	970	440	430	220	150	150

**Table 6—Teflon® Dielectric Strength (in V/mil) for 30-mil Sheets as a
Function of Temperature and Frequency**

TEMPERATURE (°C)	FREQUENCY						
	60 Hz	1 kHz	38 kHz	180 kHz	2 MHz	18 MHz	100 MHz
–55	1,080	940	660	600	400	240	160
25	850	810	540	500	380	210	140
50	800	770	530	500	360	210	140
80	780	670	530	480	360	220	140
125	870	630	560	520	350	220	140

6.3.6.5 Effect of Humidity on Flashover

The flashover strength at 100 percent relative humidity (RH) is approximately 1/2 the strength at 0 percent RH. Ice and snow do not appreciably reduce the effective flashover strength. The selection of insulating materials resistant to surface wetting and moisture absorption will greatly facilitate the maintenance of original flashover strengths. A water-repellent treatment will aid on materials that are easily wetted. As an example, table 7, Environmental Effects on Surface Flashover at 60 Hz, shows environmental effects on flashover for glass cloth and polystyrene. A safety factor of 2 is recommended where humidity can go to 100 percent with condensation. Where dirt, dust, and residual ions from plating baths, etc., may contaminate the surface between electrodes, the flashover (creepage) path should be made to be 2 to 3 times the minimum air spacing.

Table 7—Environmental Effects on Surface Flashover at 60 Hz

		1 HOUR	1 DAY	1 WEEK	1 MONTH	6 MONTHS
Glass cloth (kV)	85 °C (dry)	7.8			9.0	9.4
	125 °C (dry)	7.0			9.4	9.3
	25 °C (100% RH)	9.5	^a 3.6	^a 2.5	^a 2.5	
	50 °C (100% RH)	8.8	^a 2.4	^a 2.4	^a 2.4	
Polystyrene (kV)	25 °C (100% RH)	1.7				5.5
	50 °C (100% RH)	10.3			6.2	5.1

^aInternal flashover.

6.4 Breakdown of Solids

Solid-insulating materials play an important role in electrical systems, because they act as mechanical support as well as electrical insulation.

6.4.1 Polarization

The dielectric constant of a dielectric material is a frequency-dependent parameter over the entire electromagnetic spectrum. A typical dielectric material (solid or liquid) may have four distinct resonant regions as shown in figure 41, Dielectric Polarization (Dunbar, 1988). Between these resonant frequencies, the dielectric constant appears to have constant values for the real part of the dielectric constant as a function of frequency. These resonances are the result of polarization induced by the applied field at that particular frequency. The distinct regions correspond to different physical mechanisms by which the material responds to the time-varying electric field. At very low frequencies, the material tracks the field through all four mechanisms so they all contribute to the polarization and the resulting change in dielectric constant. As the frequency increases, each mechanism in turn becomes unable to keep up with the field and ceases to contribute.

Changes in the real part of the dielectric constant (k') are associated with a significant change in the imaginary part (k''). In general, the interfacial polarization (α_s) may occur at up to several thousand Hertz, depending on the temperature and relaxation time of the material. The dipole polarization (α_d) would occur from 10^4 to 10^{12} Hz. Raising or lowering the material temperature can respectively increase or decrease the resonance frequency for both of these effects, shown graphically as curves T1-T3. The atomic polarization (α_a) is in the visible and near infrared frequency range, and the electronic polarization (α_e) occurs at frequencies above the optical frequency range (cosmic rays such as x-rays, vacuum UV, and other radiation frequencies). When a material is operated at a frequency that includes one or more of the polarization regions (resonant frequencies), the dielectric will absorb energy from the field, resulting in dielectric heating.

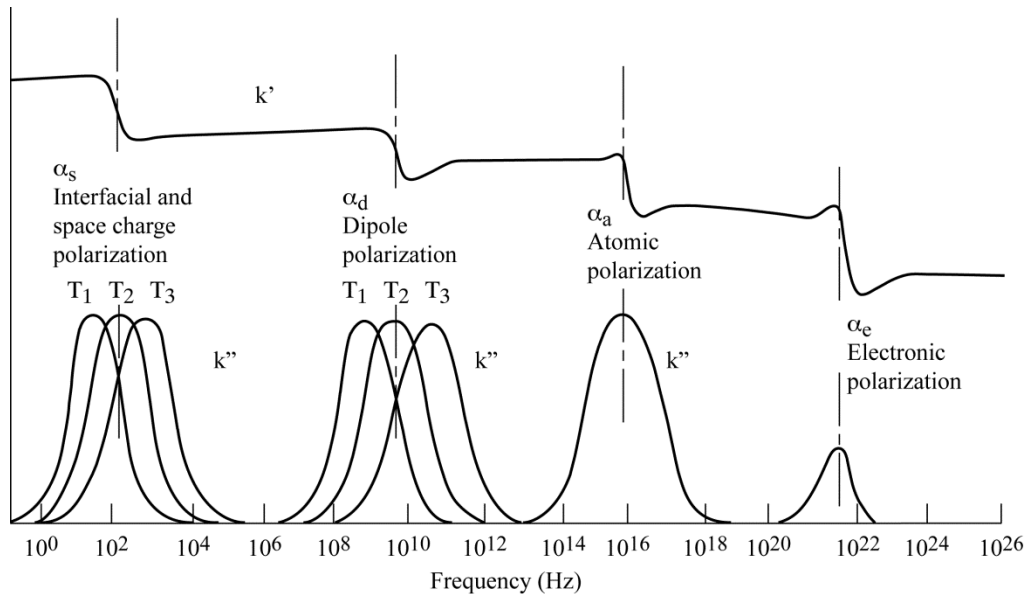


Figure 41—Dielectric Polarization

Dielectric materials used for electronic designs should be evaluated for a change of dielectric constant as a function of frequency to determine polarization effects. The dielectric constant of many materials as a function of frequency is given in Von Hippel (1954). The interfacial polarization is broadband and may be further broadened by wide temperature excursions. This implies that an electronic circuit should be evaluated through the full operating temperature range, instead of the temperature extremes (Greenfield, 1972).

6.4.2 Dielectric Constant and Dissipation Factor

Dielectric strength, dielectric constant, and the dissipation factor are the most readily measured electrical properties. Dielectric strengths and dielectric constants are well documented for high-voltage materials. Fewer data are available, however, on the dissipation factor, also called loss tangent, which is defined as

$$\tan \delta = \frac{\sigma}{\omega \epsilon} \quad (\text{Eq. 12})$$

where

σ is the ac conductivity

ω is the frequency in rad/s.

ϵ is the permittivity

The dissipation factor and dielectric constant both vary with frequency and temperature. Elevated values of the dissipation factor cause the dielectric heating in the insulation system and result in power loss. There are some frequency ranges for a given dielectric material for which the dissipation factor is above the acceptable design requirements. The system should be

operated in a regime where the dielectric constant has a constant value over the operating frequency and temperature ranges, and the dissipation factor should be relatively low to avoid dielectric heating and instability of the impedances. If the dielectric properties are functions of temperature, operating conditions have to be controlled to provide stable and predictable system performance. Most measurements of dissipation factors are made at 1000 Hz and 23 °C, but quite often the insulation has to function between 400 Hz and 1 MHz and at -40 to +200 °C. As a result, the designer has the problem of measuring the dissipation factor or searching for meaningful data and tends to extrapolate whatever data are available to the desired frequency range. This may be an important problem because electronic circuits, if operated near the frequency singularities, can be affected by fluctuating inter-electrode capacitance changes (Von Hippel, 1954; and Greenfield, 1972).

As shown in figure 41, sharp decreases occur in the dielectric constant when the relaxation time of the particular polarization involved becomes equal to or less than the period of the applied field. In general, α_s is effective up to several thousand Hertz; α_d can be effective from 10^4 up to 10^{12} Hz, and even this wide range can be increased further into the low-frequency area by reducing temperatures; α_a becomes effective in the infrared spectrum and α_e in the optical region and above.

6.4.3 Dielectric Strength

The dielectric strengths of insulating materials quoted in manufacturers' literature are based on the statistical average breakdown of constant thickness samples. These values should be used with caution in equipment design for the following reasons:

- a. Variations in manufacturing tolerances.
- b. Variations in material compositions.
- c. The manufacturers' data are based on testing at 23 °C.
- d. Large-area samples may have a few pinholes or voids.
- e. Data are for a small surface area sample.
- f. Voltage transients are rarely considered.
- g. Field stress variations with changes in electrode shapes are not considered.
- h. Aging effects on dielectric strength are not considered.
- i. Changes in material properties due to moisture/humidity

For example, the following four figures from Dunbar (1968), show the effect on the dielectric strength data for Kapton[®]-H film taken at different environmental and mechanical conditions:

Figure 42, Temperature Effects on ac Dielectric Strength of Kapton® Type-H Film, figure 43, High Humidity Effects on the Dielectric Strength of Kapton® Type-H Film, figure 44, Insulation Thickness Effects on Dielectric Strength of Kapton® Type-H Film, and figure 45, Film Area Versus Dielectric Strength of Kapton® Type-H Film.

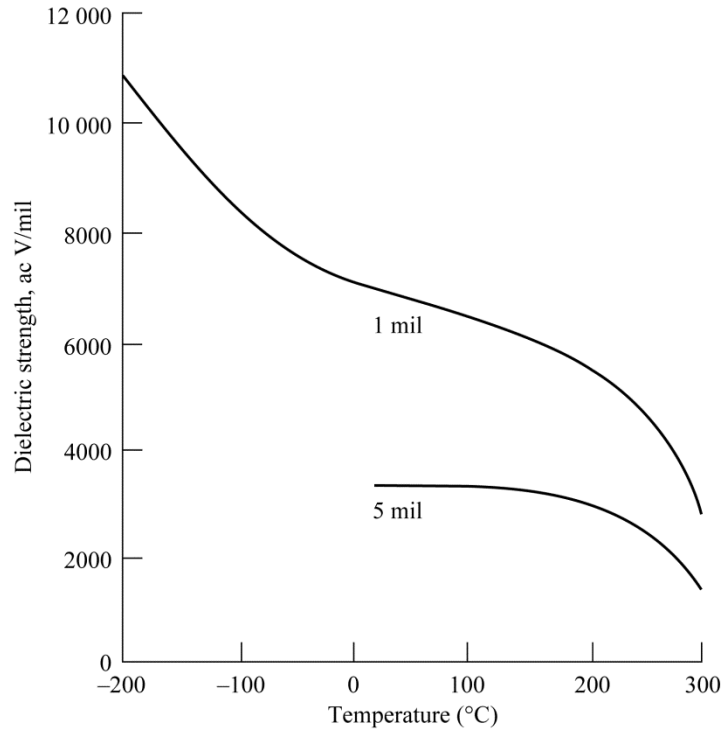


Figure 42—Temperature Effects on ac Dielectric Strength of Kapton® Type-H Film

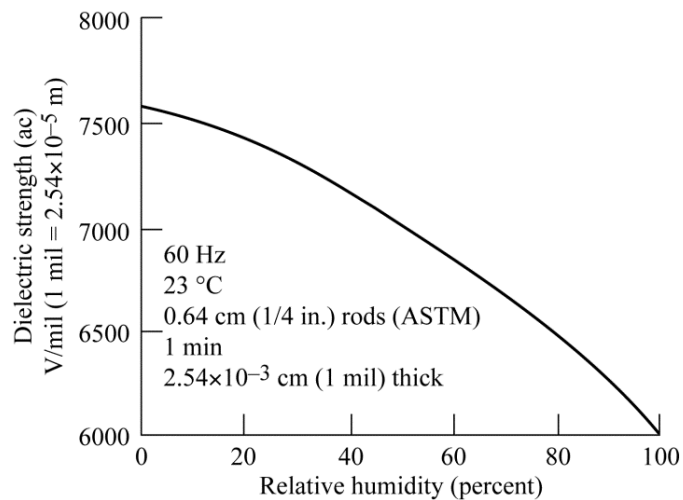


Figure 43—High Humidity Effects on the Dielectric Strength of Kapton® Type-H Film

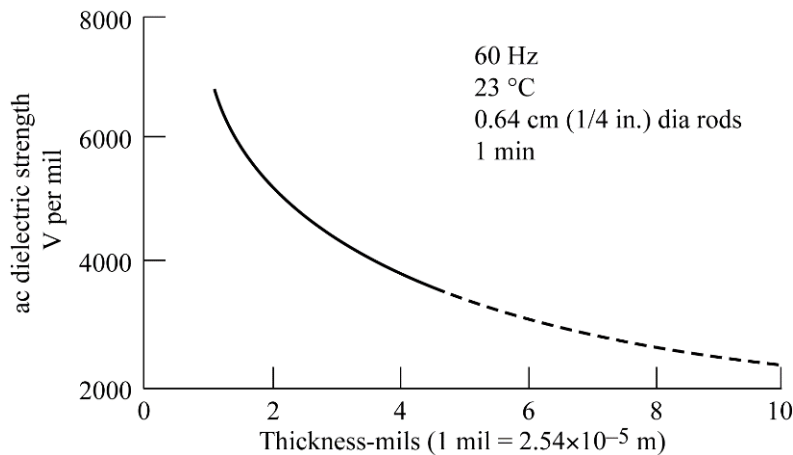


Figure 44—Insulation Thickness Effects on Dielectric Strength of Kapton® Type-H Film

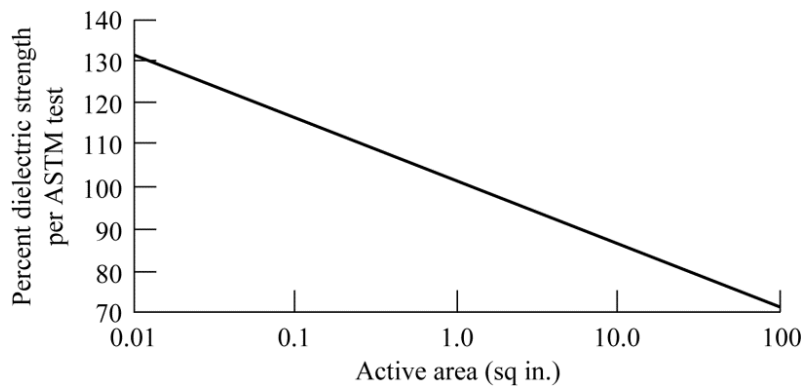


Figure 45—Film Area Versus Dielectric Strength of Kapton® Type-H Film

In spacecraft applications, the highest average operating temperature for a unit is usually specified (60 °C is typical). This temperature should not be taken as the insulation design value. The insulation design temperature has to be that of the hottest point within the equipment. For instance, the hot spot created by high current densities near an electrical component may be as much as 20 °C higher than the nominal temperature in the insulation.

Most insulation test samples are either 1 or 5 mil thick. In high-voltage work, thin insulation has insufficient dielectric strength, often requiring composite insulations having several layers. The dielectric strength (V/mil) of insulation decreases with thickness, as shown in figure 44.

The active surface area of insulation data is often not provided in a manufacturer's literature and data sheets. A deviation of dielectric strength can be caused by roughness of electrode surfaces and non-uniform thickness of the manufactured insulation. Because of these effects, a de-rating of the manufacturer's data is generally needed. For areas of a few square centimeters, a less than

5-percent de-rating of the manufacturer's dielectric strength data is usually sufficient. For large areas, the required de-rating is considerable, as shown in figure 45.

Finally, it should be noted that recent work indicates that many quoted values of dielectric strength are in error as the samples were not properly outgassed, dried out, etc. This has become a particular issue in space applications where materials need to be tested at very low temperatures, high vacuum, and under radiation environments. For a discussion of problems and issues with previous dielectric measurements, see Dennison (2014).

6.4.4 Treeing

The first published treeing experiments were demonstrated by Kitchin and Pratt (1962). In that work, a sharpened sewing needle was partially embedded in a block of polyethylene and used as one of the electrodes. The base of the square block, 2.5 cm by 2.5 cm by 6.5 mm thick, was placed on a metal plate that served as the other electrode. The voltage was adjusted until one half of a group of samples initiated a "tree" within one hour. This was named "the characteristic voltage."

Over the years, investigators have argued about the initiation mechanism of an electrical tree. A probable cause is the bombardment of the surface of the insulation adjacent to a high electrical field stress by high-energy electrons. The source of the electrons may be high-intensity ionization in a void, the field emission from the surface of a point, or the emission from an impurity embedded in a non-homogeneous insulation system.

Treeing is usually associated with a solid organic insulation; therefore, the tree initiates and spreads along the molecular interfaces rather than atomically. Thus, the tree branches may disperse throughout the insulation, eventually resulting in electrical failure. Experimentally, it has been determined that the tree is often initiated by a large electrical pulse inducing charges exceeding 200 pC. Furthermore, partial discharge pulses are recorded as tree branches extend from the initiating point toward the base plate. The branches may move upward as well as downward in their continual path of least resistance toward the ground plane (McMahon, 1978; and Mason, 1960). An example of electrical treeing is shown in figure 46, Electrical Treeing in Plexiglass (author: Bert Hickman). In the figure, high voltage breakdown within a block of plexiglass creates the beautiful fractal pattern known as a Lichtenberg figure. The branching discharges ultimately become hairlike, but are thought to extend down to the molecular lever. While extremely dangerous in high voltage insulation, the effect is often used to create works of art as shown.

There are several types of treeing. Much activity has been given to water tree growth in utility power cables in recent years. In addition, the chemical inclusions of sulfur and other debris have been found to serve as initiators for treeing (Tabata et al., 1971; Dissado et al., 1988; and Steennis and Kreuger, 1990).



Figure 46—Electrical Treeing in Plexiglass (author: Bert Hickman)

6.4.5 Breakdown Between Insulated Wires

In this section we discuss breakdown between insulated wires with respect to CIV and CEV. In figures 47 to 50, we note that for all wire samples the CIV is larger than CEV, as expected. The tests reported here were also used to study temperature effects on aging and a more detailed description of test methodology is given in section 6.4.8.2 below. Twisted-pair insulated conductors have a higher CEV than a single insulated conductor to a ground plane configuration, as shown in figure 47, Corona Initiation and Extinction Voltages of Sample T1, Twisted Pair and Wire-to-Ground Configuration Shown in Figure 11, as a Function of Pressure. An “as-received” wire sample T1 was used in these data. For a twisted pair, there are two dielectrics in series with the gas-filled space between the two insulations on the conductors. When gas breakdown calculations were made, it was found that the effective gas-filled gap was approximately 10 to 30 percent larger between the twisted pair as compared to the insulated wire to ground plane.

The voltage between an insulated conductor and a ground plane is a combination of the voltage across the wire insulation and the voltage across the gap between the wire insulation and the ground plane. The insulation around the conductor has nearly constant thickness, but the gap spacing between the solid dielectric and ground plane may vary from 0.017 cm to over 1 cm at

very low pressure as shown for samples P1 and R3. The CIV and CEV curves for these samples are shown in figure 48, CIV and CEV Data for Sample P1 Type Wire, and figure 49, CIV and CEV Data for Sample R3 Type Wire. When the pd dimension attempts to remain at the Paschen minimum in the varying gap distance, the voltage across the solid dielectric decreases, reducing the insulation effectiveness to a minor role, as shown in figures 48 and 49. The insulation effectiveness is shown for test samples R2 in figure 50, CIV as a Function of Altitude (Pressure) of Sample R2 Aged Several Hours at 304 °C. These data are obtained after 20-h thermal soak at 304 °C before testing at 288 °C.

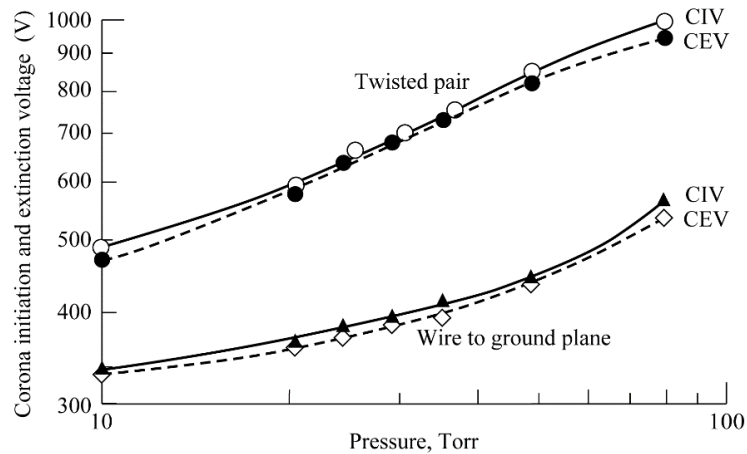


Figure 47—Corona Initiation and Extinction Voltages of Sample T1, Twisted Pair and Wire-to-Ground Configuration Shown in Figure 11, as a Function of Pressure

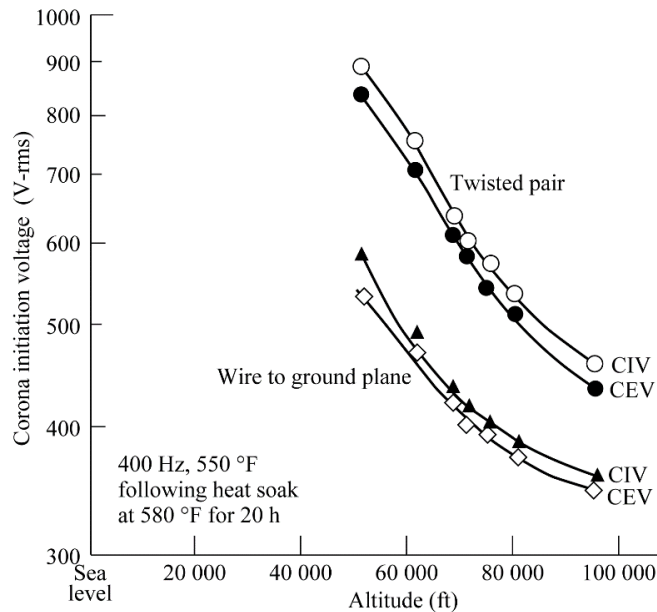


Figure 48—CIV and CEV Data for Sample P1 Type Wire

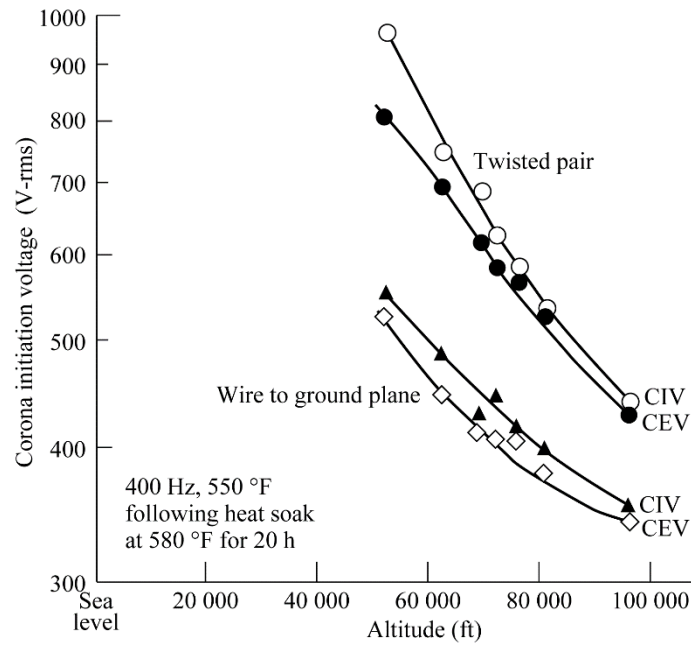


Figure 49—CIV and CEV Data for Sample R3 Type Wire

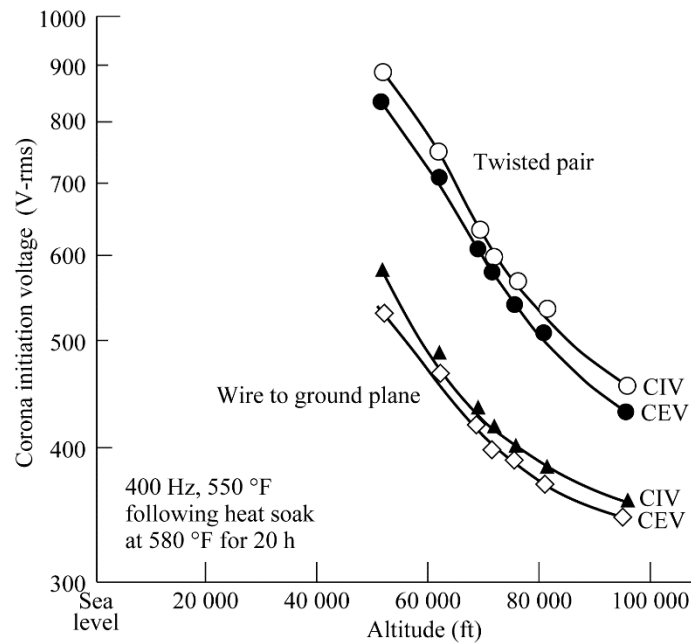


Figure 50—CIV as a Function of Altitude (Pressure) of Sample R2 Aged Several Hours at 304 °C

6.4.6 Resistivity

A high-volume resistivity reduces heating of the dielectric. Values greater than $10^{12} \Omega\text{-cm}$ are adequate for most power equipment. High-voltage insulation should have a volume resistivity greater than $10^{14} \Omega\text{-cm}$. Polyamides in high-voltage service should be operated at temperatures lower than 200°C , as suggested in figure 51, Volume Resistivity of Kapton® Type-H Film at 1 kHz (Dunbar, 1988). Surface resistivity has to be greater than $10^9 \Omega$ to prevent tracking and surface flashover events. New insulations usually have surface resistivities greater than $10^{12} \Omega$ at 23°C and 50 percent RH. This value becomes much lower at higher humidity and temperature values. If the surface resistivity is reduced from $10^9 \Omega$ to $10^8 \Omega$ by contamination, a significant surface leakage current will flow. This will form a “dry band” on the surface of the dielectric. In some cases, the dry band can be bridged by a small electrical discharge when the stress locally exceeds the breakdown stress of air at the air-solid interface. Consequently, local heat from the discharge will decompose the insulation and form a conducting path on the surface. With time, the paths will propagate, forming a tree, and resulting in eventual breakdown (Chapman et al., 1955).

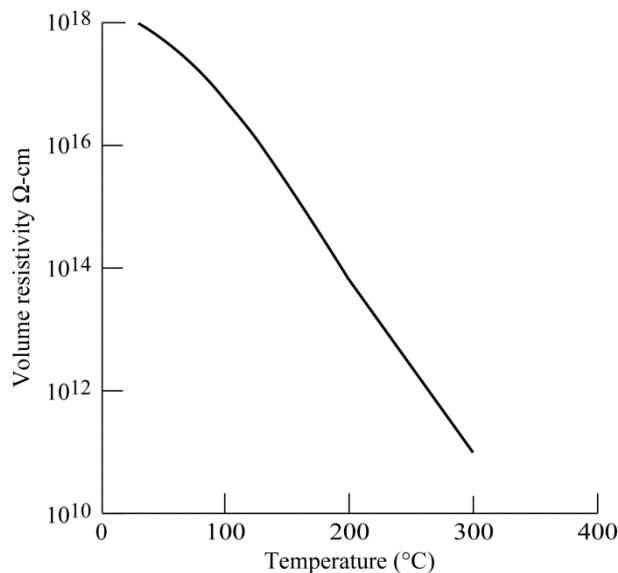


Figure 51—Volume Resistivity of Kapton® Type-H Film at 1 kHz

6.4.7 Temperature Effects

The CIV and the CEV are used to describe the presence of corona, glow discharge, or voltage breakdown in this report. Unfortunately, any sustained discharge will heat the gas locally (around conductors) as well as in enclosed spaces (voids). The resulting temperature rise will change the extinction voltage, thus giving inconsistent results. Therefore, the elapsed time between CIV and CEV is critical to the accuracy of the test results. This effect has less impact in the vicinity of the Paschen minimum. Readings at higher pressure-times-spacing values will be influenced by temperature rise during test.

As an example, the impedance between asbestos-insulated nichrome as a function of temperature and pressure in contaminated MoO_3 gas is shown in figure 52, Impedance of Two-Conductor Shielded Cable in Molybdenum Trioxide Vapor (Dunbar, 1966). The shunt impedance between conductors poses a serious problem for thermocouple wires and instrumentation wiring inside a braided stainless-steel shield.

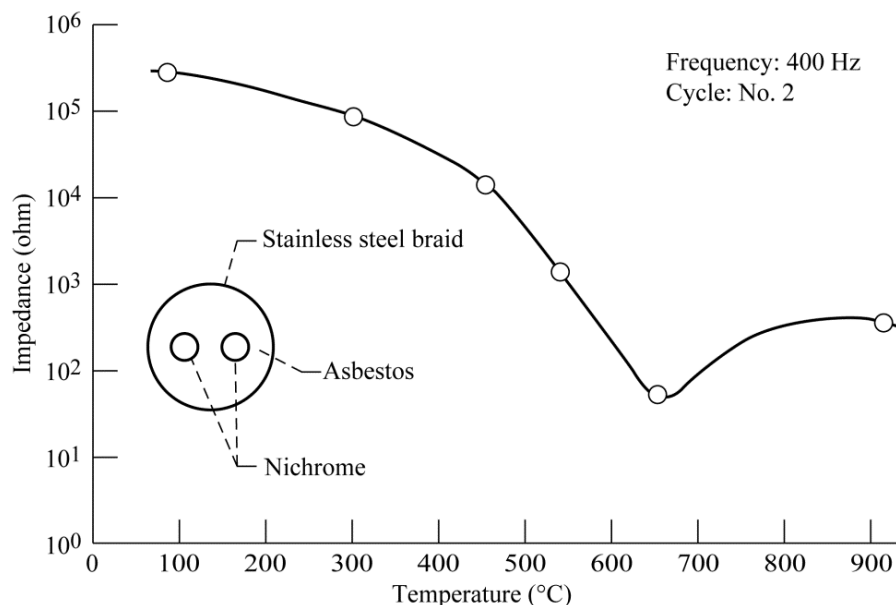


Figure 52—Impedance of Two-Conductor Shielded Cable in Molybdenum Trioxide Vapor

When testing for partial discharges in voids of solid dielectrics, internal temperature rise related to sustained discharges affects CIV and CEV. When the walls of the void are heated by dielectric losses, the insulation outgases, changing the gas pressure and possibly the gas mixture inside the void. This affects the voltage difference between the CIV and CEV across a simple void in a solid dielectric, resulting in test results that are not representative of operational conditions.

6.4.8 Aging

Aging is the end result of chemical and physical changes in electrical materials or electrical systems, resulting from the passage of time. There are several aging processes, such as thermal, electrical, mechanical, radiation, and chemical. Both thermal cycling and chronological aging diminish the dielectric and tensile strengths of dielectric materials and potted compounds. Most early aging studies were performed using thermal stress as the prime degradation process where a 10°C temperature increase above nominal operating conditions for an electrical insulation resulted in 50 percent decrease of life. Aging criteria were refined by the use of the chemical theory of Arrhenius (Dakin et al., 1954), which describes the effects of temperature on the speed of a chemical reaction. There are a number of excellent articles relating aging to temperature and time (Dakin et al., 1954, and Hewitt and Dakin, 1963), and the article by Cooke (1983) shows the changes in the slope of the Arrhenius plot with respect to several insulating materials.

Most manufacturers' data provides only the 1-min dielectric strength test results conducted at 23 °C and 60 Hz between 0.5-in.-diameter electrodes, telling little or nothing about the aging characteristics of the material. Figure 53, Life as a Function of Voltage for Kapton® Type-H Film (Dunbar, 1988), shows aging data for a polyethylene film exposed and unexposed to corona at two different operating temperatures.

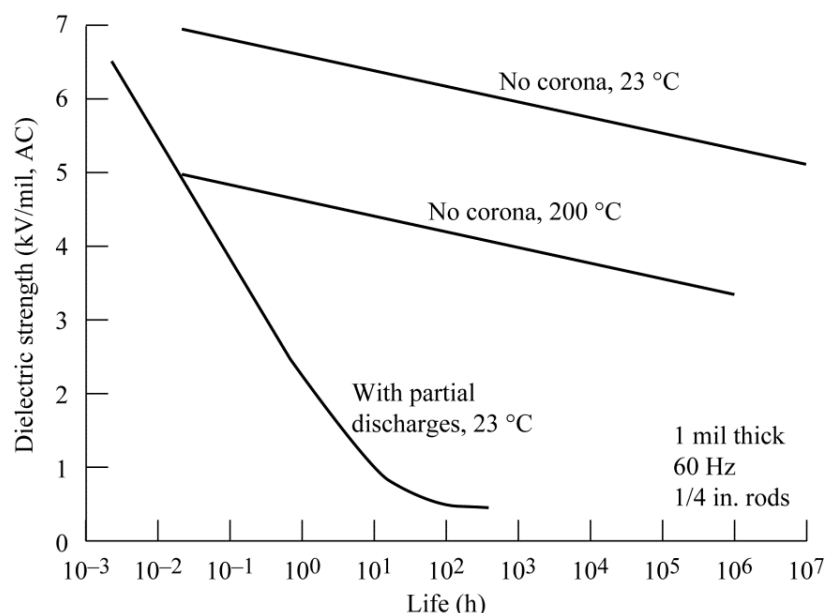


Figure 53—Life as a Function of Voltage for Kapton® Type-H Film

The characteristic life of a material can be evaluated as a function of temperature when data are plotted as Arrhenius plots (figure 54, Heat Reduces the Time for Kapton® Type-H Film to Fall to Half of Original Dielectric Strength). The baseline dielectric strength in figure 54 is 7000 V/mil, for 1 in² at 23 °C, 50 percent RH, and 60 Hz.

Data for a life-temperature plot are obtained as follows:

- a. Numerous samples are kept at constant test temperatures.
- b. Periodically, a few samples are withdrawn, and their breakdown voltages are measured.
- c. When the statistically developed breakdown voltage of the withdrawn samples is 50 percent of the initial 1-min breakdown voltage, the end of life is assumed to be reached for the specific sample at that temperature.

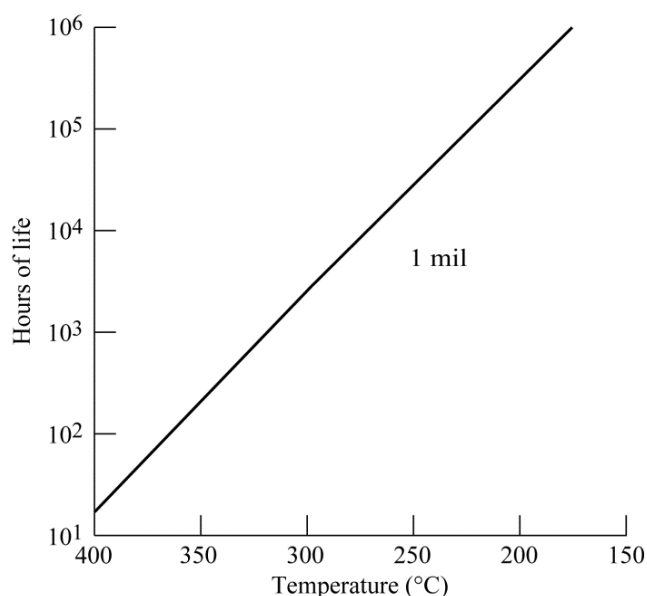


Figure 54—Heat Reduces the Time for Kapton® Type-H Film to Fall to Half of Original Dielectric Strength

Life testing should be conducted at several temperatures to obtain significant, useful data. Table 8 Life Field Stress (1 h) (Dunbar, 1988), shows the maximum field stresses for 1 h of operation of three generic-type encapsulating materials. The lower values are for very thick insulations. Higher values are for insulation less than 10 mil thick.

Table 8—Life Field Stress (1 h)

MATERIALS	MAXIMUM FIELD STRENGTH (V/MIL)
Epoxies	200 to 350
Silastics	300 to 600
Urethanes	250 to 500

Note that the data in table 8 are for 1 h life only, not 10,000 h. To obtain 10,000 h, the maximum stress has to be decreased considerably. The voltage stress has to be decreased by 8 to 10 percent for each order-of-magnitude increase in service life. For 10,000 h, the stress should be decreased to about 65 percent of the values shown in table 8. Figure 55, Insulation Life as a Function of Field Stress (Dunbar, 1988), can be used as a generic curve that may help in design work. This curve shows the voltage stress in V per mil as a function of life. This generalized curve has already included many insulation de-rating factors normal to electronic circuits. Not included are frequency, temperatures greater than 85 °C, and units with volumes greater than 500 in³.

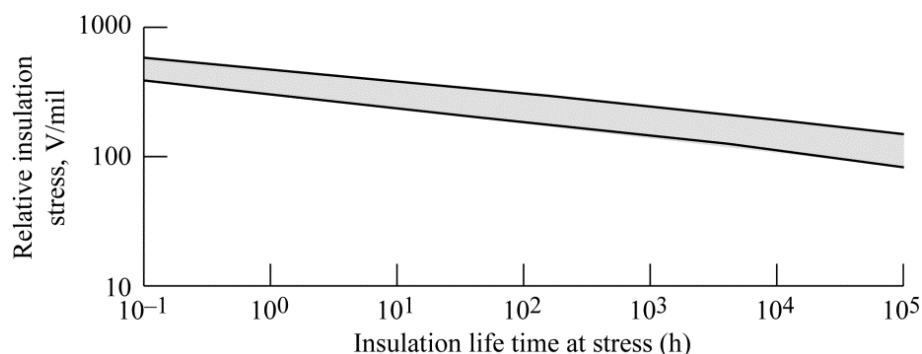


Figure 55—Insulation Life as a Function of Field Stress

Other factors that significantly decrease insulation life are improper materials preparation, encapsulation, bonding, and voids. Use of the term "void-free" to describe an electrically insulated set of electrodes does not imply the insulation is flawless; it means that the insulation is free of any "significantly large" voids. However, as time passes and insulation deteriorates, small voids will increase in size, resulting in higher energy discharges and ultimately in insulation failure.

Another life-degrading factor is frequency. Tests have shown that insulation life is inversely proportion to the ac operating frequency. When frequency, temperature, and voltage stress de-rating factors are all combined, insulation with a rating of 10,000 V for the 1-min test may be reduced to less than a few hundred volts in operational application (Nelson, 1974; Morel et al. 1980; and Montanari and Pattini, 1986). To further demonstrate the life temperature failure rate, the Arrhenius plot of insulation life as a function of temperature is shown in figure 54.

Prediction of material aging is an estimation of probabilities rather than an exact science, because of material chemical composition variables as well as processing and workmanship variables. Finally, there are the aging variables, such as environmental and electromechanical. Therefore, it is readily seen that a simple formulation that may adequately determine the aging quality of a specific material under a specific application may be in error for another material.

6.4.8.1 Multifactor Aging

It became obvious to several researchers that partial discharges and corona degraded polymeric materials much faster than temperature alone (Dakin et al., 1954; Hewitt and Dakin, 1963; Cooke, 1983; Nelson, 1974; Morel et al., 1980; Montanari and Pattini, 1986; Montanari, 1990; Dixon, 1990; Yianakopoulos et al., 1990; Cygan and Laghari, 1990; and Stone et al., 1992).

As a result, many tests and test procedures for material evaluation as well as theoretical analyses and models for materials aging under electrical, temperature, mechanical, radiation, and chemical stress conditions were developed (Montanari, 1990; Dixon, 1990; Yianakopoulos, et al., 1990; Cygan and Laghari, 1990; Stone, et al., 1992; Montanari, 1992; Khachen and Laghari, 1992; Densley, et al., 1993; Kimura, 1993; Simoni, et al.; Bruning and Campbell, 1993; Sanche,

1993; Li and Unsworth, 1994; Khachen and Laghari, 1994; Agarwal, 1995; Montanari, 1995; Galski and Krivda, 1995; and Dissado, et al., 1995).

Most of the data in the literature is for materials used in utility power systems; therefore, it is important for the space industry to evaluate accelerated aging of materials for specialty applications.

6.4.8.2 Temperature Effects on Aging

In general, insulation aging is accelerated at elevated temperatures. Aging effects due to temperature were apparent in the study discussed in section 6.4.5. The test samples in this study consisted of many identical specimens. Each sample type, such as R3 (figure 49), included 10 identical specimens for each temperature setting. One specimen was removed for test evaluation following each 10 percent of total test time until 100 percent test time in thermal and temperature cycling was achieved. The specimens removed were visually inspected; the corona was tested and the sample was then preserved until the end of the test program. Thus, Sample P1 started with 80 specimens for the 8 different temperatures. This accounts for a variation from specimen to specimen related to physical dimension variations during wire manufacture and the mechanical attachment to the corona test fixture.

Samples R2 shown in figure 50 demonstrate corona test results following thermal aging. The information from these data indicates that the CIV decreased somewhat as a function of thermal cycling time. Indeed, one specimen had a melted spot on the insulation, giving it a lower partial discharge reading at the higher temperatures. However, all the undamaged specimens were visually and mechanically tested and passed. Within 20 percent of test time, the specimens at both temperatures failed, and the CIV decreased. The visual test indicated a very roughened surface. Following a mechanical wrap-unwrap test, many cracks were found along the full length of the specimen, indicating failures.

6.4.9 Corona Extinction Voltage as a Function of Composite Materials

The CIV and CEV of insulated wires depend upon the electrical properties of the electrical insulation composition. Parameters for each material of the composite insulation system that are to be considered are dielectric constant, volume resistivity, surface resistivity, and thickness. The other parameters are conductor size, configuration, the environmental pressure, and temperature. Insulated conductor configurations include coaxial, shielded, wire-to-ground plane, twisted pair, and proximity to an adjacent conductor or ground plane. These parametric configurations are to be carefully considered when designing interconnecting wiring.

The ac CIVs for many insulation compositions were also tested during the study referred to above. The metal conductors were all the same diameter to obtain consistent results; however, the insulation materials and processing for each test sample varied by manufacturer. Composite and glass covered insulation systems differed but they appeared to have less variation in CIV as shown in figure 56, Minimum CIV of Several Wire Types and Wire Sizes (Dunbar, 1966). The

single dielectric insulation systems, such as Teflon®-insulated wire, were not affected by the high temperature.

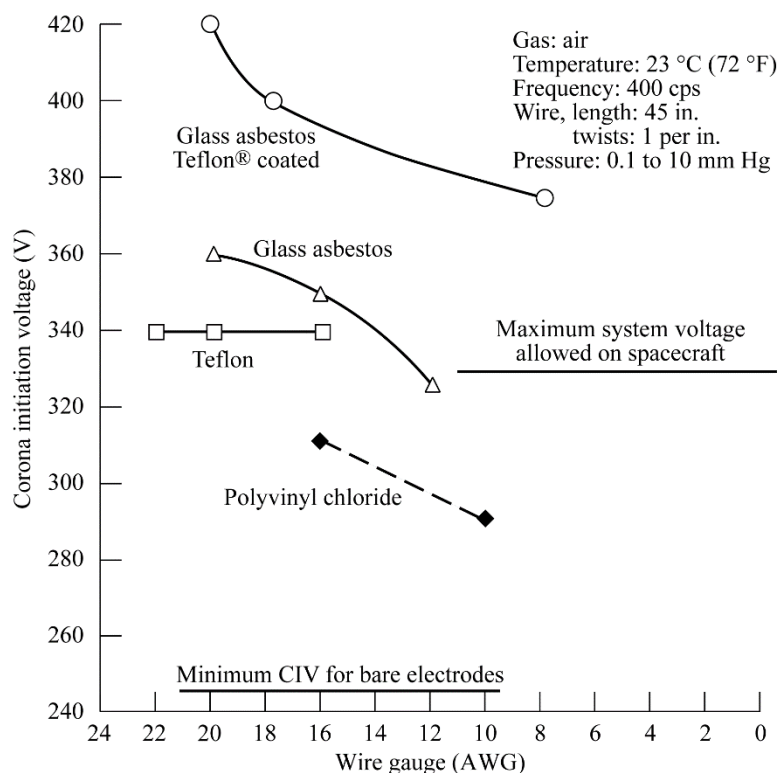


Figure 56—Minimum CIV of Several Wire Types and Wire Sizes

The conductor insulation compositions shown in figure 56 are for specific test samples and may differ somewhat from other test samples of similar composition because of supplier materials and manufacturing processes. Samples with similar thickness were selected to show the effects of dielectric constant when tested with ac. The dc applications are controlled by the volume and surface resistivities rather than by dielectric constant.

6.4.10 Corona Extinction Voltage as a Function of Insulation Thickness

Similar testing with several insulation samples was performed to show the effects of insulation thickness on the CIV/CEV. The greatest variance in insulation thickness was found for composite insulation systems. Significant variances were observed because of the following parameters: the number of Teflon® layers, the type of Teflon® insulations applied to the conductor, and whether the insulations were applied as an outer cover or jacket, all of which led to a wide variance in CEVs, as shown in figure 57, Minimum CIV as a Function of Insulation Thickness.

NASA-HDBK-4007 W/CHANGE 2

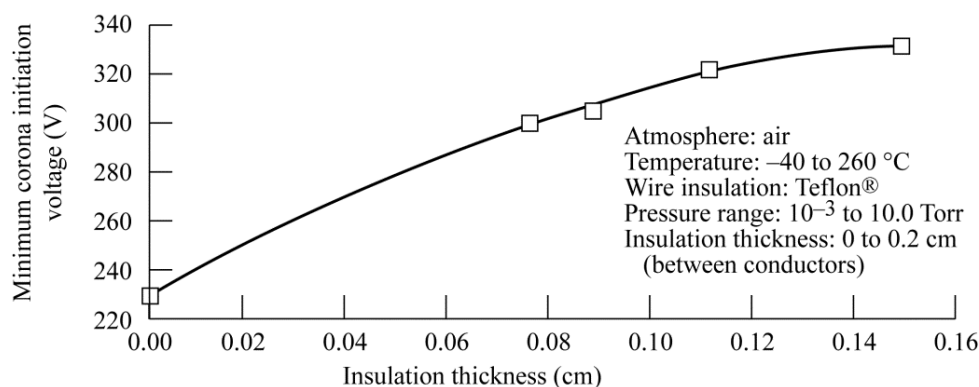


Figure 57—Minimum CIV as a Function of Insulation Thickness

6.5 References

6.5.1 Government Documents

NASA

MSFC-STD-531 High Voltage Criteria

Graves, Timothy P. (2014). *Standard/Handbook for Radio Frequency (RF) Breakdown Prevention in Spacecraft Components*. Air Force Space Command. Aerospace Report No. TOR-2014-02198

6.5.2 Non-Government Documents

Agarwal, V.K.; Banford, H.M.; Bernstein, B.S.; Brancato, E.L.; Fouracre, R.A.; Montanari, G.C.; Parpal, J.L.; Seguin, J.N.; Ryder, D.M.; Tanaka, J. (May/June 1995). "The Mysteries of Multifactor Ageing," *IEEE Electrical Insulation Magazine*. Vol. 11, No. 3, pp. 37-43.

Amjadi, Houman. (2000). "The Mechanism of Voltage Decay in Corona-Charged Layers of Silicon Dioxide During UV Irradiation," *IEEE Transactions on Dielectrics and Electrical Insulation*. Vol. 7, pp. 222-228.

August, G.; Chown, J.B.; Nanevich, J.E. (December 1967). *Rocket Antenna Multipactor Breakdown Under Dynamic Pressure Conditions*. Report Nos. AFCRL-68-0155 and SR-6. Menlo Park, CA: Stanford Research Institute. Available from Stanford Research Institute.

August, G.; Chown, J.B. (April 1969). *Power-Handling Capability of Radiating Systems in the Exoatmosphere*, Final Report. Report No. ESD-TR-69-107. Menlo Park, CA: Stanford Research Institute. Available from Stanford Research Institute.

APPROVED FOR PUBLIC RELEASE—DISTRIBUTION IS UNLIMITED

NASA-HDBK-4007 W/CHANGE 2

August, G.; Chown, J.B. (June 1970). *Reduction of Gas-Discharge Breakdown Threshold in the Ionosphere Due to Multipacting*. Published in Proceedings of the Second Workshop on Voltage Breakdown in Electronic Equipment at Low Air Pressure, March 1969; Report No. JPL-TM-33-447, Pasadena, CA: Jet Propulsion Laboratory, p. 193.

Bashara, N.M.; Green, F.M.; Lederer, D. (March 1965). "Pulse Height and Temporal Distribution at Dielectric Surfaces under Corona," *IEEE Transactions on Electrical Insulation*. Vol. EI-1, No. 1, pp. 12-18.

Bewley, Loyal Vivian. (1948). *Two-Dimensional Fields in Electrical Engineering*. New York, NY: Macmillan Co.

Billings, Malcolm J.; Humphreys, Keith W. (August 1968). "An Outdoor Tracking and Erosion Test of Some Epoxide Resins," *IEEE Transactions on Electrical Insulation*. Vol. EI-3, No. 3, pp. 62-70.

Billings, M.J.; Smith, A.; Wilkins, R. (December 1967). "Tracking in Polymeric Insulation," *IEEE Transactions on Electrical Insulation*. Vol. EI-2, No. 3, pp. 131-136.

Billings, Malcolm J.; Warren, Leonard; Wilkins, Robert. (June 1971). "Thermal Erosion of Electrical Insulating Materials," *IEEE Transactions on Electrical Insulation*. Vol. EI-6, No. 2, pp. 82-90.

Birks, J.B.; Schulman, James Herbert. (1959). *Progress in Dielectrics*. Vol. 1, New York, NY: John Wiley & Sons, Inc.

Bourat, C.; Joly, J-M. (December 1989). "On Multipactor Effect in a 600 MHz rf Cavity Used in Electron Linear Accelerator," *IEEE Transactions on Electrical Insulation*. Vol. 24, No. 6, p. 1045.

Bowers, A.; Cath, P.G. (1941). *The Maximum Electrical Field Strength for Several Simple Electrode Configurations*. Philips Technical Review. No. 6, p. 270.

Bruning, A.M.; Campbell, F.J. (October 1993). "Aging in Wire Insulation under Multifactor Stress," *IEEE Transactions on Electrical Insulation*. Vol. 28, No. 5, pp. 729-754.

Buchalla, H.; Hund, R.; Koch, H.; Pfeiffer, W. (June 1992). *Long Time Exposure Influence of Partial Discharge (PD) to Coated Printed Circuit Boards*. Conference Record of the 1992 IEEE International Symposium on Electrical Insulation. Baltimore, MD.

Bunker, E.R., Jr., Ed. (1966). *Proceedings of the Workshop on Voltage Breakdown in Electronic Equipment at Low Air Pressures*. Report No. Technical Memo 33-80. Pasadena, CA: Jet Propulsion Laboratory.

NASA-HDBK-4007 W/CHANGE 2

Bunker, E.R., Jr., Ed. (June 1970). *Proceedings of the Second Workshop on Voltage Breakdown in Electronic Equipment at Low Air Pressure*. Report Nos. JPL-TM-33-447. Washington, DC: National Aeronautics and Space Administration.

Chapman, J.J.; Frisco, L.J.; Smith, J.S. (July 1955). "Dielectric Failure of Volume and Surface Types," American Institute of Electrical Engineers. Transactions, Communications and Electronics, Vol. 74, pt. I, No. 3, pp. 349-356.

Cooke, C.M. (1983). *Accelerated Aging to Estimate Life of Short Cable Assemblies*. Paper presented at Conference on Electrical Insulation and Dielectric Phenomena. 16-20 October 1983, Buck Hill Falls, PA.

Cygan, P.; Laghari, J.R. (October 1990). "Models for Insulation Aging under Electrical and Thermal Multistress," *IEEE Transactions on Electrical Insulation*. Vol. 25, No. 5, pp. 923-934.

Dakin, T.A.; Mullen, G.A. (December 1972). "Continuous Recording of Outdoor Insulator Surface Conductance," *IEEE Transactions on Electrical Insulation*. Vol. EI-7, No. 4, pp. 169-175.

Dakin, T.W.; Philofsky, H.M.; Divens, W.C. (May 1954). *Effect of Electric Discharges on the Breakdown of Solid Insulation*. Paper presented at the AIEE Winter General Meeting. Paper No. 54-70, New York, NY, p. 155.

Damas, M.C.; Robiscoe, R.T. (1988). "Detection of Radio-Frequency Signals Emitted by an Arc Discharge," *Journal of Applied Physics*. Vol. 64, pp. 566-574.

Dennison, J.R. "The Dynamic Interplay Between Spacecraft Charging, Space Environment Interactions and Evolving Materials", 13th Spacecraft Charging Technology Conference, Pasadena, CA, 2014

Densley, J.; Bartnikas, R.; Bernstein, B.S. (January/February 1993). "Multi-Stress Ageing of Extruded Insulation Systems for Transmission Cables," *IEEE Electrical Insulation Magazine*. Vol. 9, No. 1, pp.15-17.

Dissado, L.; Mazzanti, G.; Montanari, G.C. (December 1995). "The Incorporation of Space Charge Degradation in the Life Model for Electrical Insulating Materials," *IEEE Transactions on Dielectrics and Electrical Insulation*. Vol. 2, No. 6, pp. 1147-1158.

Dissado, L.A.; Wolfe, S.V.; Filippini, J.C.; Meyer, C.T.; Fothergill, J.C. (1988). "An Analysis of Field-dependent Water Tree Growth Models," *IEEE Transactions on Electrical Insulation*. Vol. 23, No. 3, pp. 345-356.

Dixon, Robert R. (August 1990). "Environmental Aging of Insulating Materials," *IEEE Transactions on Electrical Insulation*. Vol. 25, No. 4, pp. 667-671.

APPROVED FOR PUBLIC RELEASE—DISTRIBUTION IS UNLIMITED

NASA-HDBK-4007 W/CHANGE 2

Dunbar, W.G. (1966). *Corona Onset Voltage of Insulated and Bare Electrodes in Rarefied Air and Other Gases; Final Report, Jul.-Dec. 1965*. Report No. AFAPL-TR-65-122. Wright-Patterson Air Force Base, OH: Air Force Aero Propulsion Laboratory.

Dunbar, W.G. (1983). High Voltage Design Guide. Report No. AFWAL-TR-82-2057-VOL-4. Wright-Patterson Air Force Base, OH: Air Force Wright Aeronautical Laboratory.

Dunbar, William G. (August 1988). Design Guide: *Designing and Building High Voltage Power Supplies, Volume 2; Topical Interim Report*. Report No. AFWAL-TR-88-4143-Volumes I and II. Wright-Patterson Air Force Base, OH: Air Force Wright Aeronautical Laboratories.

Dunbar, W.G., Schweickart, D.L.; Horwath, J.C.; Walko, L.C., "High Frequency Breakdown Characteristics of Various Electrode Geometries in Air," Proceedings of the 23rd International Power Modulator Symposium. Rancho Mirage, CA, 22-25 June 1998, pp.221-224.

Frisco, L.J.; Chapman, J.J. (April 1956). "The Flashover Strength of Solid Dielectrics," *Power Apparatus and Systems, Part III. Transactions of the American Institute of Electrical Engineers*. Vol. 75, pt. III, pp. 77-83.

Galan, L.; Moranti, C.; Rueda, F.; Sanz, J.M. (1988). *Study of Secondary Emission Properties of Materials Used for High Power RF Components in Space; Final Report*. Report No. ESA-CR(P)-2587. Paris, France: European Space Agency.

Galstjan, Eugene A.; Ravaev, Alexander A. (April 1995). "Microwave Surface Flashover of Dielectrics in Vacuum," *IEEE Transactions on Dielectrics and Electrical Insulation*. Vol. 2, No. 2, pp. 312-316.

Given, M.J.; Banford, H.M.; Mackersie, J.; Fouracre, R.A. (2000). *Radiation Effects in Polyimide Foils Subjected to a Simulated Space Environment*. Paper presented at the Conference on Electrical Insulation and Dielectric Phenomena. Victoria, BC, pp. 768-771.

Greenfield, Eugene W. (1972). *Introduction to Dielectric Theory and Measurements*. Pullman, WA: Washington State University.

Gulski, Edward; Krivda, Andrej. (August 1995). "Influence of Aging on Classification of PD in HV Components," *IEEE Transactions on Dielectrics and Electrical Insulation*. Vol. 2, No. 4, pp. 676-684.

Harwood, J.J. (1958). *The Metal Molybdenum*. Cleveland, OH: American Society of Metals.

He, D.; Hall, D.R. (May 1984). "Frequency Dependence in RF Discharge Excited Waveguide CO₂ Lasers," *IEEE Journal of Quantum Electronics*. Vol. QE-20, No. 5, pp. 509-514.

NASA-HDBK-4007 W/CHANGE 2

Herlin, Melvin A.; Brown, Sanborn C. (1948). "Breakdown of a Gas at Microwave Frequencies," *Physical Review*. Vol. 74, No. 3, pp. 291-296.

Hewitt, G.W.; Dakin, T.W. (December 1963). "Voltage Endurance Tests of Insulating Materials Under Corona Conditions," *IEEE Transactions on Power Apparatus and Systems*. Vol. 82, No. 69, pp. 1033-1039.

Hughes Aircraft Company (July 1966). *The Study of Multipactor Breakdown in Space Electronic Systems*. Report No. NASA CR-448, Washington, DC: National Aeronautics and Space Administration.

Ishimaru, A.; Woo, R. (December 1967). "A Similarity Principle for Multipacting Discharges," *Journal of Applied Physics*. Vol. 38, pp. 5240-5244.

Khachen, W.; Laghari, J.R. (October 1992). "Estimating Lifetime of PP, PI and PVDF under Artificial Void Conditions Using Step-stress Tests." *IEEE Transactions on Electrical Insulation*. Vol. 27, No. 5, pp. 1022-1025.

Khachen, W.; Laghari, J.R. (December 1994). "Determination of Aging-model Constants under High Frequency and High Electric Fields," *IEEE Transactions on Dielectrics and Electrical Insulation*. Vol. 1, No. 6, pp. 1034-1038.

Kimura, Ken. (May/June 1993). "Progress of Insulation Ageing and Diagnostics of High Voltage Rotating Machine Windings in Japan," *IEEE Electrical Insulation Magazine*. Vol. 9, No. 3, pp. 13-20.

Kind, Dieter; Karner, Hermann. (1985). *High-Voltage Insulation Technology: Textbook for Electrical Engineers*. Braunschweig, Germany: Friedrich Vieweg Und Sohn Publishing.

Kitchin, D.W.; Pratt, O.S. (June 1962). "An Accelerated Screening Test for Polyethylene High-Voltage Insulation," Paper No. 62-54, *Transactions of the AIEE*. Vol. 81.

Korzekwa, R.; Lehr, M.; Krompholz, H.; Kristiansen, M. (August 1989). "Inhibiting Surface Flashover With Magnetic Fields," *IEEE Conference Publications*. Vol. 1, pp. 441-445.

Krieg, J.F.; Neerman, C.J.; Savage, M.W.; Titus, J.L.; Emily D.; Dunham, G.W.; Van Vonno, N.; Swonger, J. (December 2000). "Comparison of Total Dose Effects on a Voltage Reference Fabricated on Bonded-Wafer and Polysilicon Dielectric Isolation," *IEEE Transactions on Nuclear Science*. Vol. 47, No. 6, pp. 2561-2567.

Kurtz, Mo. (June 1971). "Comparison of Tracking Test Methods," *IEEE Transactions on Electrical Insulation*. Vol. EI-6, No. 2, pp. 76-81.

Labrum, N.R. (1947). *Investigation of the Breakdown of Gases by Pulsed Radio-Frequency Electric Fields*. Australia: Council for Scientific and Industrial Research. Report No. C.S.I.R. Australia RPR 85.

APPROVED FOR PUBLIC RELEASE—DISTRIBUTION IS UNLIMITED

NASA-HDBK-4007 W/CHANGE 2

Lassen, H. (1931). "Frequency Dependence of the Breakdown Voltage in Air," *Archiv Fur Elektrotechnik*. Vol. 25, pp. 322-332.

Lee, C.; Lim, K.J.; Park, Y.G.; Ryu, B.H. (2000). *Radiation Effects on Electrical Treeing Resistance and Mechanical Characteristics of Low Density Polyethylene Containing Barbituric Acid Derivatives*. Proceedings of the 6th International Conference on Properties and Applications of Dielectric Materials. Vol. 1, pp. 501-504.

Lewis, D.J.; McCarty, D.K. (April 1966). "Multipactor Effects in X-Band Waveguide Slots," *Proceedings of the IEEE*. Vol. 54, pp. 713-714.

Li, Y.; Unsworth, J. (February 1994). "Effect of Physical Aging on Dielectric, Thermal and Mechanical Properties of Cast-epoxy Insulators," *IEEE Transactions on Dielectrics and Electrical Insulation*. Vol. 1, No. 1, pp. 9-17.

Loeb, Leonard B. (1965). *Electrical Coronas, Their Basic Physical Mechanisms*. Berkeley, CA: University of California Press.

Luck, R. (June 1967). High Voltage Design Guide for Spacecraft. Department, General Electric Spacecraft Department. Document No. S30110

MacDonald, A.D.; Brown, Sanborn C. (1949). "High Frequency Gas Discharge Breakdown in Helium," *Physical Review*. Vol. 75, No. 3, pp. 411-418.

Mackersie, J.W.; Given, M.J.; MacGregor, S.J.; Fouracre, R.A. (2001). *Gamma Radiation Effects in Polyethylene Naphthalate—Electrical Properties*. Paper presented at the Annual Conference on Electrical Insulation and Dielectric Phenomena. Waterloo, pp. 183-187.

Mason, J.H. (December 1960). "The Resistance of Sheet Insulation on Surface Discharges," *Power Engineering*. Vol. 107A, pp. 551-563.

Mattingley, J.M.; Ryan, H.M. (1973). *Correlation of Breakdown in Compressed Air and SF6 for Non-uniform Fields*. Paper presented at Conference on Electrical Insulation and Dielectric Phenomena. National Academy of Sciences, Washington, DC, pp. 222-233.

McMahon, Eugene J. (1978). "A Tutorial on Treeing," *IEEE Transactions on Electrical Insulation*. Vol. EI-13, No. 4, p. 277.

Meek, J.M.; Craggs, J.D. (1978). *Electrical Breakdown of Gases*. New York, NY: John Wiley & Sons, Inc.

Mohr, H.J.; Putz, J.L. (August 1966). *X-Band Multipactor Switch Final Report*. Report No. 66-CA-268. Palo Alto, CA: Varian Associates.

APPROVED FOR PUBLIC RELEASE—DISTRIBUTION IS UNLIMITED

NASA-HDBK-4007 W/CHANGE 2

Montanari, Gian Carlo. (October 1992). "Electrical Life Threshold Models for Solid Insulating Materials Subjected to Electrical and Multiple Stresses: Investigation and Comparison of Life Models," *IEEE Transactions on Electrical Insulation*. Vol. 27, No. 5, pp. 974-986.

Montanari, G.C. (August 1995). "Aging and Life Models for Insulation Systems Based on PD Detection," *IEEE Transactions on Dielectrics and Electrical Insulation*. Vol. 2, No. 4, pp. 667-675.

Montanari, G.C.; Pattini, G. (February 1986). "Thermal Endurance Evaluation of Insulating Materials: A Theoretical and Experimental Analysis," *IEEE Transactions on Electrical Insulation*. Vol. EI-21, No. 1, p. 69.

Montanari, Gian Carlo. (April 1990). "A New Thermal Life Model Derived by the Aging Compensation Effect," *IEEE Transactions on Electrical Insulation*. Vol. 25, No. 2, p. 309.

Moore, A.D. (1927a). *Fundamentals of Electric Design*. New York, NY: McGraw-Hill Book Co.

Moore, A.D. (1927b). "Mapping Techniques Applied to Fluid Mapper Patterns," *AIEE Transactions*. Vol. 71.

Morel, J.F.; Dung, Phung Nhu; Joly, J.C. (August 1980). "Thermal Aging of Bi-Axially Oriented PET Films: Relation Between Structural Changes and Dielectric Behavior," *IEEE Transactions on Electrical Insulation*. Vol. EI-15, No. 4, p. 335.

Nanevicz, J.E.; Vance, E.F. (December 1967). *Multipactor Discharge Experiments*. Report No. AFRCL-68-0083. Palo Alto, CA: Stanford Research Institute.

Nelson, Wayne. (March 1974). "A Survey of Methods for Planning and Analyzing Accelerated Tests," *IEEE Transactions on Electrical Insulation*. Vol. EI-9, No. 1, p. 12.

Orbeck, T.; Niemi, R.F. (1973). *Study of Surface Leakage Current and "Dry-Band-Arcing" on Synthetic Insulation Materials and Porcelain Under Wet High Voltage Conditions*. Paper presented at the Conference on Electrical Insulation and Dielectric Phenomena, 1973 Annual Report, pp. 43-50.

Paschen, Friedrich. (1889). "Ueber die zum Funkenubergang in Luft, Wasserstoff und Kohlensaure bei Verschiedenen Drucken Erforderliche Potentialdifferenz," *Annalen der Physik*. Vol. 37, pp. 69-96.

Pfeiffer, W. (April 1991a). "High-frequency Voltage Stress of Insulation: Methods of Testing," *IEEE Transactions on Electrical Insulation*. Vol. 26, No. 2, p. 239.

Pfeiffer, Wolfgang. (April 1991b). "Partial-discharge Testing of Components for Low-voltage Equipment," *IEEE Transactions on Electrical Insulation*. Vol. 26, No. 2, p. 247.

APPROVED FOR PUBLIC RELEASE—DISTRIBUTION IS UNLIMITED

NASA-HDBK-4007 W/CHANGE 2

Pfeiffer, W.; Richter, K.; Schau, P.V. (1987). "Electric Strength of Small Insulating Distances," *IEEE Transactions on Electrical Insulation*. Vol. EI-22, No. 4, pp. 397-404.

Pim, J.A. (1949). "The Electrical Breakdown Strength of Air at Ultra-High Frequencies," *Proceedings of the Institute of Electrical Engineers*. Vol. 96, pt. III, pp. 117-137.

Prowse, W.A. (November 1950). "The Initiation of Breakdown in Gases Subject to High Frequency Electric Fields," *Journal of the British Institution of Radio Engineers*. Vol 10, issue 11, pp. 333-347.

Ryan, H. McL. (1967). "Prediction of Alternating Sparking Voltages for a Few Simple Electrode Systems by Means of a General-Discharge-Law Concept," *Proceedings of the Institute of Electrical and Electronics Engineers*. Vol. 114, pp. 1815-1821.

Ryan, H. McL.; Walley, C.A. (1967). "Field Auxiliary Factors for Simple Electrode Geometries," *Proceedings of the Institute of Electrical and Electronics Engineers*. Vol. 114, pp. 1529-1536.

Saito, Y. (April 1995). "Surface Breakdown Phenomena in Alumina rf Windows," *IEEE Transactions on Dielectrics and Electrical Insulation*. Vol. 2, No. 2, pp. 243-250.

Saito, Y.; Matuda, N.; Anami, S.; Kinbara, A.; Horikoshi, G.; Tanaka, J. (December 1989). "Breakdown of Alumina RF Windows," *IEEE Transactions on Electrical Insulation*. Vol. 24, No. 6, pp. 1029-1032.

Sanche, Leon. (October 1993). "Electronic Aging and Related Electron Interactions in Thin-film Dielectrics," *IEEE Transactions on Electrical Insulation*. Vol. 28, No. 5, pp. 789-819.

Sato, N.; Haydon, S.C. (1984a). "Time-Resolved Observations of RF Corona in Air and Nitrogen," *Journal Physics Digest: Applied Physics*. Vol. 17, pp. 2009-2021.

Sato, N.; Haydon, S.C. (1984b). "Nanosecond Time-Resolved Spectroscopic Investigations of RF Corona With High Spatial Resolution," *Journal Physics Digest: Applied Physics*. Vol. 17, pp. 2023-2036.

Schwaiger, Anton; Sorensen, Royal Wasson. (1932). *Theory of Dielectrics*. New York, NY: John Wiley & Sons, Inc.

Seebok, R.J.; Kohler, W.E. (1988). "Temporal Intensity Modulation of Spectral Lines in a Low-Frequency Discharge in Argon," *Journal of Applied Physics*. Vol. 64, No. 8, pp. 3855-3862.

Simoni, L.; Mazzanti, G.; Montanari, G.C.; Lefebvre, L. (June 1993). "A General Multi-stress Life Model for Insulating Materials with or without Evidence of Thresholds," *IEEE Transactions on Electrical Insulation*. Vol. 28, No. 3, pp. 349-364.

NASA-HDBK-4007 W/CHANGE 2

Smythe, William Ralph. (1968). *Static and Dynamic Electricity*. New York, NY: McGraw-Hill Book Co.

Steennis, E.F.; Kreuger, F.H. (October 1990). "Water Treeing in Polyethylene Cables," *IEEE Transactions on Electrical Insulation*. Vol. 25, No. 5, pp. 989-1028.

Stojadinovic, N.; Djoric-Veljkovic, S.; Manic, I.; Davidovic, V.; Golubovic, S. (2001). *Effects of Elevated-Temperature Bias Stressing on Radiation Response in Power VDMOSFETs*. Paper presented at the 8th Annual International Symposium on Physical and Failure Analysis of Integrated Circuits, pp. 243-248.

Stone, G.C.; van Heeswijk, R.G.; Bartnikas, R. (April 1992). "Electrical Aging and Electroluminescence in Epoxy under Repetitive Voltages Surges," *IEEE Transactions on Electrical Insulation*. Vol. 27, No. 2, pp. 233-244.

Stratton, Julius Adams. (1941). *Electromagnetic Theory*. New York, NY: McGraw-Hill Book Co.

Suganomata, Shinji; Ishikawa, Itsuo; Ohmoto, Shinichiro; Akitsu, Tetsuya; Saito, Yukinori. (1989). "Spatiotemporal Variation of Light Emission From SF₆ Parallel-Plate Discharge at Frequencies of 100 and 500 kHz," *Japan Journal of Applied Physics*. Vol. 28, pp. L2265-L2266.

Tabata, Toshio; Nagai, Hiroshi; Fukuda, Teruo; Iwata, Zensuke. (1971). *Sulfide Attack and Treeing of Polyethylene Insulated Cables—Cause and Prevention*. Paper presented at the IEEE Summer Meeting and International Symposium on High Power Testing Transactions. Paper No. 71 TP 551-PWR, Portland, OR.

Toriyama, Yotsuo; Okamoto, Hideo; Kanazashi, Motonori. (September 1971). "Breakdown of Insulating Materials by Surface Discharge," *IEEE Transactions on Electrical Insulation*. Vol. EI-6, No. 3, pp. 124-129.

Vaughn, J.R.M. (November 1968). "Observations of Multipactor in Magnetrons," *IEEE Transactions on Electron Devices*. Vol. ED-15, pp. 883-889.

Vlieks, A.E.; Allen, M.A.; Callin, R.S.; Fowkes, W.R.; Hoyt, E.W.; Lebacqz, J.V.; Lee, T.G. (December 1989). "Breakdown Phenomena in High-power Klystrons," *IEEE Transactions on Electrical Insulation*. Vol. 24, No. 6, pp. 1023-1028.

Von Hippel, Arthur R. (1954). *Dielectric Materials and Applications*. New York, NY: John Wiley & Sons, Inc. Chapter 3.

Wachowski, H.M. (May 1964). *Breakdown in Waveguides Due to the Multipactor Effect*. Report No. TDR-269/9990/-5. El Segundo, CA: Aerospace Corporation.

APPROVED FOR PUBLIC RELEASE—DISTRIBUTION IS UNLIMITED

NASA-HDBK-4007 W/CHANGE 2

Wallace, C.F.; Bailey, C.A. (December 1967). "Dip-Track Test," *IEEE Transactions on Electrical Insulation*. Vol. EI-2, No. 3, pp. 137-140.

Walter, John E.; Hershberger, W.D. (1946). "Absorption of Microwaves by Gases, II." *Journal of Applied Physics*. Vol. 17, No. 10, p. 814.

Weber, Ernst. (1950). *Electromagnetic Fields*. New York, NY: John Wiley & Sons, Inc.

Woo, Richard (1968a). "Multipacting Discharges Between Coaxial Electrodes," *Journal of Applied Physics*. Vol. 39, No. 3.

Woo, R. (April 1968b). "Multipacting Breakdown in Coaxial Transmission Lines," *Proceedings of the IEEE*. Vol. 56, pp. 776-777.

Wu, C.T.; Cheng, T.C. (June 1978). "Formation Mechanisms of Clean Zones During the Surface Flashover of Contaminated Surfaces," *IEEE Transactions on Electrical Insulation*. Vol. EI-13, No. 3, pp. 149-156.

Yianakopoulos, G.; Vanderschueren, J.; Niezette; Thielen, A. (August 1990). "Influence of Physical Aging Processes on Electrical Properties of Amorphous Polymers," *IEEE Transactions on Electrical Insulation*. Vol. 25, No. 4, pp. 693-701.

7. DESIGN APPLICATIONS

7.1 Introduction

The primary purpose of an electrical insulation is to isolate one conducting surface from another and from their surroundings, restricting current flow to the conductors. Many insulation designs have the additional functions of supporting the parts and structural components in their exact position to eliminate electric field overstresses from vibration, shock, and structural deformations. They also serve in efficient heat transfer from the parts to a thermal controlled surface. High-power, high-voltage spacecraft equipment is densely packaged, and the denser the packaging is, the more functions the electrical insulation is required to perform.

7.2 Materials and Processes

Encapsulated electronic circuits incorporate a wide variety of materials about which the designer should be knowledgeable. The designer should know the mechanical, thermal, and electrical properties of each material used in the potted circuit and should be aware of the compatibility between the materials associated with all parts, components, and structural members.

Encapsulating materials are critical to proper and reliable operation and aging of the electronic circuits. They provide the electrical insulation between parts of different voltages and provide a thermal path for transfer of heat from the heat-generating sources. Proper selection and application of the encapsulating material is critical to the success of the manufacturer's design.

APPROVED FOR PUBLIC RELEASE—DISTRIBUTION IS UNLIMITED

NASA-HDBK-4007 W/CHANGE 2

Because improper selection or application are the source of many of problems, it is important that the manufacturer has a thorough understanding of the encapsulating material and processing.

Each manufacturer has preferred material selection and processing techniques based on the application and design. It is best to evaluate these processes for each application before a design starts. One supplier may be a specialist in one material and processing, therefore this supplier should be considered first. A study related to these issues can be found in Harper et al. (1979) and Dunbar (1988).

The epoxy and silicone materials described in Harper et al. (1979) and Dunbar (1988) are both complicated and difficult to use. They are best avoided unless absolutely necessary and have been qualified to be used in specific applications. The materials used in Hughes/Northrop Grumman (December 1995) are well defined and easily applied with minimum development by materials engineers.

7.3 Pressure Sensing

Some equipment is pressure sensitive and is designed to operate only at high vacuum, for example, at pressures less than $1.33 \times 10^{-3} \text{ N/m}^2$ (1×10^{-5} Torr). Therefore, it is recommended that pressure switches be installed in the flight vehicle to shut down the experiment at higher pressures, that is, pressures greater than $1.33 \times 10^{-3} \text{ N/m}^2$ (1×10^{-5} Torr).

When pressure sensors are installed near equipment containing gases other than air, the pressure sensors may require calibration in a gaseous mixture similar to that anticipated in operation. For instance, the continuous leakage of gas A and the purging of gas B and/or gas C may result in a unique mixture, which may require the pressure sensors to be calibrated for that particular gaseous mixture.

If operational requirements or test protocols permit, pressure-sensitive equipment should be powered down whenever pressure approaches the Paschen minimum. Equipment that must operate near the minimum should be carefully monitored and will need to be de-energized as rapidly as possible if a pressure surge occurs. There should be a requirement that the pressure sensors have inputs to the power system automatic control system, if one exists, so that the pressure-sensitive equipment can be turned off in time to prevent permanent damage. Override control circuitry should be installed to compensate for a failed pressure sensor circuit.

Instrumentation computer space, weight and volume restrictions, and system complexity restrict the number of pressure sensors that may be installed inside the high-voltage instrumentation compartment. First, the pressure sensors may be limited to the most sensitive circuit or instrument. Second, the instrument should be essential either to the operation of the spacecraft or an essential part of the mission objectives. The sensors may be placed next to the pressure-sensitive instrument, in the instrument compartment, or near the instrument outgassing port where external pressure can be sensed before compartment pressurization.

7.4 System Voltages

Insulation degradation related to aging occurs at all voltages, including the very low voltages associated with solid-state devices. Water-induced corrosion, oxidation, and chemical reactions all enhance the aging process of electrical insulation systems. More rapid degradation is caused by over-voltage electrical stress, partial discharges, and corona usually associated with, but not limited to, high voltage. Some properties of different voltage regimes are investigated in the following paragraphs.

7.4.1 0 to 50 Volts

When the appropriate conditions exist, corona can occur at any voltage level greater than the ionization potential of the material. The 0 to 50 V region is usually considered corona-free for dc voltages and low-frequency ac peak voltages (less than 500 MHz). This also assumes that the environment temperature is less than 250 °C and free of concentrations of noble gases and radioactive and other contaminants known to lower the CIV.

7.4.1.1 0 to 50 Volts Good Workmanship Practices

When the voltage stress in air is less than 50 V/mil (2,000 V/mm), creepage and tracking should not exist, provided the following good workmanship practices are performed during design, packaging, assembly, and test:

- a. Select materials and dimensions that can withstand the worst-case voltage gradients near the energized conductors.
- b. Avoid contamination on conductor and insulation surfaces.
- c. Avoid small gaps between thinly insulated or bare conductors.
- d. Select high quality insulating materials that have low dielectric constants and maximum resistivity and dielectric strength.
- e. Base all calculations on the instantaneous peak abnormal over-voltage.
- f. Select materials with suitable outgassing properties.
- g. Select packages with adequate sealing or venting.
- h. Protect the circuit from radiation and direct exposure to plasma environments.
- i. Select materials whose characteristics are favorable to the application environment.
- j. Avoid sharp points and rough electrode surfaces.

NASA-HDBK-4007 W/CHANGE 2

- k. Avoid high localized regions of mechanical stress (e.g. sharp bends) in insulating materials.
- l. Inspect workmanship for simple contamination such as fingerprints.
- m. Avoid overstressing of screws, bolts (which can lead to cracks), and through-holes (possible sites for surface flashover).

7.4.1.2 0 to 50 Volts Typical Problem Areas

Typical problem areas are as follows:

- a. Low-voltage tracking may occur across contaminated insulating surfaces where low current (nanoamperes) may eventually char the insulation.
- b. Metal migration may occur over extended operating times, resulting in a short circuit when the migrating metal bridges a gap between electrodes.
- c. Corrosion from salt spray, outgassing products, and oils may create critical pressures that may affect nearby high-voltage circuitry.
- d. Cold-flow, the process by which the insulation will move from a stress point; a common concern with PTFE insulations.

7.4.2 50 to 250 Volts

This voltage range is usually considered corona-free for dc voltages and sinusoidal ac peak voltages with frequencies less than 50 kHz. This also assumes the ambient temperature is less than 250 °C, and free of concentrations of noble gases and radioactive and other contaminants known to lower the CIV.

7.4.2.1 50 to 250 Volts Good Workmanship Practices

When the voltage stress in air is less than 50 V/mil (2000 V/mm), creepage and tracking should not exist, provided the following workmanship practices are followed during design, packaging, assembly, and test, in addition to the precautions stated for the 0 to 50 V ranges:

- a. Eliminate triple points by forming a small gap between the dielectric and the metal.
- b. Recess terminals and encapsulate with void-free bonded potting materials.
- c. Use nontracking materials for printed circuit boards.
- d. Prevent condensation of liquids on all circuit parts.
- e. Lengthen flashover gaps with skirts, grooves, and undercuts.

APPROVED FOR PUBLIC RELEASE—DISTRIBUTION IS UNLIMITED

NASA-HDBK-4007 W/CHANGE 2

- f. Inspect the bonding of all materials and joints. Insulator and metal bonds are to be void free.
- g. Use smooth rounded surfaces and edges wherever possible.
- h. Where possible, avoid tracking in low-voltage circuits by reducing voltage stress to less than 50 V/mil (2000 V/mm).
- i. Reduce metal migration by conformally coating circuit boards.
- j. Keep contaminants from entering the circuit environment.
- k. Check pressure seals with a gas other than helium. If helium is used, ensure that it is totally removed from the circuits, parts, and enclosures before flight.
- l. Use surge protection devices to reduce over-voltages.
- m. Minimize capacitive coupling between circuits.
- n. Over-design for abnormal faults and transients.
- o. Ensure conductor spacing on circuit boards is compliant with IPC-2221A standard.
- p. Use conformal coatings to protect the circuit from faults, eliminate moisture penetration, and inhibit glow discharges and corona.
- q. Avoid multipactor in RF circuits by proper selection of frequency, spacing parameters, and materials (see section 6.3.5).
- r. Separate high-voltage and low-voltage circuits as much as possible.
- s. Ensure the field stresses have a maximum value of less than 100 V/mil (400 V/mm).
- t. Design gaps between conductors with significant voltage differentials to eliminate flashover, creepage, and tracking.
- u. After cleaning with solvents or water, thoroughly dry all parts and framework by heating and, where possible, outgassing in a vacuum.
- v. Only place high-voltage wires and cables close to ground planes with if sufficient insulation is provided. Sharp bends and clamps can generate standing waves at high frequency and result in breakdown.
- w. Over-design for maximum transients and over-voltages to prevent creepage and flashover related to repetitive transients.
- x. Prevent over-voltage stress by conducting repeated dielectric withstanding voltage (DWV) tests.

APPROVED FOR PUBLIC RELEASE—DISTRIBUTION IS UNLIMITED

7.4.2.2 50 to 250 Volts Typical Problem Areas

Typical problems for circuits in this voltage range are as follows:

- a. Corona, enhanced by the presence of concentrations of noble gases and hydrogen.
- b. Sharp edges on dielectrics (equivalent to sharp edges on metals).
- c. Over-tightened clamps and ties on shielded and unshielded insulated conductors resulting in over-voltage reflections and failures.

7.4.3 Voltages Over 250 Volts

This is the normal high-voltage range where most problems exist because of voltage overstress, flashover, and voltage breakdown.

7.4.3.1 Voltages Over 250 Volts Good Workmanship Practices and Precautions

Design features to be added to the good workmanship and precautions described previously are listed below:

- a. Eliminate voids. Small voids are subject to partial discharges; larger gaps may result in voltage breakdown leading to arcing and bulk discharges.
- b. Corona, partial discharges, and glow discharges all have different frequency signatures. Select test equipment to detect each specific phenomenon.
- c. Control magnetic fields near high-voltage circuits. The breakdown voltage between conductors can be raised or lowered in the presence of a magnetic field.
- d. Shield circuitry and high-voltage conductors from exposure to the solar environment, temperature extremes, plasma, and ionizing radiation and particles.
- e. Encapsulate with void-free materials.
- f. When using materials or circuits with large gas-filled volumes, either pressurize them or operate them in hard vacuum.
- g. Use lossy dielectric materials for shielding of high-voltage conductors and parts.
- h. Polish conductors to eliminate all rough spots or jagged surfaces.
- i. Use radiation-proof gaskets on hermetically sealed packages.
- j. Ensure that material aging in a radiation field is considered.
- k. Shield to limit aging caused by atomic oxygen and radiation.
- l. Inspect for debonding of conformal coatings.

- m. Eliminate bubbles in liquid dielectrics.
- n. To the extent practicable, limit temperature excursions which can lead to delaminations

Pressurizing with hermetic sealing or total encapsulation may be required for circuits that operate at voltages above 5 kV and at pressures between 1×10^{-5} to 100 Torr (1×10^{-2} and 1×10^4 Pa). A gas with a high dielectric strength and large molecules, such as sulfur hexafluoride (SF_6), is recommended to assure leak-free operation for long periods of time.

7.4.3.2 Voltages Over 250 V Typical Problem Areas

Most frequent failures for this voltage range include the following:

- a. Incomplete bonding of materials, such as Teflon[®] to epoxy.
- b. Voids in encapsulating materials caused by incomplete outgassing during processing.
- c. Cracked encapsulation by insufficient post encapsulation curing, specifically inadequate mechanical stress relief.
- d. Partial discharges in voids.
- e. Creepage and tracking.
- f. Insulation cracking and treeing caused by temperature stresses in materials with insufficient temperature coefficients of thermal expansion.
- g. Delamination of materials resulting in voids.
- h. Bubbles formed in a liquid at zero gravity, which have a tendency to move toward the center of the mass, result in partial discharges and voltage breakdown.

A summary chart for system voltages operating in air and other gases is shown in table 9, Power System Voltages.

NASA-HDBK-4007 W/CHANGE 2

Table 9—Power System Voltages

PARAMETERS		GASEOUS ATMOSPHERE			
		AIR/N ₂ —AIR	HYDROGEN	HELIUM	OXYGEN/ CARBON DIOXIDE
Minimum breakdown voltage (bare electrodes)	Volts (ac-rms)	230	206	134	300
	Volts (dc-peak)	327	292	190	425
Minimum pressure region (Torr)	Contact and terminals	20 to 0.025	10 to 0.02	100 to 0.1	
	Insulated conductors (twisted)	10 to 0.025	5 to 0.2	100 to 5	3 to 0.025
	Wires in shielded coaxial; not extruded	10 to 0.1			
	Coaxial cables with connectors (MIL—SPEC)	10 to 1.0		100 to 10	
	Circuit breakers contacts	5 to 0.05			
System voltage	115 V; 400 Hz; 3 phase	Normal design, no special protection		Protect for transients over 180 V-peak	Normal design, no special protection
	115 V; 1600 Hz; 3 phase				
	270 V; dc	<ul style="list-style-type: none"> • All wiring and bare contacts are to be insulated with at least 10-mil insulation. • Glow discharges will exist during transients. 	<ul style="list-style-type: none"> • All conductors shielded. • All connectors potted or pressurized. 	<ul style="list-style-type: none"> • All conductors shielded. • All components potted or pressurized. 	
	230 V; 400 Hz; 3 phase	<ul style="list-style-type: none"> • All 3-phase wiring and bare contacts pressurized or shielded. • Single phase to neutral may be treated as 115-V system. 	Same as air.	<ul style="list-style-type: none"> • No exception for single phase lines. • All conductors shielded. • All components pressurized or potted. 	Same as 115-V system
	650 V; dc	<ul style="list-style-type: none"> • All lines in coaxial configuration for all gases. • All components pressurized or protected. 			
	440 V, 20 kHz; 1 phase				

APPROVED FOR PUBLIC RELEASE—DISTRIBUTION IS UNLIMITED

7.5 Solid Insulation

Solid insulation can be in two forms: either a conformal coating or an encapsulation. A conformal coating is defined as the application of two or more individual coats of low-viscosity liquid insulation to a circuit or printed circuit board. Each coat is cured, resulting in a solid coating that is free of voids. Encapsulation (potting) is defined as the immersion of all electrical and structural components, circuits, and printed circuit boards into a liquid insulation, which, when cured, forms a void-free solid insulation.

7.5.1 Solid Materials Selection Data

When selecting an insulating material for a high-voltage application, the right data may be difficult to find. Mechanical and chemical data are usually abundant; however, the electrical data are a simple tabulation of constants, with no hint of how these constants will vary with respect to operating conditions. Most published data need to be adjusted or translated for the application at hand.

Table 10, Properties of Interest for Insulating Materials (Bruins, 1968), summarizes the electrical, mechanical, thermal, and chemical properties that need to be considered for solid insulation. Sometimes, solid potted insulation is specified to be transparent so that the packaging engineer can assess parts stressing and bonding. Weight, water adsorption, and outgassing are often specified. Most important for all categories of high-voltage insulation is life, which is dependent upon the electrical stress and environment.

Table 10—Properties of Interest for Insulating Materials

MECHANICAL	ELECTRICAL	THERMAL	CHEMICAL	MISCELLANEOUS
1. Tensile, compressive, shearing, and bending strength	1. Dielectric strength	1. Thermal conductivity	1. Resistance to reagents	1. Specific gravity
2. Elastic moduli	2. Surface breakdown strength	2. Thermal expansion	2. Effects upon adjacent materials	2. Refractive index
3. Hardness	3. Liability to track	3. Primary creep	3. Electro-chemical stability	3. Transparency
4. Impact and tearing strength	4. Volume and surface resistivity	4. Plastic flow	4. Stability against aging and oxidation	4. Color
5. Viscosity	5. Permittivity	5. Thermal decomposition, spark, arc, and flame resistance	5. Solubility	5. Porosity
6. Extensibility	6. Loss tangent	6. Temperature coefficients of other properties	6. Solvent crazing	6. Permeability to gases and vapors

NASA-HDBK-4007 W/CHANGE 2

MECHANICAL	ELECTRICAL	THERMAL	CHEMICAL	MISCELLANEOUS
7. Machine-ability	7. Insulation resistance	7. Melting point		7. Moisture adsorption
8. Fatigue	8. Frequency coefficient of other properties	8. Pour point		8. Surface adsorption to water
9. Resistance to abrasion		9. Vapor pressure		9. Resistance to fungus
10. Stress crazing				10. Resistance to aging by light

Operating voltage, frequency, temperature, ambient gas composition, pressure, radiation, and structural requirements must be known when designing insulation for high-voltage equipment. This includes the steady-state operating voltage as well as higher voltage transients, their duration, and their frequency of repetition.

7.5.2 Conformal Coatings

Open construction refers to modules that have few or no solidly potted submodules. In this type of construction, circuit boards are to be conformally coated to reduce breakage related to vibration and shock, to inhibit corrosion and fungus during handling and storage, and to reduce surface tracking along board surfaces between high-voltage and low-voltage parts, terminations, or connections. Circuits selected for conformal coatings are to be either limited to low voltage, installed within a module floating at high voltage, or only operate when the gas pressure surrounding the board is less than 10^{-5} Torr. Conformal coatings are put on low- and high-voltage circuits to prevent short circuits caused by conducting debris that sometimes appears after launch. The parts on a circuit board are spaced so that the region outside the conformal coating is quickly evacuated when the system is placed in a vacuum chamber or as the spacecraft is boosted into orbit. Epoxy and polyurethane resins are the most frequently used materials for conformal coating.

Before a board is conformally coated, it should be inspected. Flat surfaces mounted parallel to the board surface should be staked 0.5 to 1.0 mm above the circuit board to allow the insulating coating material to flow into the space between the parts and the board and fill the voids between the parts and the board. Then, the following rules apply:

- a. All boards, conductors, wiring, and electrical components are to be cleaned according to the specification before the unit is conformally coated. This includes solder flux, fingerprints, and particles from the work bench and dust.
- b. The circuit boards should be conformally coated with at least three separate layers of a low-viscosity insulation. This is recommended to eliminate the pinholes (continuous leakage path) and uncoated areas that normally occur in single- or double-coating processes. Application of the dielectric material may be either by dipping or brushing with each layer applied at right

angles to the preceding layer. The completed process should be checked with standard tests such as resistivity or dielectric withstanding.

c. The final step in an electrical assembly is the joining of the printed circuit board assembly. If wired, the wire and solder joints are to be cleaned and conformally coated with the same precaution as the electrical networks on the printed circuit boards after the connections are made to other boards and subassemblies within the module.

In some cases, a conformally coated board is then potted to attain better bonding. The board and assembled parts are to be cleaned, and care taken to ensure good bonding at the conformal coating and potting material interface. Some materials that are used for conformal coatings include Conathane[®] CE 1155 and Arathane[®] 5750. Two materials that require a post-cure vacuum bake to meet the outgassing specification are Hysol[®] PC 18M and Solathane[®] 113.

7.5.3 Encapsulated Circuits

One method of preventing a gas discharge voltage breakdown is to exclude gases from the high-voltage areas. This can be accomplished by encapsulating the high-voltage circuitry. Encapsulation provides the system with mechanical protection from external damage, gives structural support to the components against shock and vibration, and protects the high-voltage system from gas discharge damage.

The decision to encapsulate should be made during the conceptual design phase and incorporated in the subsequent hardware design. In this manner, a total system approach to the design can be taken, yielding an electronic component with minimum problems that can arise from encapsulation or potting. This will permit the optimum choice of components, parts, materials, mechanical arrangements, manufacturing techniques, and the methods of functional and environmental testing. This approach will reduce the failure probability. In a survey of U.S. Air Force, NASA, and industry, encapsulated electronics failures fell into the following categories: High electric stress (packaging); improper selection or use of parts (design); poor bonds, board delamination (material); and voids, cracks, workmanship, and handling (processes). The distribution of these failures is summarized in table 11, Summary of Failure Analysis Form (Stinthal, 1982).

**Table 11—Summary of Failure
Analysis Form**

ITEM	PERCENT
Materials	15
Packaging	24
Design	25
Processes	36

7.5.4 Modularized Electronic Circuits

Many electronic circuits are either encapsulated or conformally coated and pressurized to avoid arcing and partial discharges. Conformally coated and pressurized circuits require large heavy enclosures to ensure no leakage. Even then, excessive vibration and mechanical shock can cause flaws in seals, causing the unit to depressurize, resulting in possible circuit failure.

Encapsulation always adds material and weight to the circuit but may be necessary in some cases. The workmanship involved during encapsulation should be scrutinized by visual and test analysis to assure there are no cracks or voids in the finished product. Another aspect of encapsulated circuits is the number and size of parts. Large volumes are more apt to have voids and flaws than very small volumes. Materials matching is easier in a unit with a few parts than when a large number of parts are used in the volume. Therefore, consideration should be given to the use of encapsulated parts or circuits where necessary, while conformally coated parts and circuits should be used for the remainder of the unit. Encapsulated parts and circuits should be carefully considered whenever operating voltages may exceed the Paschen minimum. Conformally coated circuits may be used for voltages less than 300 V in air, as long as the circuits are in a debris-free environment.

7.5.5 Radiation and Chemical Factors

Other environmental factors affecting insulation are UV radiation, nuclear radiation, and exposure to solvents and chemicals. Addition of UV radiation and chemicals tends to lower insulation breakdown voltage, either instantaneously or as exposure and deterioration progress.

7.6 Packaging

New packaging concepts are to be analyzed and evaluated for large high-voltage spacecraft modules. In small spacecraft with loads up to 5 kW, solidly encapsulated modules, conformally coated circuit boards, gas-pressurized modules, and a few liquid-filled modules have been used. Most of the enclosed gas- and liquid-filled modules had volumes of less than 0.25 m³. Likewise, most of the conformally coated high-voltage circuit boards operated at voltages less than 10 kV. Some future high-voltage spacecraft components may require voltages of 50 to 100 kV with volumes more than 1 m³. This will necessitate new and different packaging concepts, and there will be reasons for using liquids or gases as insulating materials. These design solutions require further careful analysis and considerations to prevent leakage and contamination of other components.

7.6.1 Wiring and Connectors

Partial discharges and corona in electrical circuits and components generate electromagnetic noise. Typically, the noise signature is between 20 kHz and 20 MHz. If the partial discharges are extensive, noise can also be induced in neighboring low-power level circuits. In high-frequency systems such as radar, the wave shapes of the electrical signals can carry partial discharge signals. Furthermore, these partial discharges produce ozone, optical emission, and acid from

decomposition of material, which can cause deterioration of dielectrics. If corona persists for several hours, the dielectric may start to deteriorate and eventually a breakdown will result.

Coaxial cable shielding is often cured using intense electron beams. This is known under some conditions to leave a strong charge in the shielding that can lead to unexpected breakdowns and arcing later. Recent spacecraft anomalies have been attributed to subsequent insulation breakdown and resulting arcing (Catani, 2007).

Internal electrostatic discharge (IESD) results from charge buildup (from the radiation belts) in cable insulation or in circuit boards (or on isolated insulators inside the spacecraft Faraday cage) can cause serious arcing and permanent shorts. Designers need to be aware of such effects, which are addressed in NASA-HDBK-4002A.

7.6.2 Gas Pressure

The pressure of gas between spaced electrodes in an electrostatic field is a parameter that is required when determining the location of the Paschen minimum. This gas pressure between electrodes may differ from the surrounding ambient gas pressure and may vary as a function of time. With higher temperatures and mechanical stress, air trapped in the insulation layers may rupture or force voids in the insulation when the surrounding air pressure is reduced. Figure 58(a) Outer Jacket Rupture and (b) Center Conductor Delamination (Dunbar 1988), shows such voids created by gas trapped in layers near the center conductor and near the outer shield of a coaxial cable.

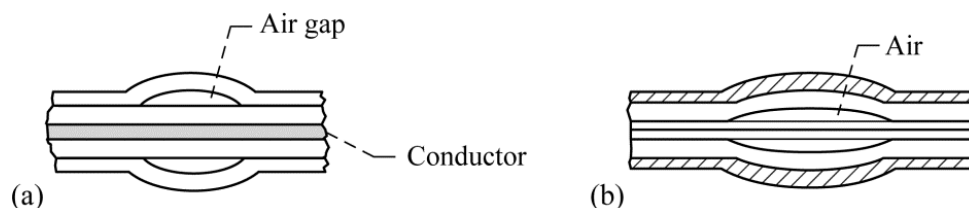


Figure 58—(a) Outer Jacket Rupture and (b) Center Conductor Delamination

7.6.3 Temperature

Each electrical insulation material has maximum temperature limits and temperature-life limits. Therefore, it is necessary to know the short-duration temperature and the continuous temperature exposure, both ambient and local.

7.6.4 Gases

In addition to the fill-gas between electrodes (such as air), there will be outgassing products of the insulation and the conductor material. Therefore, the Paschen curves will deviate from the known fill-gas curves, and should not be relied on exclusively.

7.6.5 Mechanical Requirements

Requirements to be satisfied include shock, abrasion, stability, strength, and flexure from vibration.

7.6.6 Frequency

Most of the published partial discharge initiation voltage data are in either 60 Hz or dc. The dc initiation voltage for point-to-plane electrode configurations is affected by the polarity of the point. The configuration with the point negative breaks down at a lower voltage. The ac initiation voltage always corresponds to the lower value as determined by dc polarity experiments. At high frequencies, the interference generated by partial discharges is worse than at low frequencies. The rate of deterioration of insulation by partial discharges is usually proportional to frequency. The dielectric strength of insulators is inversely proportional to frequency. Sample values of loss of dielectric strength with frequency is shown in tables 5 and 6 in section 6.3.6.4.

7.7 Interconnection Systems

The high-voltage insulation design starts with a circuit diagram showing all parts and their anticipated design voltage levels. The parts are then arranged in a preliminary package, which minimizes the net voltage between parts and voltage drop across each part. In designing high-voltage assemblies, it is important to avoid wire and part crossovers that put a low-voltage surface on one part next to a very high voltage surface of another part. Circuits containing resistive or capacitive voltage dividers require careful design, especially if the resistor or resistor string is extended. For example, a resistor or group of resistors may form a voltage divider between the high-voltage terminal and local ground. The normal plan is to zigzag many resistors from the high-voltage terminal to the ground terminal or to have one resistor with one end attached to the high-voltage terminal and the other end grounded. Sometimes, other high-voltage parts near the center of the resistor or resistor chain may be at full voltage or at ground potential, stressing a zone that is not normally designed for voltage stress. This is poor design practice and to be avoided.

7.7.1 Connector Test Data

There are two basic types of high-voltage connector designs: multi-pin connectors for power and electronic equipment and single-pin connectors between electronic packages and high-voltage power supplies. Closely spaced, small-pin, multi-pin connectors are not recommended for high-

voltage unpressurized equipment, especially if there is a probability that the voltage between pins will exceed 450 V-peak in the pressure region between 50 and 0.1 Pa.

This problem was demonstrated by a three-part evaluation test of a 55-pin connector in a simulated high-altitude chamber (Dunbar, 1974). Then, the CIV was measured between the pins. Figure 59, Round Wire Connector (Dunbar, 1988) illustrates the pin construction and indicates the air gaps of the test article. The tests were performed with the connector shell electrically grounded and the connecting wires and unwired pins encapsulated with 1.25-mm silicone rubber on each end of the connector. In the first test, a pair of 22-gauge, twisted, Teflon[®]-insulated wires (0.025-mm-thick) were connected to adjacent connector pins and then fed through the vacuum chamber wall to the corona test facility. The second test was like the first, except that the wires were connected to nonadjacent pins. In the third test, one lead was disconnected from the assigned pin and then reconnected to an adjacent pin on the other mating half of the connector to eliminate the possibility of partial discharges between the parallel conductors.

The contacts within a connector should float to allow for manufacturing tolerances and pin insertion and extraction. To do this, small spaces surround each contact. Furthermore, small air gaps will form about the wire insulation unless the insulation is pressed firmly against the contact. Many connectors are made with spring-loaded or crimp contacts, which leave an air gap above each contact as shown in figure 58. These air gaps are ideal for partial discharges, that is, the air gaps are located in the highest field stress volumes.

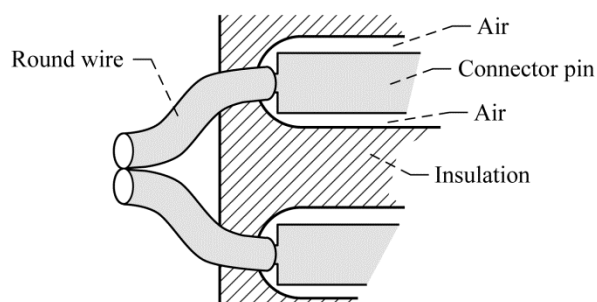


Figure 59—Round Wire Connector

The curves obtained from the test data are shown in figure 60, Connector-55 Pins in Air at 24 °C—Terminals Not Potted (Dunbar, 1988). The data show that the highest CIV was derived from the test in which the pins were energized from opposite connector halves. In this test, the initiation voltage for the connector was less than that of wires spaced 5 cm apart (the length of the connector) and greater than that of twisted, closely spaced conductors. This low CIV exhibited by the connector is related to air passages within the connector construction, as shown in figure 59. The design voltage for this connector was too low, between pins, to provide adequate high-voltage design practice. Curves for the other two tests have corona initiation voltages equal to those of twisted insulated conductors (Dunbar, 1974).

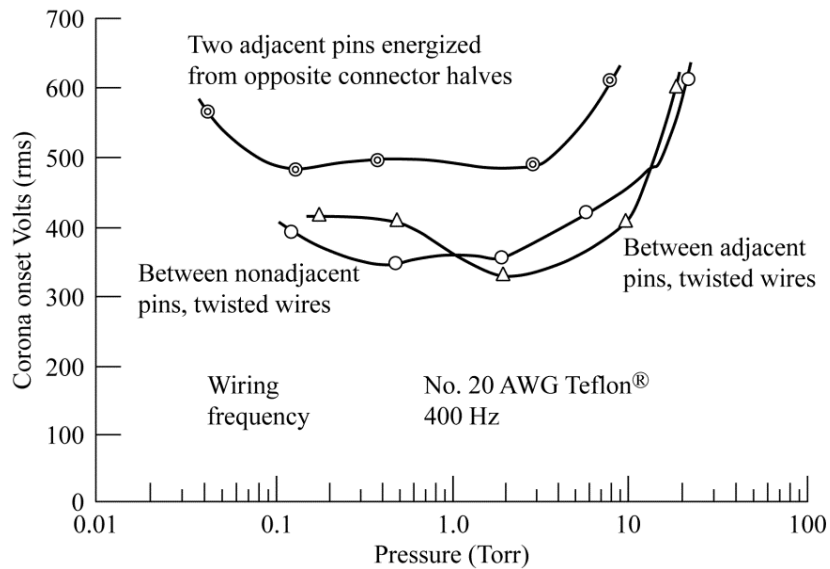


Figure 60—Connector-55 Pins in Air at 24 °C—Terminals Not Potted

7.7.2 High-Voltage Connectors

Connectors are also to be designed to eliminate air voids between conducting surfaces. One successful method for very high voltage (over 50 kV) applications is to make one side of the mating-interface from soft, pliable insulation as shown in figure 61, High-Voltage Connector (Dunbar, 1988). When mated, the pliable insulation conforms closely to the opposite dielectric. The pliable insulation should first contact the molded insulation near the center conductor, and then the contact should progress out to the shell without trapping air between the two contact surfaces. A thin layer of silicone grease may be applied to the insulation surfaces of some connectors to fill micro-pores in the insulation. Too much grease (more than 5 mil) tends to prevent complete closure of the connector, introduce air cavities, or deform the pliable insulation. Therefore, silicone or other additives are not recommended for properly constructed high-voltage connectors. Commercial HV connectors are available, such as the successful and widely used product line from Reynolds Industries that implement these principles.

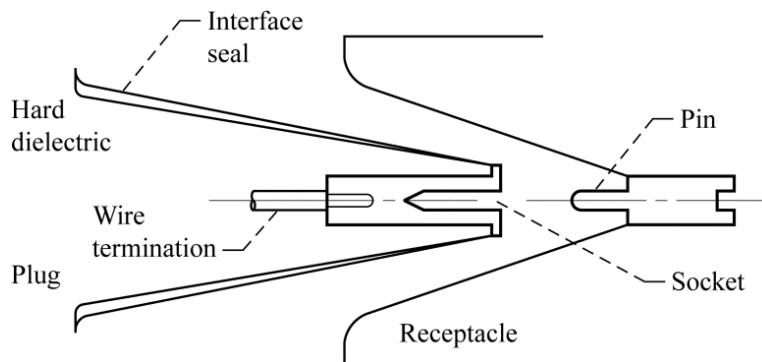


Figure 61—High-Voltage Connector

7.7.3 Feedthroughs

Some feedthroughs are designed with a shallow well around each termination or pin as shown in figure 62, Connector Pin With Air Gap (Dunbar, 1988). These wells should be completely filled with an encapsulant or provided with a generous opening for outgassing to space. The well, if left open or partially filled with encapsulant, will be subject to partial discharges, even at low voltages. The voltage across a bubble at the bottom of the well can be found by corona testing the encapsulated article between each pin and the metal frame. The feedthrough insulator shown in figure 63, Acceptable Stand-Off Connections (Dunbar, 1988), is an excellent design. It is designed with corona shields on each end and has no air gaps between the conductor and metal base plate.

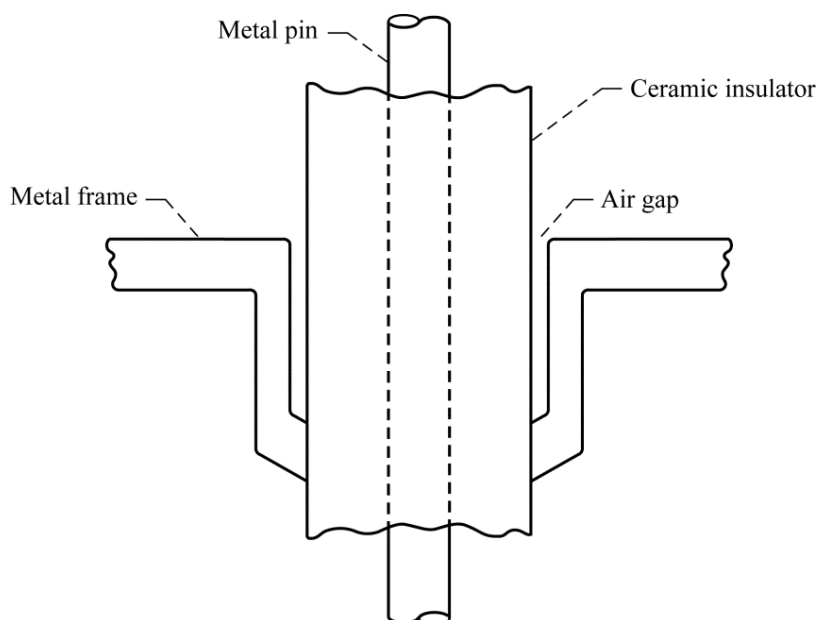


Figure 62—Connector Pin With Air Gap

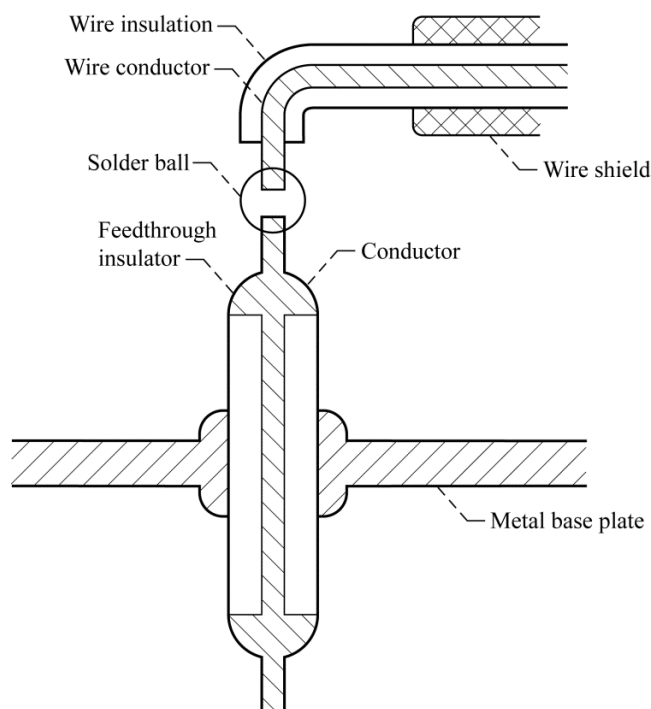


Figure 63—Acceptable Stand-Off Connections

Occasionally it is necessary to pass several conductors through a wall evacuated on one side and pressurized on the other side. It should be remembered that the small spaces between the conductor strands are like small air pipes. To be successful, it is required that the wire strands in that section be filled completely with a potting compound or solder to work. It is best to use solder with a solder ball or corona shield surface (Dunbar, 1988). The solder balls should be in the center of the feedthrough. The potting material should be allowed to penetrate the conductor ends to seal the insulation. Vented connectors should be avoided because they perform poorly because of slow venting rates, thus resulting in a high probability of partial discharges.

7.7.4 Wiring Selection

Cables for large high-power spacecraft may be required to operate at either high voltage or high current or both, depending on the type of the power source and the load power requirements. The design of the power distribution system will require that the line losses be kept to an acceptable level without jeopardizing the thermal characteristics of the lines or subjecting them to arc-over events.

Distribution system mass is of prime importance to the design of large high-power spacecraft. The mass of the distribution system includes the lines and interconnections and the required heat rejection equipment (Finke, et al., 1978). That weight required for distribution wiring for dc or single-phase ac circuits (in grams) can be calculated by the following equation:

$$W_l = 2l(A_1 D_1 + A_2 D_2) \quad (Eq. 13)$$

where

l is distribution line length in cm

A_1 and A_2 are cross sectional area of the conductor and the insulator, respectively, in cm^2

D_1 and D_2 are the density of conductor and the insulator, respectively, in g/cm^3

The factor 2 is included in the formula because two lines are required, a positive and a negative (or return) line. Since most of the larger spacecraft may be designed using high-resistivity material such as graphite epoxy, a return line is necessary (return through structure may not be feasible or desirable). This distribution system mass should be equal to or less than the weight required for heat rejection. That weight required for heat rejection for the two conductors (in grams) is given by the following equation:

$$W_H = \frac{2I^2 \rho l \alpha_H}{A_1} \quad (Eq. 14)$$

where

I is distribution line current in A

ρ is line resistivity in $\Omega\text{-cm}$

l is distribution line length in cm

α_H is added conduction specific weight of the heat rejection system in (g/W)

A_1 is the area per unit length in cm^2/cm .

This conductor weight is required to radiate heat so that the conductor temperature can be stabilized at a given upper temperature limit.

The mass of the heat rejection system depends on the shape and orientation of the conductors, the operating temperature of the conductors, and the conductor material. Cylindrical conductors present minimum surfaces for radiative cooling, whereas rectangular conductors present more surface area for cooling. For simplified analysis, it will be assumed that the conductors will be constructed from wide, thin, aluminum sheets, with the largest cross-section dimension oriented toward free space. Aluminum sheet is an excellent material because it is lightweight, low cost, has good mechanical strength, and can be easily fabricated. Other materials that may be used as conductors are shown in table 12, Conductor Materials.

Table 12—Conductor Materials

MATERIAL	RESISTIVITY ($\mu\Omega\text{-cm}$ AT 20 °C)	DENSITY (g/cm^3 AT 20 °C)
Aluminum	2.828	2.7
Beryllium	5.9	1.82
Copper (annealed)	1.729	8.89
Graphite	1,589.0 (avg.)	1.58
Lithium	8.55	0.54
Magnesium	4.6	1.74
Silver	1.629	10.5
Sodium	4.3	0.97

Table 12 should be used with care. Several materials, for example, have lower density than aluminum while lithium and sodium have much better resistivity-density characteristics. These materials, along with beryllium and magnesium, are difficult to fabricate and require special storage. Copper, silver, and silver alloys are heavier than aluminum but are much easier to join and should be considered for the connector materials. Aluminum materials tend to crack and set with time. Continual flexing (caused by electrical transients) could cause joints to weaken with time. Graphite structural characteristics are such that it should not be considered for the ground return; its resistivity is much higher than most metals.

7.7.5 Wire Terminations

High-voltage interconnections between power supplies and electronic circuits are difficult to design, assemble, and assess, especially if the interconnecting shielded wire is flexed or strained after it is attached to one or both terminals. Linear stressing can break one or all of the bonded joints between the shield, conductor, or wire insulation and the terminal and encapsulating material. Any delamination at the insulation bond will form a void and can result in corona and eventual voltage breakdown. When the wire is bent at the terminal (figure 63) and the high-voltage conductor is flexed or stressed, there is a probability of delamination at the wire-encapsulant surface.

The wire shield and insulation preparation are as important as the connection. One method of preparing the wire termination is to cut the wire and shield to length and then place three or more turns of a small conductor or formed metal ring over the end of the wire shield and insulator as shown in figure 64, Wire Termination. This method holds the shield end strands in place and forms a round conformal metal surface at the end of the shield. When three or more turns of wire are used, as for breadboard demonstration, the wire should be soldered in place with a low-heat iron as to avoid melting or deforming the insulation.

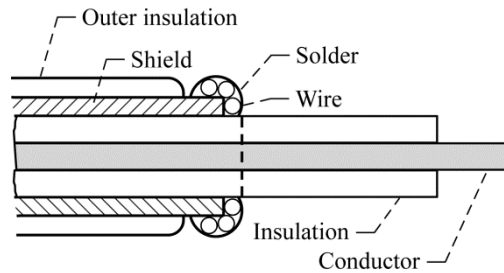


Figure 64—Wire Termination

Solder joints on circuit boards, especially printed circuit boards, are designed to have minimum solder. This leaves the electrical post termination protruding through the solder on the circuit interconnection. Often, the post terminal is clipped after soldering, leaving sharp edges protruding above the circuit board's metal surface. This is unacceptable for circuits with voltage exceeding 250 V-peak. Sketches of acceptable and unacceptable solder joints for high-voltage circuits are shown in figure 65, Acceptable Solder Terminations, and figure 66, Unacceptable Solder Terminations. Whenever a solder-draw or sharp edge protrudes from a circuit, the probability of corona and voltage breakdown is enhanced. First, the conformal coating applied to the circuit board and circuits may not cover the sharp point or edges. Second, solder has more free electrons than a conformal coating. It can be assumed that a solder joint has corona initiation and breakdown voltages of 85 percent that of steel (W.G. Dunbar, unpublished data). Third, any ionization from a solder joint will result in surface heating of the solder, and the solder will tend to evaporate a thin layer across the insulation surface between the conductors, resulting in tracking and arc over. This phenomenon may occur within only a few minutes between high-voltage conductors.

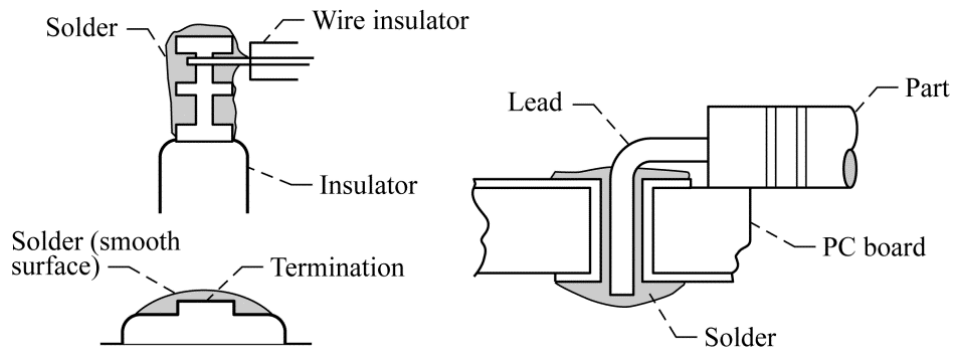


Figure 65—Acceptable Solder Terminations

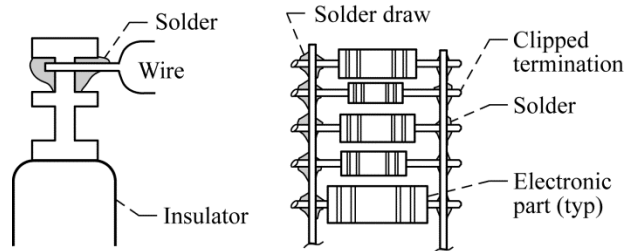


Figure 66—Unacceptable Solder Terminations

7.7.6 High-Voltage Leads

Leads made of metal tubing between high-voltage parts should be round bent, polished to a smooth surface. Nickel-plated metals or steel are preferred, but other softer metals are often used because they are easier to fabricate. The radius of curvature on all bends should be at least 2.5 times the conductor (tube) diameter to avoid flattening or crushing the tube at the bend. When necessary, the ends of the tubes should be flattened as little as possible. The corona suppression shield should extend over the edges of the flattened end, as shown in figure 67, High-Voltage Lead and Bushing (Dunbar, 1988). Ample space should be provided between the inside surface of the insulator (high-voltage bushing in figure 67) and the metal tube. A safe design would be based on the assumption that the full voltage stress exists on the top edge of the bushing.

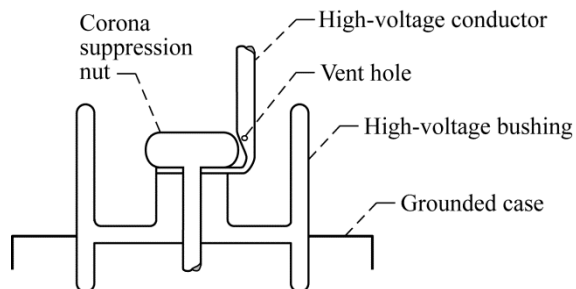


Figure 67—High-Voltage Lead and Bushing

Hollow tubing should be vented. Vent holes should be drilled through one wall of the tubing at both ends of the tube. The vent hole should face the corona shield, and no other holes should be drilled in the tubing.

7.7.7 Lead Terminals

High-voltage flexible lead termination should be designed to eliminate pressure points on the terminal board (figure 68, High-Voltage Terminals (Dunbar, 1988)). Pressure points may cause delamination and enhance internal tracking or corona. Also, the terminal should be protected with a corona ball or shield.

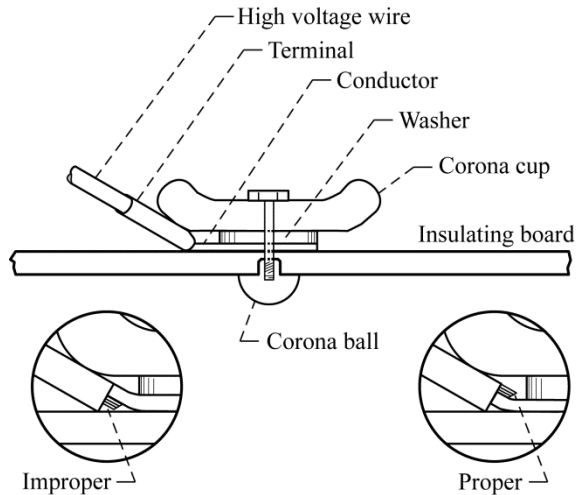


Figure 68—High-Voltage Terminals

Other insulation techniques include either burnishing or enameling over the knots in ties. Otherwise, the feathered ends will become points from which corona discharges can emanate (figure 69, High-Voltage Ties (Dunbar, 1988)).

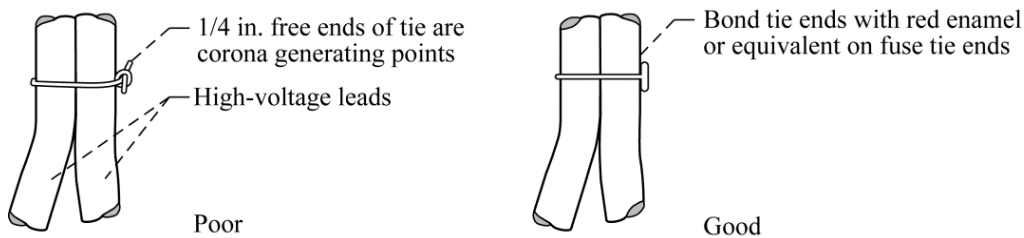


Figure 69—High-Voltage Ties

Encapsulated coils and coil supports should have rounded corners as shown in figure 70, Round Corners on Encapsulated Coils (Dunbar, 1988). Rounding the corners eliminates high stress points or low utilization factors in the media between the encapsulated coil and its support frame.

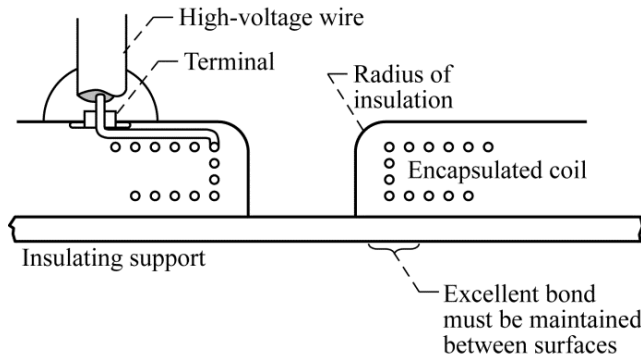


Figure 70—Round Corners on Encapsulated Coils

7.7.8 Taps and Plates

Occasionally, a voltage tap is required at the center of the part strings. This tap should be made of material having the same diameter as the part surface and be thick enough for attachment of a round tubular connection. Soldered joints should not be used because most soldered electrodes have lower breakdown potentials than metals such as steel, nickel, brass, copper, and aluminum.

Parts should be stacked in such a way that there are no drastic potential differences between them. A potential shaping surface within a stack of series-connected diodes can be a thin plate of metal provided with a large-radius edge as shown in figure 71, Curved Edge on High-Voltage Plate (Dunbar, 1988). This curved edge suppresses corona.

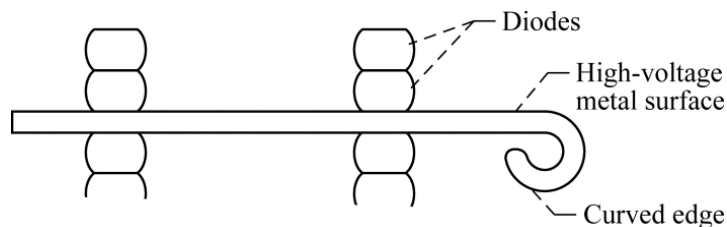


Figure 71—Curved Edge on High-Voltage Plate

7.7.9 Insulated High-Voltage Wiring

A designer may have to interconnect two or more components with a high-voltage flexible wire that has insulation inadequate to sustain the full electrical stress of the applied voltage. This can be done only if the following are observed:

- a. The outside diameter of the wire is increased with more insulation.
- b. Adequate and rigidly controlled spacing is provided between the wire and ground planes.

Generally, extra-flexible wire should be used only when the bending and placement of the tubing through the high-voltage volume is too difficult or will mechanically stress parts during installation. Terminations on extra-flexible wire will not stay in place as they will with solid tubing. Therefore, the terminations are to be keyed either to a slot in the insulation barrier or to a special locking device be developed for the termination and/or wire end.

7.7.10 Control Wiring and Circuits

Electrically controlled switches may also be required for voltage regulation and performance measurements. These functions are performed with components such as fan motors, relays, motor-driven switches, instrumentation, sensors, and circuits that operate at voltages less than 250 V-rms or V-dc. These devices and circuits, normally insulated, are incapable of withstanding the induced transient voltages. Therefore, these circuits and their wiring must be well shielded.

Low-voltage devices and their wiring should be well separated from the high-voltage circuit wiring. Low-voltage conductor shielding typically has rough surfaces that behave like multiple points that enhance field gradients with respect to the high voltage. This will result in lowering the breakdown voltage between high-voltage parts, or conductors, and the low-voltage shields.

7.8 Parts and Components

7.8.1 Resistors

Solid-core resistors should be used throughout the high-voltage module. Hollow-core resistors, if sealed on the ends, will slowly depressurize at high altitude and arc from end to end along the hollow-core surface.

Resistor coatings can be a problem. One supplier made resistors with light or dark blue coatings. The light blue coatings were well bonded to the elements. The dark blue coatings tended to debond. The resulting air gaps then depressurized, and the resistors failed.

Some resistors are constructed similar to the design shown in figure 72, High-Reliability Resistor (MSFC-STD-531). This design is acceptable only if the gas voids are filled or potted with solid insulations. Voids and gas-filled gaps will cause corona or breakdown and failure. If needed, resistors should have conformal coating on their entire surface. The terminations will be coated or encapsulated on the circuit board.

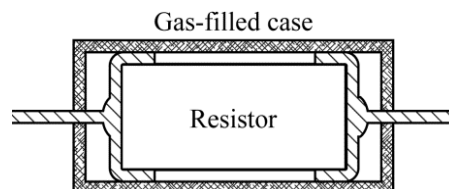


Figure 72—High-Reliability Resistor

7.8.2 High Voltage Capacitors

This section deals only with high-voltage capacitors. Many dielectric configurations that are quite appropriate for low-voltage, high-performance capacitors used in solid-state communication equipment are not applicable to high-voltage work and are not covered here.

Dielectrics used for high-voltage capacitors include liquids, liquid-impregnated paper or film, electrolytics, plastic film, paper-plastic combinations, mica, ceramics, glass, compressed gas, and vacuum. Among these, liquid-impregnated paper or plastic film capacitors offer the best energy-space-cost combination, unless special requirements with respect to temperature, stability, radiation resistance, or packaging are involved. Consequently, they are more widely available as high-voltage capacitors.

The most important design features of capacitors are low dissipation factor, high dielectric stress, and yields at acceptable failure rate. The dc capacitors for continuous duty also require a low dissipation factor because some ac ripple is usually present. High insulation resistance is usually required for applications. The dc energy storage capacitors require design features that permit extremely high currents as well as very fast charge and discharge rates.

Series connection of sections necessitates careful attention to conductor insulation, clearances, geometry, and workmanship, while the necessity for liquid impregnation requires meticulous control of initial material purity, as well as prevention of contamination during processing.

7.8.2.1 Dielectrics for Capacitors

Where viable, liquid impregnation is the most effective means of ensuring corona-free performance at rated voltage. All papers and films have surface irregularities caused by wrinkles and stretching that trap air when stacked between metal electrodes. Another advantage of liquid impregnation is replacing air with higher dielectric strength liquid that results in a more compact capacitor. Impregnation with solids such as waxes or resins is feasible for some applications. Unimpregnated plastic film capacitors are also suitable for some applications but are usually subject to partial discharge damage at ac voltages above 225 V-rms.

In addition to the requirements listed in table 13, Capacitor Requirements, high-voltage capacitors should be selected that are made from dielectric materials having the highest available dielectric strength and having the longest demonstrated life at rated stress.

Table 13—Capacitor Requirements

ac CAPACITORS	dc CAPACITORS	ENERGY STORAGE CAPACITORS
Low dissipation factor High partial discharge threshold	Low dissipation factor Low insulation resistance	Low equivalent series resistance (ESR) Low insulation resistance High current capacitance Low inductance

NASA-HDBK-4007 W/CHANGE 2

Dielectrics successfully used in high-voltage capacitors include, but are not limited to, the materials shown in table 14, Acceptable Impregnates, and the following materials:

- a. Polystyrene dielectric capacitors. Because of their low dielectric absorption and RF losses, these capacitors are intended primarily for use in calculators, computers, integrators, time-base oscillators, laboratory standards, and other pulse applications. The outstanding characteristics of these capacitors are low-temperature performance and stability.
- b. Polyethylene terephthalate dielectric capacitors. These capacitors are intended for use in high-temperature applications, similar to those served by hermetically sealed paper capacitors, but where higher insulation resistance at the upper temperature limits is required.
- c. Paper and polyethylene terephthalate dielectric capacitors. These capacitors are intended for applications where small case sizes and high-temperature operation are required.
- d. Polytetrafluoroethylene dielectric capacitors. These capacitors are intended for high-temperature applications that require high insulation resistance, small capacitance change, and low dielectric absorption. These capacitors exhibit excellent insulation resistance values at high temperatures.

7.8.2.2 Acceptable Impregnates

Acceptable impregnates for high-voltage capacitors include, but are not limited to, the materials, listed in Table 14. Other materials historically used include

- a. Castor oil and cyanoethyl sucrose: These impregnating liquids tend to freeze at -20 °C and are unacceptable for spacecraft equipment.
- b. Polyvinylidene fluoride film (K-F polymer)/silicone oil: Polyvinylidene fluoride film (K-F polymer) impregnated with silicone oil performs well in capacitors used in pulsed applications.
- c. K-F polymer/DAP: K-F polymer impregnated with diallyl phthalate has excellent radiation resistance, but some interaction was observed between the DAP and K-F polymer (Ramrus, 1980).
- d. Polysulfone film: Polysulfone film is an acceptable film for high-voltage capacitors (Bullwinkel and Taylor, 1982).

Table 14—Acceptable Impregnates

IMPREGNATES	DIELECTRIC CONSTANT
Tricresyl phosphate (TCP)	6.9
Monoisopropyl biphenyl (MIPD)	2.5
Silicone oil (DC-200)	3.6
Diallyl phthalate monomer (DAP)	10.0

7.8.2.3 Ceramic Capacitors

The acceptance criteria for ceramic capacitors vary according to the application for the part. Likewise, qualification and acceptance specifications are usually interpreted and implemented according to the requirements. In addition, acceptance testing may be limited to the measurement of capacitance and to the complete characterization of the substrate and developed capacitor. Substrates should be examined for cracks, delaminations, flaws, and voids using an acoustical examination such as a Scanning Laser Acoustic Microscope (SLAM) or C-mode Scanning Acoustic Microscope (C-SAM). This examination reveals manufacturing defects and may result in an initial rejection rate that is high. Characterization tests for ceramic substrates include capacitance (C), equivalent series resistance (ESR), equivalent series inductance (ESL), dissipation factor, DWV, physical dimensions and materials workmanship, vibration, and accelerated life test. Temperature and voltage ratings should also be considered in design selection, since capacitance characteristics can degrade with temperature and voltage variations.

Ceramic capacitors are made in a variety of styles and shapes, but the most commonly used designs are variants of Multilayer Ceramic Chip (MLCC). Many designs now include metal layers embedded in the dielectric between anode and cathode and floating electrode construction, (called floating electrodes) that can offer significant performance advantages. Three examples of plate arrangement are shown in figure 73, Relative Spacing (Stress) of X7R Dielectric Ceramic Capacitors (Stinthal, 1982).

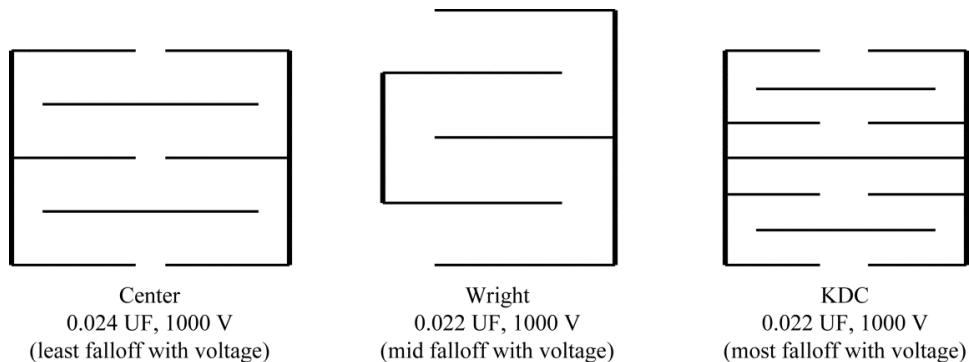


Figure 73—Relative Spacing (Stress) of X7R Dielectric Ceramic Capacitors

The number of plates within the construction affects the temperature and voltage characteristics; the greater the number of plates, the lower the electrical stress between plates. However, very thin plates may result in more voids and cracks, which degrade the dielectric and lower the reliability and aging for the capacitors as illustrated in figure 74, Capacitance Versus Applied Voltage Data for 0.022 μF , 1000 V, X7R Ceramic Capacitors (Stinthal, 1982) where each data point is an average of 10 to 12 capacitors.

NASA-HDBK-4007 W/CHANGE 2

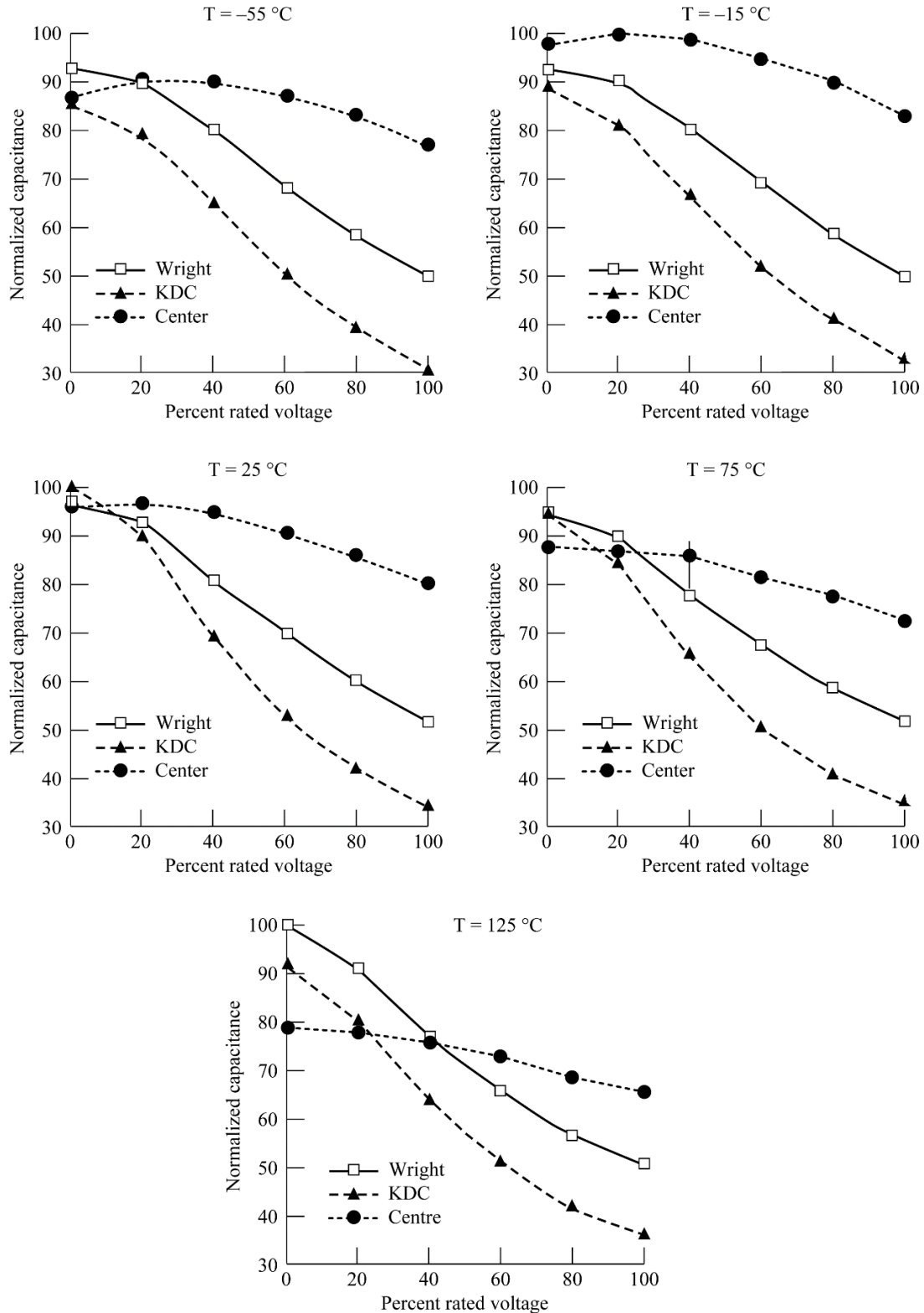


Figure 74—Capacitance Versus Applied Voltage Data for 0.022 μ F, 1000 V, X7R Ceramic Capacitors

APPROVED FOR PUBLIC RELEASE—DISTRIBUTION IS UNLIMITED

7.8.2.4 Mica-Paper Capacitors

Reconstituted mica-paper capacitors are used for power supply and regulator filters. Reconstituted mica is ground mica mixed in a slurry to form very thin sheets of multilayer mica chips. The resulting thin mica sheet is then bonded to a paper film resulting in a high dielectric constant, high working voltage material with excellent aging characteristic. The drawback to the process is the presence of a large quantity of microvoids and cracks in the mica slurry product. Above the CIV, there will be a large number of partial discharge pulses. These partial discharge pulses will have small magnitudes in microvoids and larger magnitudes in cracks and debonds. For high quality capacitors, the partial discharge rate should not exceed 20 pC/s. Partial discharges should be measured and baselined before and after thermal stress and vibration tests, and should not increase more than 3 percent above the baseline for the component to be acceptable.

Tests on mica paper include C, ESR, ESL, DF, CIV, CEV, vibration, accelerated life test, and physical dimensions and materials workmanship.

7.8.2.5 Film Capacitors

Film capacitors are subject to workmanship errors such as wrinkles in the dielectric, poor dielectric thickness, and a large number of voids per square meter. When a paper film is oil or liquid impregnated, the oil will fill the voids and wrinkles at the beginning of life, passing all the acceptance criteria. Accelerated life testing usually causes some of the liquid to escape from the wrinkles and large voids lowering the CIV and CEV and raising the partial discharge rate. As the capacitors dry and partial discharges accumulate in the voids and wrinkles, the liquid will polymerize, and hydrogen can replace air and significantly lower the CIV and CEV and increase the partial discharge number and magnitudes. Tests for film capacitors are the same tests for mica-paper capacitors.

7.8.3 Solid State and Vacuum Parts

Sometimes in spacecraft construction, live high-voltage circuits have to be switched on or off using devices such as hard-vacuum tubes, thyratrons, silicon-controlled rectifiers, and vacuum switches. The effect of switching on other circuit components such as resistors, capacitors, wiring, magnetic devices, isolation transformers, electro-optical isolators, and triggering circuits should be considered. Withstand voltages of such devices are typically rated for continuous applications; however, the switching or impulse withstand of the devices may differ considerably from the continuous rating. Boards, terminals, bushings, and other insulation should be impulse tested.

7.8.3.1 Diodes

Characteristics that should be evaluated by test include forward voltage drop (as a function of current), reverse breakdown voltage, reverse leakage current, and reverse recovery time (t_{rr}). All tests should be done as a function of temperature over the operational range.

Of these parameters, the $t(rr)$, is very important when selecting a diode for high-frequency applications. A slow recovery time at the higher temperatures may lead to thermal runaway and rapid aging. The other parameters are self-explanatory and should be judged by comparing components with the same specified characteristics.

7.8.4 Transformers

Transformers have several inherent failure modes that may be controlled by proper design, material selection, and workmanship. Wire fatigue can be eliminated by placing a strain relief curve at the terminating end of the wire at the anchor tap. In addition, the end of the wire to be terminated should be stripped without damage by cutting, elongating, or bending the wire. Finally, soldering the wire to the eyelet or to the termination post should be completed without excessive solder wicking or using an over-heated soldering iron. The potting or conformal coating material is to have characteristics compatible with the wire, the metal core, and the termination support material. For HV transformers in particular, vacuum potting usually produces the best results. Debonding of the insulation material from the wire, the core, or structure must be avoided as it will result in either a crack or a void, which may eventually be a source of partial discharges and accelerated aging.

High-frequency multi-winding transformers should be designed to eliminate differences in coupling coefficients as a function of frequency and avoid mutual induced currents as a function of frequency. Current sharing can be forced by interleaving the primaries and secondaries. This will reduce hot spots within a winding and promote load sharing between transformer windings. Since connecting multiple windings in series can result in very high voltages, one should consider parallel primary windings on opposite legs of the transformer and, likewise, with the secondary windings.

7.9 Printed Circuit Boards

There are two basic printed circuit designs: curved and square-cornered, as shown in figure 75, Curved and Square-Corner PWB Test Structures. Test results between curved and square-cornered circuits in air and Freon[®] and with conformal coating indicate that, with the same spacing between conductors, the curved circuits in air have 2 to 10 percent higher CIV and breakdown voltage for spacing less than 30 mil and 15 to 30 percent higher CIV and voltage breakdown for spacings greater than 60 mil as compared to square cornered ones. Freon[®]-immersed printed circuit boards had an improvement of 5 to 10 times than that of air-insulated circuits. Conformally coated printed circuit boards had 10 to 40 times higher breakdown voltage and CIV than air-insulated circuits. However, a consideration that is not to be overlooked is the workmanship and application of the coating material. Voids or incomplete filling and bonding to the metal circuits will greatly reduce both CIV and breakdown voltage. Test results and recommendations are available for a variety of epoxies rated for high voltage applications, including testing for corona (Hughes/Northrop Grumman, December 1995). Materials and conductor spacing should be compliant with IPC-2221A standard.

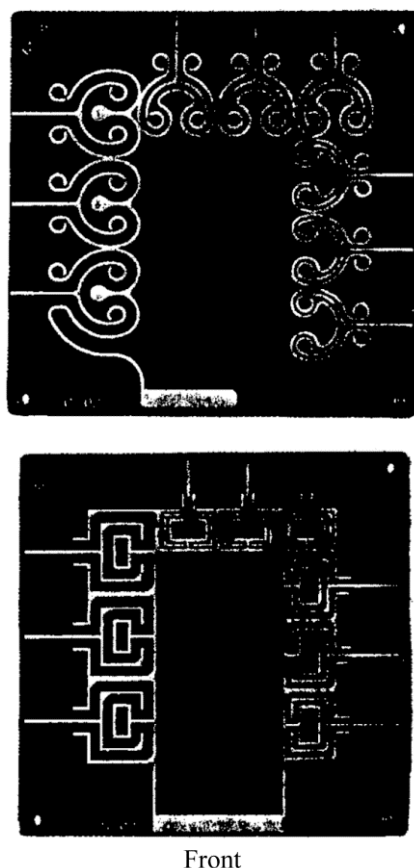


Figure 75—Curved and Square-Corner PWB Test Structures

7.10 Grounding and Bonding

Spacecraft either now exist or are under consideration that have power requirements ranging from a few watts, in the case of smallsats, to several hundred megawatts needed for large spacecraft using solar electric propulsion. The bonding and grounding of these units will vary considerably. Smaller spacecraft with powered loads to 5 kW will use standard, single-point grounding techniques with the solar arrays referenced to the central load module. Larger spacecraft using multiple solar array sections, capable of being transported to space and assembled there, may have a main load center and several remote load centers. Those spacecraft will require special bonding and grounding considerations.

7.10.1 Composite Structures

Spacecraft respond to the natural space environment by assuming a range of potentials relative to the plasma potential, depending on the plasma density, charged particle flux, and solar illumination. To equalize the potentials, it is necessary to maintain continuous electrical paths throughout the structure. Present spacecraft with composite structures already use conducting coatings to alleviate the spacecraft's charging problem with reasonable success. The use of a

composite structure will change the nature of the spacecraft ground and complicate grounding procedures. Concerns such as electrical continuity through the structure will become more important whenever a composite joint is encountered. However, initial results with composite spacecraft have indicated that composite joint designs are workable when properly grounded and bonded. There is still a potential corrosion problem. The design criteria shown in table 15, Recommendation in Designs Where Graphite/Epoxy is Coupled With Other Materials (Dunbar, 1988), have been suggested for composite/metallic joints in spacecraft (Brantley, 1978).

Table 15—Recommendation in Designs Where Graphite/Epoxy is Coupled With Other Materials

METAL GROUPING			
a,b I	a,b II	a,b III	c IV
Magnesium and magnesium alloys	Aluminum alloys, cadmium, and zinc plate	Lead, tin, bare iron, and carbon or low alloy steels	CRES, nickel, and cobalt-based alloys, titanium, copper, brass, and chrome

^aDo not couple Group I, II, or III metals directly to graphite/epoxy.

^bWhen Group I, II, or III metals are within 3 in. of graphite/epoxy and connected by an electrically conductive path through other structures, isolate the graphite/epoxy surface and edges. (Isolation system should be one layer of Tedlar[®] or type 120 glass fabric with a compatible resin or finish.)

^cTitanium, CRES (A286 or 300 series stainless steel), nickel, and cobalt-based alloys may be coupled to graphite/epoxy structures; when other Group IV metals are coupled, isolate the graphite/epoxy surface and edges. (Isolation system should be one layer of Tedlar[®] or type 120 glass fabric with a compatible resin or finish.)

7.10.2 Composite Joints

Conduction between two composite members may be provided by either a screen joint, by an adhesive bond using a conductive metal-filled epoxy, or by metal fasteners such as rivets or bolts. Six joint configurations (Dunbar, 1988) are shown in figure 76, Multiple Screen Interleaved Lap Joint; figure 77, Multiple Exposed Screen, Mechanically Fastened Stepped Lap Joint; figure 78, Butt, Scarf, and Stepped Lap Joints; figure 79, Mechanically-Fastened Joints; figure 80, Metal Connector; and figure 81, Center Screen Stepped Lap Composite-to-Metal Joint.

Metal connectors shown in figure 80 are recommended for large space structures. Although the initial cost is high, the ease of fabrication in space may make this system the most cost effective. The second best method is a screen technique shown in figure 77. The metal-filled epoxy joints, mechanically fastened joints, and metal splices shown in figure 78, figure 79, and figure 80, respectively, need much improvement or research and development before they can be considered as applicable for assembly in space. An assessment of these configurations is shown in table 16, Bonding/Grounding Concept Assessment (Dunbar, 1988).

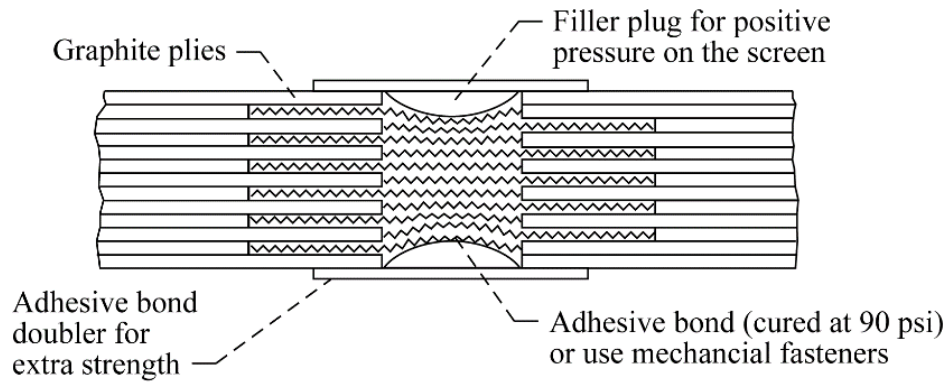


Figure 76—Multiple Screen Interleaved Lap Joint

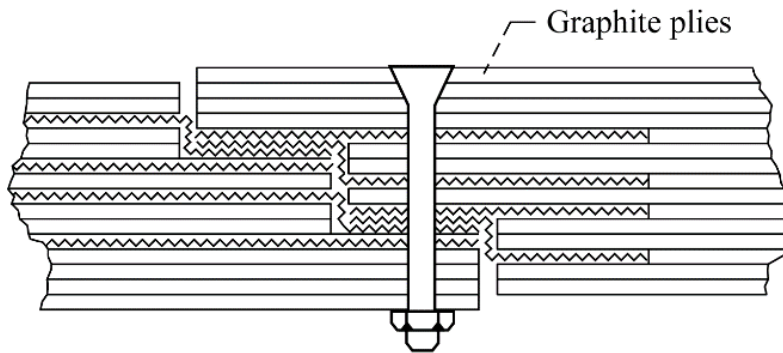


Figure 77—Multiple Exposed Screen, Mechanically Fastened Stepped Lap Joint

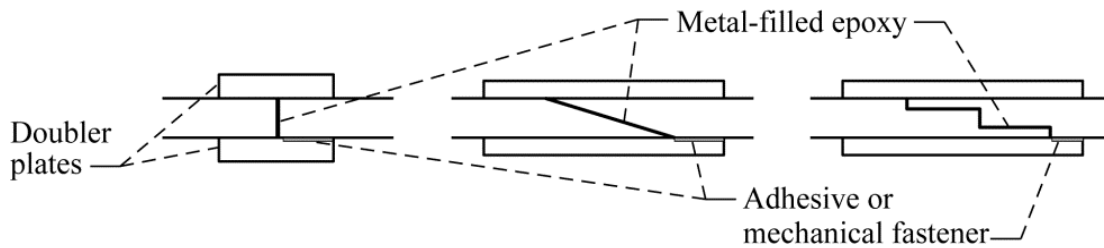


Figure 78—Butt, Scarf, and Stepped Lap Joints

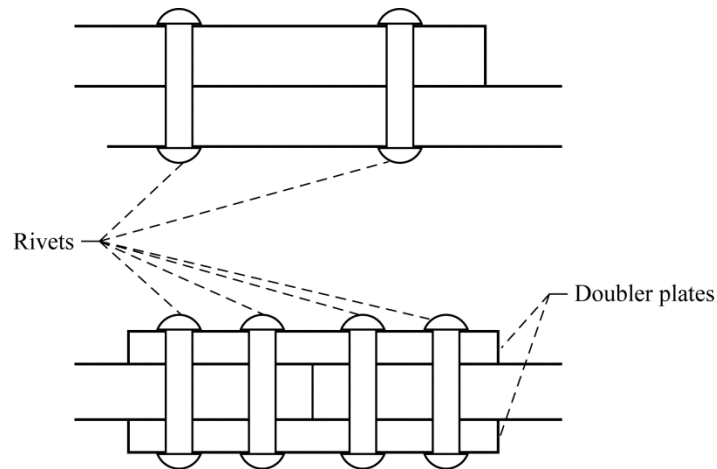


Figure 79—Mechanically Fastened Joints

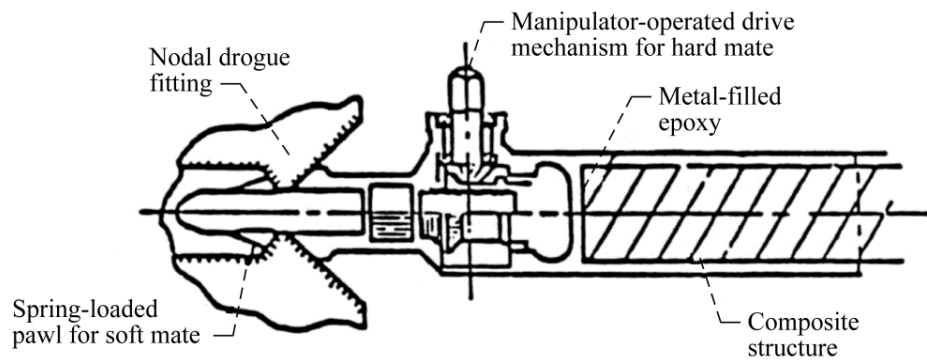


Figure 80—Metal Connector

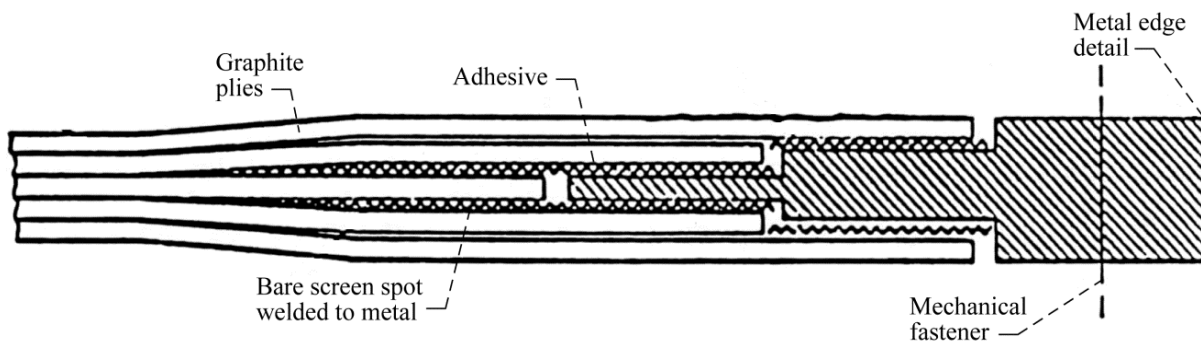


Figure 81—Center Screen Stepped Lap Composite-to-Metal Joint

NASA-HDBK-4007 W/CHANGE 2

Table 16—Bonding/Grounding Concept Assessment

JOINT	ADVANTAGES	DISADVANTAGES
Screen (Figure 76)	<ul style="list-style-type: none"> • Good electrical conduction 	<ul style="list-style-type: none"> • Difficult to fabricate in space • Requires individual component layup • Requires doublers for mechanical strength
Screen (Figure 77)	<ul style="list-style-type: none"> • Good electrical conduction • Inherent mechanical strength • Can be fabricated in space with prelaunch preparation 	<ul style="list-style-type: none"> • Requires individual component layup
Metal-Filled Epoxy (Figure 78)	<ul style="list-style-type: none"> • Good electrical conduction • Can be used on cut ends of continuously formed members 	<ul style="list-style-type: none"> • Difficult to fabricate in space • Requires doublers for mechanical strength
Mechanical Fasteners (Figure 79)	<ul style="list-style-type: none"> • Inherent mechanical strength • Can be fabricated in space • Components may be joined at positions other than ends • Allows use of continuously formed members 	<ul style="list-style-type: none"> • Poor electrical conduction
Metal Connectors (Figure 80)	<ul style="list-style-type: none"> • Good electrical conduction • Inherent mechanical strength • Suitable for truss structures • Easily fabricated in space with prelaunch preparation • Can be used on cut ends of continuously formed members 	<ul style="list-style-type: none"> • Requires expensive and heavy connectors • Limited to truss structures
Metal Splice (Figure 80)	<ul style="list-style-type: none"> • Good electrical conduction • Inherent mechanical strength for joining panels 	<ul style="list-style-type: none"> • Cannot be fabricated in space • Requires individual component layup

7.10.3 Static Drain

To support the use of graphite-epoxy composite structures in space, joints are to be developed to provide electrical conduction between composite structural members for static drain and for a fault current return path. The static drain path is necessary because the effect of vehicle charging can be detrimental where the conducting sections of the vehicle are not bonded together. For example, consider a vehicle that is charged triboelectrically on the forward surfaces and discharged through corona or the plasma from the skirt at the edges. If the forward section is not electrically connected to the aft section, charge acquired on the forward section cannot flow to the aft section unless the potential difference between the sections becomes large enough for a spark discharge to occur. These spark discharges can be quite energetic, since the capacitance between the sections may be several thousand picofarads and the sparkover voltage may be several kilovolts. Furthermore, the spark discharge will seek the easiest electrical path between

the sections. If there is some electrical wiring routed across this gap, it is possible that the spark will travel through a shorter gap from the section to the wiring, through the wiring, and then through another short spark gap to the aft section. This, of course, would put a tremendous noise pulse on any data line. Also, there is the possibility that these spark discharges could fire pyrotechnic devices.

7.11 Design Examples of Successful High-Voltage Power Supplies

The creation of high-voltage power supplies or any other high-voltage assembly or device falls into two stages: the electrical/electronic design and layout/packaging/insulation buildup. The two stages are intertwined, and both have to be kept in mind throughout the theoretical planning and the practical hardware fabrication. Several examples of good high-voltage design are presented in a report by Bever, et al (2006). Operational guidance for test and flight qualification of each high-voltage power supply is also very important. An example of one such set of instructions is included with the same report.

7.12 References

7.12.1 Government Documents

NASA

MSFC-STD-531 High Voltage Design Criteria

Bever, Renate S.; Ruitberg, Arthur P.; Kellenbenz, Carl W.; and Irish, Sandra M. (July 2006). *High Voltage Power Supply Design Guide for Space*. Report No. NASA/TP—2006-214133. Washington, DC: National Aeronautics and Space Administration.

7.12.2 Non-Government Documents

Brantley, Lott W. (1978). *Power Modules and Projected Power Systems Evolution*. Report No. NASA Conference Publication 2058. Washington, DC: National Aeronautics and Space Administration.

Bullwinkel, E.P.; Taylor, A.R. (May 1982). *Improved Capacitor Dielectrics for High Energy Density Capacitors; Final Report*. The Schweitzer Company, Kimberly-Clark Corporation, Lee, MA.

Bruins, Paul F., Ed. (1968). *Plastics for Electrical Insulation*. New York, NY: Interscience Publishers.

Catani, J.P. *Flight Failures by Arcing on Power Lines*, 10th Spacecraft Charging Technology Conference, Biarritz, France, 2007.

NASA-HDBK-4007 W/CHANGE 2

Dunbar, W.G. (January 1974). *High-Voltage Connections for Flight Vehicles; Spacecraft Electrical Insulation Reliability*. Proceedings of the National Aerospace and Electronics Conference. Dayton, OH, pp. 311-316.

Dunbar, William G. (August 1988). Design Guide: *Designing and Building High Voltage Power Supplies, Volume 2; Topical Interim Report*. Report No. AFWAL-TR-88-4143-VOL-II. Wright-Patterson Air Force Base, OH: Air Force Wright Aeronautical Laboratories.

Finke, Robert C.; Myers, Ira T.; Terdan, Fred F.; Stevens, N. John. (1978). *Power Management and Control for Space Systems*. Report No. NASA Conference Publication 2058. Washington, DC: National Aeronautics and Space Administration.

Harper, C.A.; Levitt, E.R.; Ponemone, S.J.; Zucker, R.S.; Wilson, L.E. (February 1979). *Manufacturing Technology for Spaceborne High Voltage Power Supplies, Volume I; Final Report*. Report No. AFML-TR-4014-VOL-1, Wright-Patterson Air Force Base, OH: Air Force Materials Laboratory. Available from Wright-Patterson Air Force Base.

Hughes/Northrop Grumman (December 1995). *Design and Manufacturing Guidelines for High Voltage Power Supplies*. Document ID No.: 394-000470. U.S. Air Force, Manufacturing Technology, Vol. II, III, and IV.

Ramrus, A. (October 1980). *Development of a High Energy Density Capacitor for Plasma Thrusters; Final Report*. Report No. AFRPL-TR-80-35. Edwards Air Force Base, CA: Air Force Rocket Propulsion Laboratory.

Stinthal, M.W. (April 1982). *Compilation of VCM Data on Nonmetallic Materials*. Report No. JSC-08962. NASA Johnson Space Center, Houston, TX. Revision U, Addendum 8.

8. TESTING

8.1 Introduction

In the global market, much of the high-voltage electronic equipment is designed, manufactured, and operated without regard to partial discharges. The reasons for not testing high-voltage electronics for partial discharges are varied. In many cases, industry does not recognize the value of such testing as a means of demonstrating product reliability. Manufacturing economics often influence this rationale.

It became evident early in the advent of developing high-voltage equipment for the electric power utilities that corona and partial discharges shortened the life of the electrical insulation and equipment. The first signs of such degradation led to the development of corona measuring instrumentation. Today, it is almost mandatory to measure partial discharges in most electrical utility power system equipment to identify and reject faulty materials and equipment. Similar

types of testing should be required for certain space applications as well. This would ensure normal aging of energized parts and materials without degradation caused by partial discharges. Many of the practical testing techniques commonly employed are found in Bever et al. (2006) and in MSFC-STD-531.

Most of the state-of-the-art commercial corona and partial discharge detection systems are designed and calibrated in accordance with various national and international standards organizations, for example, National Electrical Manufacturers Association (NEMA), Institute of Electrical and Electronics Engineers (IEEE), International Electrotechnical Commission (IEC), ASTM International (formerly the American Society for Testing and Materials), and SAE International. While most offer some generic testing and calibration guidelines, the specifics of equipment connection, calibration, and detection bandwidth selection are often left to the relevant power apparatus committee or component manufacturer association guidelines to tailor the testing to the application. Hence, the detection equipment options are typically focused upon meeting the requirements of specific electrical power apparatus component tests, that is, rotating machinery, utility high-voltage cable, and transformers and switchgear. As a corollary to this, much commercial instrumentation is typically designed to test all equipment with energization voltage at frequencies less than 1 kHz (including dc testing). In the case of electronic equipment that can operate at frequencies in the 20 kHz to 500 kHz regime, partial discharge test equipment has to be designed or customized to discriminate between the normal frequencies and the partial discharge event. Erroneous conclusions can be drawn about the presence or absence of partial discharges in a component if inappropriate detection equipment is used.

Through the years, the recording and display of partial discharge data has progressed from a direct visual display on an oscilloscope to digitization and storage of transient voltage pulses in computer-based instrumentation. High-speed analog-to-digital converters that can record multiple traces and aperiodic partial discharge data from dc testing (for later analysis) make this type of instrumentation invaluable. Without it, dc partial discharge activity is extremely difficult to quantify. This is particularly important to the testing of many high-voltage aerospace components, which typically operate at dc potentials. Conversely, testing with ac voltage generates partial discharge data, which are temporally more predictable and repeatable, than testing with dc potentials. This is because of the periodic reversing of polarity on the test article, which repeatedly charges and discharges the dielectric. Here, digital conversion and storage instrumentation is also useful for accurate partial discharge activity characterization, but visual display methods may be adequate.

8.2 Corona Detection Methods for Electronic Systems

It is the purpose of this section to point out some of the difficulties associated with utilizing partial discharge test equipment designed for utility power apparatus applications to evaluate aerospace electronic systems. This is not to say that such equipment is entirely unsuitable but rather to make known the need for careful application and/or possible modification before to its use in testing aerospace electronic equipment. Some problem areas fall into the following categories:

NASA-HDBK-4007 W/CHANGE 2

- a. High-frequency applications: Laboratory investigations have shown that partial discharge inception voltage levels can decrease with increasing excitation frequency.
- b. Non-sinusoidal wave forms: Pulse-width-modulated drives generate short risetime voltage surges that can apply higher voltages on turn-to-turn insulation in random-wound motors and actuators.
- c. Low-pressure or high-altitude environments: Partial discharge inception voltages are lowered as ambient pressure decreases.
- d. Environmental extremes: High temperatures can cause outgassing and degradation of polymeric insulation that can result in localized plasma discharges.

To cope with these issues, special test techniques are required. Some of the techniques described herein are empirical, with applicability being limited by instrumentation capabilities.

A power utility partial discharge detection system is usually designed to attenuate frequencies less than 30 kHz. This is to eliminate electromagnetic noise generated in power system equipment. Unfortunately, this can include the partial discharge bandwidth associated with low-pressure discharges, that is, from about 0.001 to 2 Torr. In addition, the upper cut-off frequency for certain wideband detection systems is often limited to a few megahertz. Many aerospace high-frequency power conversion electronics may include switching circuitry that generates considerable EMI in that frequency spectrum. Thus, partial discharge detection equipment designed for commercial utility applications may require substantial modification of the detection circuitry for aerospace equipment evaluations. As a minimum, equipment with selectable or tunable detection bandwidth is required.

8.3 Sensor Constraints

For best results, a partial discharge or corona detection sensor should be either directly connected to the discharge source circuitry or placed near enough to it to electromagnetically couple the discharge activity into the detection system. That is, the sensor should be placed in a position to detect but not to perturb the electric fields and/or the operating characteristics of the test article. In addition, an electromagnetically coupled sensor should be designed with sufficient sensitivity so it can be located a convenient distance from the high-voltage conductors and parts in the test circuit, such that shorting or arcing will not occur between the sensor and circuit parts.

The simplest direct-coupled detection circuit uses a low-value resistor connected in series with the ground electrode. Instrumentation can be designed to sense the minute perturbations generated by the passing of the discharge pulse current through the resistor. The transient voltage signal is then passed through a transducer or isolation amplifier and displayed or recorded. This circuit can be also used to evaluate the *pd* activity in electronic systems, which operate at high frequency and/or high altitude.

In some instances, a resistor already exists between the circuit ground and system ground. A specific criterion for the use of an existing resistor is that it be in series with the ground circuit

and that it not be bypassed by a filter. Some circuits utilize filter or shunt capacitors to reduce EMI susceptibility.

Another sensor for partial discharge testing is the Rogowski coil. The Rogowski coil is an electrical device used for measuring ac or high-speed current pulses (Wikipedia article, “Rogowski Coil,” 2013). These devices can be placed around a conductor in the test circuit, and the output of the coil can be easily recorded and stored. The sensitivity of the Rogowski coil (typically in volts/amp) must be selected for specific test purposes. The advantage of the Rogowski coil is that it allows sampling of many different locations in a test circuit without adding extra line resistance which, in many cases, will alter test results. The disadvantage of the Rogowski coil is that it will not measure dc currents and it may not have enough sensitivity to detect small partial discharge pulses. Within these limitations, the coils can work well in this application.

8.4 Pressure Sensors

Partial discharge activity in energized components is often dependent upon the ambient pressure. The environment most likely to produce partial discharge activity ranges in vacuum pressure from 10 Torr to 1 mTorr and there are many pressure sensor types that can be used to measure the pressure in this range. However most of the sensors require insight into the response of the pressure sensor in the current working gas, such as air. Many times this response limits the ability to accurately measure the pressure at the lower and upper ends of the pressure range which is the exact range where the tests must be carried out.

A capacitance manometer is a pressure gauge that has been widely used to accurately measure vacuum in the range of interest, independent of the working gas. The capacitance manometer has been used in many tests and has proven to be a highly reliable instrument.

8.5 Ultrahigh Frequency (UHF) Sensor Constraints

In UHF systems, gaseous breakdowns or glow discharges can develop and are sometimes referred to as multipactor (see section 6.3.5). Such voltage breakdown (or multipactor) generally only occurs at pressures less than 0.5 Pa (~4mTorr). UHF systems and components are usually tested for voltage breakdown and for multipactor by input/output measurements or by VSWR measurements. The presence of multipactor or voltage breakdown is measured as a change in transmitted or reflected power (Chown, et al., 1970).

Two very simple methods have been used to detect voltage breakdown or multipactor in UHF components and aerospace systems after installation has been completed. The presence of a voltage breakdown or multipactor within a cavity or waveguide produces a very slight vibration or audible noise. One technique is accomplished by attaching a very small accelerometer, strain gauge, or other vibration sensor to the component’s exterior. The vibrations generated by the internal multipactor or voltage breakdown may be sensed. If a precise location of the breakdown or multipactor is required, multiple vibration sensors may be used in a triangulation scheme. The

other technique uses an external sonic detector to recognize noise generation in proximity to the component. Of course, spatial resolution of the noise source is difficult.

8.6 Optical Detectors

Optical detectors have sensitivities compatible with the quantity of photons produced by the discharges. Some of these detectors must be operated with little or no background illumination. Most optical detectors are large, and may require fiber optic leads for direct optical viewing. This implies that the detection of corona or glow discharges may be limited to the outer surface of the test article. If the emission component of the discharge energy in the visible spectrum is large enough, unaided visual corona detection is possible and certainly cost effective.

At low pressures, the partial discharges initiated by high-frequency excitation, such as those in the UHF frequency band, can initiate very faint glows. A low-light-level camera or image intensifier may be used to detect glow discharges, provided the test article can be tested in a suitable darkened environment. One such application was on the SPEAR (He and Hall, 1984) vehicle. In this example, the camera signals (pulsed discharge events) were passed through a transducer, amplified, and transferred to the data bus system for transmission to Earth. This technology may be very helpful when testing spacecraft high-voltage systems in enclosed vacuum chambers.

Still cameras can be used, assuming the still camera synchronization between the transient discharge event and shutter speed is achieved or conditions are conducive to time exposure techniques. This is less of an issue when the discharge is of long duration or a continual glow.

Another example of an optical device used to detect partial discharge in a vacuum chamber is an infrared video system. The detection device uses specially developed cameras that sense only in the infrared spectrum, that is, 2.5 microns to 25 microns. This optical device, when combined with high-speed data acquisition, allows the digital monitoring of these test configurations many times faster than a standard video system. The advantage of the infrared video camera is that it allows the viewing of a *pd* in almost complete darkness. The infrared video camera has been used successfully for monitoring and identifying the location of partial discharge events in many tests.

8.7 Non-Explicit Detection

Various scientific instruments, such as displays, Geiger counters, mass spectrometers, photomultipliers, and curved plate analyzers, have inherent partial discharge detection capability. The electronic circuitry associated with these instruments is much more sensitive than most partial discharge instrumentation and can detect charge transfer quantities of less than 1 pC. Therefore, any extraneous transient signals generated by partial discharge within their power supplies or high-voltage electronic circuitry can be detected and displayed by the above instruments when operated at full potential. The signals will appear either as dots and dashes on visual displays or as spurious data in the signal record (Anderson and Kresge, 1957).

8.8 Electromagnetic Detectors

A simple and readily available electromagnetic-based device can be used for partial discharge detection when only very qualitative information is needed. A small hand-held radio tuned to the low end of the AM frequency spectrum (510 to 540 kHz) is one of the easiest tools to use to detect significant, continuous partial discharge activity. The radio will pick up transmitted signals from partial discharges as long as the radio antenna can be placed in close proximity and oriented toward the partial discharge signal source(s) within the test article. The partial discharge activity can be heard as a crackling or popping. This is possible since corona and partial discharges radiate a very wide frequency spectrum, as shown in figure 20. However, the exact location of the partial discharges cannot be determined by this method; only a general area in the vicinity of the partial discharge site is discernable. (Note: This detection technique is usually only applicable for equipment operated at pressures greater than 30 Torr.)

As ambient pressure is decreased from 30 Torr to less than 1 Torr, the discharges on the exterior surface of a test article change temporally. It has been observed that the frequency spectrum of such discharges in low-pressure air (0.1 to 2 Torr) is predominantly in the range of 10 to 30 kHz (Woo, 1968a; Nanevich and Hilbers, 1973; Densley, 1970; and Mason, 1978). Figure 21 shows a specific case with parallel, #16 AWG, solid copper wire electrodes spaced 4.8 cm. in air at 0.75 Torr. This limited low-frequency spectrum is undetectable by the hand-held radio method and some commercial partial discharge test equipment. A partial discharge test system with tunable detection bandwidth can detect the glow discharge frequency spectrum. Input high-pass filters may have to be modified or removed to detect the partial discharge frequency range at low pressure.

Directional antennas, dipoles, RF coils, and probes may be used as part of the sensor system to detect the RF signals radiated from partial discharge generated within an electronic circuit or system. When specialized antennas or probes are used, the test operator will be required to position and orient the sensing device with respect to the partial discharge source to achieve maximum coupling between the sensor antenna and the generated partial discharge activity. However, the test operator should be aware that the partial discharge activity may be superimposed on the circuit or system operating frequencies. In some cases, the test operator may find it necessary to develop special filter circuits to attenuate normal operating frequencies and harmonics so as not to affect the collection of partial discharge information. The available partial discharge spectrum can then be optimized, amplified, displayed, and/or recorded for future evaluation and analysis.

The sensors for RF detection schemes need not be commercially manufactured devices. Several turns of insulated #22 AWG solid copper wire wound as an approximately 2-cm diameter multiturn coil makes a simple RF pickup that can be maneuvered over the surface of an electronic circuit. The coil output leads are then impedance matched to a transmission line and connected to the detection amplifier. By attaching the coil to an insulating rod in the manner of a wand, the operator can use the directional characteristic of the probe to locate the source of partial discharge sites on an open assembly. The advantage of such a probe is that it can be oriented in any direction and moved over the surface of the test article. This type probe has been

successfully used to determine the presence of partial discharges when assessing developmental circuits and hardware.

Although excellent detection results can be obtained with this type sensor, it has one significant limitation, which is its lack of absolute calibration. First, the distance between the partial discharge activity and sensor detector is not fixed. Second, it is often difficult to introduce a known calibrating signal into the electronic test article. Finally, the orientation of the probe with respect to the plane of the partial discharge sources is unknown. Therefore, the antenna detection system should be considered primarily qualitative.

When it is necessary to quantify partial discharge activity, a capacitor-type sensor can be developed (Bartnikas, 1979; and Ahmed et al., 1979). A capacitive sensor can be constructed from a parallel plate capacitor geometry. The positive signal plate is positioned close to the test article partial discharge source. To obtain a relative calibration, it will be necessary to inject a calibration signal into the electronic circuitry under test.

It is intuitive that the synergism of different simultaneous detection methods may result in better partial discharge detection with increased resolution. This has been used on high-frequency and pulsed power components and subsystems. The following is an example describing the simultaneous use of two different detection techniques. In this case, an improvised RF probe was used while the circuitry was totally encapsulated in a dielectric media. The RF probe was placed over the suspect circuit. When the RF probe could not be used, because the circuitry was in very close proximity to a shield or ground plane, a very thin, small area ($\sim 2 \text{ cm}^2$) capacitor was utilized. The custom-developed capacitor was constructed from two conducting plates separated by a thin film dielectric (with the outer plate grounded). The partial discharge signal was transferred from the inner plate to the processing circuitry via a small diameter coaxial cable.

8.9 Spectrum Analysis

It is obvious that in some electronic circuits or systems the inherent background noise or EMI may have a frequency bandwidth that includes the majority of the partial discharge frequency spectrum. Thus, the use of band-pass or high-frequency cut-off filters to measure the partial discharge activity selectively becomes impractical. Another effective technique may be to use a spectrum analyzer to detect the presence of partial discharge activity within a circuit containing EMI and natural operating frequency spectra. For this detection technique to be effective, it may be necessary to operate the high-voltage electrical/electronic circuit at less than the rated voltage to establish a spectral baseline. Typically, the baseline data should be taken at approximately half of the rated voltage to be assured that the frequency spectrum displayed by the spectrum analyzer is free of contribution from partial discharge activity. By increasing the voltage slowly to 75 percent, 100 percent, and finally to 115 percent or 125 percent operating voltage, individual partial discharge spectral signatures can be observed and recorded. By comparing the output frequency spectrum displays, the discharge inception voltage may be determined and/or the partial discharge activity level can be characterized.

8.10 Acoustic Detection

Acoustic partial discharge detection techniques have been used widely in both commercial equipment testing and lab investigations (Meek and Craggs, 1978; Gill and von Engle, 1948; and August and Chown, 1970). They are best suited for totally enclosed circuitry, which does not lend itself to other detection schemes, by placing acoustic device(s) on the available component surface. For example, electronic power conversion equipment that is totally encapsulated inside a nonremovable shield box may be evaluated for partial discharges using acoustic emission detectors (Boggs and Stone, 1982). Acoustic devices may be selected with resonant frequencies from 50 kHz to 1 MHz. In the selection of these types of devices, one should consider the specific electrical noise and operating frequency characteristics of the test article and avoid these frequency ranges. The output of an acoustic detector is typically fed through an appropriate preamp and filter into an oscilloscope, spectrum analyzer, or dedicated data acquisition system.

8.11 References

8.11.1 Government Documents

NASA

MSFC-STD-531 High Voltage Design Criteria

Bever, Renate S.; Ruitberg, Arthur P.; Kellenbenz, Carl W.; and Irish, Sandra M. (July 2006). *High Voltage Power Supply Design Guide for Space*. Report No. NASA/TP—2006-214133. Washington, DC: National Aeronautics and Space Administration.

8.11.2 Non-Government Documents

Ahmed, Abobakr S.; Zaky, Asser A. (October 1979). "Calibration of Partial Discharge Detectors for Pulse-Height Distribution Analysis," *IEEE Transactions on Electrical Insulation*. Vol. EI-14, no. 5, p. 281.

Anderson, J.G.; Kresge, J.S. (September 1957). "An Electronic Electrometer as a Versatile Corona Detector," *American Institute of Electrical Engineers Transactions*, Part I, Vol. 76, pp. 449-454.

August, G.; Chown, J.B. (June 1970). *Reduction of Gas-Discharge Breakdown Thresholds in the Ionosphere Due to Multipacting*. Published in Proceedings of the Second Workshop on Voltage Breakdown in Electronic Equipment at Low Air Pressure, March 1969; Report No. JPL TM 33-447. Pasadena, CA: Jet Propulsion Laboratory, p. 193.

Bartnikas, R.; McMahon, E.J., Eds. (1979). *Engineering Dielectrics: Volume 1, Corona Measurement and Interpretation*. ASTM Special Technical Publication 669. Philadelphia, PA: American Society for Testing and Materials, pp. 285-326.

NASA-HDBK-4007 W/CHANGE 2

Boggs, S.A.; Stone, G.C. (April 1982). "Fundamental Limitations in the Measurement of Corona and Partial Discharge," *IEEE Transactions on Electrical Insulation*. Vol. EI-17, no. 2, pp. 143-150.

Chown, J.B.; Nanevich, J.E.; Vance, E.F.; (June 1970). "VHF Breakdown on a Nike-Cajun Rocket." Published in Proceedings of the Second Workshop on Voltage Breakdown in Electronic Equipment at Low Air Pressure, March 1969; JPL TM 33-447, Pasadena, CA: Jet Propulsion Laboratory.

Densley, John. (December 1970). "Partial Discharges in Electrical Insulation Under Combined Alternating and Impulse Stresses," *IEEE Transactions on Electrical Insulation*. Vol. EI-5, no. 4, pp. 96-103.

Gill, E.W.B.; von Engel, A. (March 1948). *Proceedings of the Royal Society of London*. London, England: Cambridge University Press, Series A, Vol. 192, p. 446.

He, D.; Hall, D.R. (May 1984). "Frequency Dependence in RF Discharge Excited Waveguide CO₂ Lasers," *IEEE Journal of Quantum Electronics*. Vol. QE-20, pp. 509-514.

"High Pressure & Vacuum," *Omega Engineering*. Retrieved May 9, 2014, <http://www.omega.com/literature/transactions/volume3/high3.html>.

Mason, J.H. (August 1978). "Discharges," *IEEE Transactions on Electrical Insulation*. Vol. EI-13, no. 4, p. 211.

Meek, J.M.; Craggs, J.D., Ed. (1978). *Electrical Breakdown of Gases*. New York, NY: John Wiley & Sons, Inc.

Nanevich, J.E.; Hilbers, G.R. (July 1973). *Titan Vehicle Electrostatic Environment; Final Report*. Report No. AFAL-TR-73-170. Menlo Park, CA: Stanford Research Institute.

"Rogowski Coil," *Wikipedia, The Free Encyclopedia*. Retrieved September 30, 2013, http://en.wikipedia.org/wiki/Rogowski_coil.

Vance, E.F.; Nanevich, J.E. (June 1966). *Rocket Motor Charging Experiments*. Menlo Park, CA: Stanford Research Institute.

Woo, R. (April 1968b). "Multipacting Breakdown in Coaxial Transmission Lines," *Proceedings of IEEE*. P. 776.